

# Effects of sympathetic nerve activity on the stiffness of conduit arteries

George Lindesay (*BMedSc, Hons*)

A thesis submitted to Macquarie University in fulfilment of the requirements for the degree of Doctor of Philosophy



The Australian School of Advanced Medicine  
Faculty of Human Sciences  
Macquarie University

Supervisor: Professor Alberto Avolio  
Co-supervisor: Dr Mark Butlin

December 2013

*“I learned very early the difference between knowing the name of something and knowing something.”*

Richard P. Feynman

# Abstract

Sympathetic nerve activity (SNA) regulates blood pressure by controlling vascular smooth muscle tone in peripheral arterioles. However, the function of SNA on vascular smooth muscle affecting the function of large conduit arteries is not as well established. It is hypothesized that SNA modulates smooth muscle tone, differentially loading the passive structural elements of the aortic wall, leading to changing arterial stiffness. This thesis presents a series of *in-vivo* experimental studies which aim to quantify the contribution of SNA on arterial stiffness. Techniques developed for quantification of arterial stiffness involved high fidelity measurements of diameter and pressure in the rat aorta. Sympathetic denervation was performed in different rodent strains (normotensive, WKY; hypertensive, SHR; hypertensive kidney disease and increased calcification, LPK) with varied baseline SNA to ascertain the effects of both chronic and acute changes in SNA. Denervation was achieved by unilateral splanchnicectomy or ganglionic blockade with hexamethonium. Aortic stiffness measurements (pulse wave velocity, compliance, distensibility) were performed across a range of mean arterial pressures to characterise the pressure dependent effect of SNA on stiffness of the abdominal aorta. Phase relationships between pressure and diameter enabled characterisation of neurogenic effects on wall viscoelasticity. Findings showed that: (i) unilateral physical denervation is insufficient to produce a change in stiffness of the abdominal aorta; (ii) sympathetic denervation by ganglionic blockade produces a maximal decrease in aortic stiffness at resting blood pressure in WKY rats; (iii) chronic exposure to high blood pressure induces vascular remodelling which alters aortic diameter, reducing the effect of SNA in SHR; (iv) modulation of cardiac function due to SNA can significantly affect arterial viscoelasticity by altering the dynamic loading characteristics of the wall of conduit arteries; this effect is more pronounced in LPK rats; (v) pressure-distension profile in the rat aorta is distinctly different to that in human arteries due to the large difference in heart rate. These findings demonstrate that the effect of SNA on arterial stiffness is mediated by direct neurogenic effect on arterial smooth muscle tone and by effects on cardiac contraction affecting the dynamic loading of conduit arteries.

# Statement of originality

I hereby declare that the work presented in this thesis has not been submitted for a higher degree to any other university or institution. To the best of my knowledge this submission contains no material previously published or written by another person, except where due reference is stated otherwise. Any contribution made to the research by others is explicitly acknowledged.

George Lindesay

Australian School of Advanced Medicine  
Faculty of Human Science  
Macquarie University

December 2013

# Acknowledgments

I would like to acknowledge the following people for their contribution to the work contained in this thesis. In alphabetical order, by first name:

*Professor Albert Avolio.* Albert has been a constant source of supervision, inspiration, enthusiasm and wisdom throughout the entirety of my research career. From the moment I walked into his laboratory he has challenged me to truly understand a concept down to its very core elements. This ethos has allowed me to delve into what were once unfamiliar concepts explored throughout this thesis, with the confidence that my understanding was true and founded in the fundamentals of the universe, or in his words “all things are mass, energy and time”. I have also thoroughly enjoyed our late night musical jamborees spurred on by wine and delicious food.

*Barbara Zangerl.* Barbara helped in both the care and surgeries of the Lewis and LPK rats. Her love of animals was ever apparent as evidenced by the rescued marsupials that she would care for under her desk. This care undoubtedly helped the fragile LPK rats survive until surgery.

*Dr Cara Hildreth.* Cara provided assistance in the calculation of baroreceptor sensitivity curves as well as the statistical tests required for analysing these curves.

*Professor Jacqueline Phillips.* Jackie helped in the design of the polycystic kidney disease study. She was also a fantastic source of information regarding the physiology of the Lewis Polycystic Kidney Disease rat. Jackie also provided welcome critical appraisal and insight into the understanding of my results throughout my candidature.

*Kayla Viegas.* My Canadian confidante. As the only other member of our vascular group doing electrophysiology, Kayla served as my ever sympathetic companion through both difficult experiments and successes. She was also there to help in the understanding of new concepts brought forth from Albert. Whilst I was first commissioned as her teacher, I feel that I ended up learning much more from her.

*Dr Mark Butlin.* My supervisor in the trenches. It was Mark’s initial work on aortic smooth muscle tissue that led to the hypotheses explored throughout this thesis. Mark has been my ever present guide, mentor and friend throughout the writing of this thesis. He has helped me in the development of my surgical techniques, writing and statistical analysis among a host of other skills which have furthered my development as a scientist. He has also been a great lunch time conversation companion. I will miss our “walk-and-talks”.

*Dr Melissa Inglott.* Melissa demonstrated the process of sympathetic nerve recording. Melissa also served as my “rig buddy” through many long days and nights of surgery. I would like to thank her for enduring my long running podcast episodes.

*Parisa Kouchaki.* Parisa helped perform the surgeries for the baroreceptor stimulation study explored in the appendix. I wish her luck in the further exploration of this and related topics.

*Professor Paul Pilowsky.* Paul provided very useful oversight and advice throughout the baroreceptor stimulation study. He was also always happy to provide helpful advice regarding both experimental methodology and statistical analysis.

*Peter Brands.* Peter provided training for the Art.Lab vessel tracking software used throughout this thesis.

*Dr Simon McMullan.* Simon helped me both in the establishment of my electrophysiology rig and furthered my understanding on the acquisition of electrophysiological data. Simon also helped in establishing an analysis technique that allowed for the generation of pressure-distension curves. Simon was also a fine source of interesting and varied conversations and a great drinking companion throughout the rugby world cup among other events.

I would like to thank the Australian Postgraduate Award scheme for the scholarship awarded to me throughout this thesis.

I would also like to thank my family and friends not mentioned above, but without whom I would not have been able to complete this thesis. Your friendship, hospitality and encouragement have been invaluable.

# List of Publications

## Journal publications

1. A.P. Avolio, M. Butlin, Y.-Y. Liu, K. Viegas, B. Avadhanam, **G. Lindesay**, Regulation of arterial stiffness: Cellular, molecular and neurogenic mechanisms, *Artery Res.* 5 (2011) 122–127.

## Conference abstracts published in journals

2. Z. Kouchaki, G. **Lindesay**, M. Butlin, A.P. Avolio, Effect of carotid baroreceptor activation on the dynamic relation between arterial pressure and pulse transit time in the spontaneously hypertensive rat., *Pulse.* 1 (2013) 75.
3. M. Butlin, A. Hammond, **G. Lindesay**, K. Viegas, A.P. Avolio, In-vitro and in-vivo use of vasoactive agents in characterising aortic stiffness in rats: testing the assumptions, *J. Hypertens.* 30 (2012) e42.
4. **G. Lindesay**, M. Butlin, A.P. Avolio, Sympathetically mediated age related changes in abdominal aortic stiffness parameters in the rat, *J. Hypertens.* 30 (2012) e44–e45.
5. **G. Lindesay**, M. Butlin, A.P. Avolio, Differential changes in large artery haemodynamics following sympathectomy in normo and hypertensive rats, *Hypertension.* 60 (2012) 493.
6. K.D. Viegas, **G. Lindesay**, M. Butlin, A.P. Avolio, Aortic stiffness is dependent on direction of mean arterial pressure change, *Hypertension.* 60 (2012) 497.
7. **G. Lindesay**, M. Butlin, A.P. Avolio, Effects of sympathetic blockade on pressure dependent abdominal aortic stiffness in the spontaneously hypertensive rat, *Artery Res.* 6 (2012) 181.
8. **G. Lindesay**, K.D. Viegas, M. Butlin, A.P. Avolio, Sympathetic activity contributes to abdominal aortic compliance and wall distensibility in rats, *J. Hypertens.* 29 (2011) e485.
9. M. Butlin, **G. Lindesay**, K.D. Viegas, I. Tan, A.P. Avolio, Cardiovascular parameters other than mean arterial pressure are predictive of dynamics changes in aortic stiffness in the rat, *Artery Res.* 5 (2011) 160.
10. I. Tan, M. Butlin, Y.Y. Liu, **G. Lindesay**, K. Ng, A.P. Avolio, Heart rate-dependence of aortic pulse wave velocity in the rat, *Hypertension.* 55 (2010) 1511.
11. **G. Lindesay**, I. Tan, M. Butlin, A.P. Avolio, Large artery stiffness increases with local neurogenic blockade in rats, *Hypertension.* 55 (2010) 1503.

### Conference abstracts published in conference proceedings

12. M. Butlin, **G. Lindsay**, D. Georgakopoulos, P.M. Pilowsky, E. Goldys, G. Town, et al., Effect of baroreceptor field stimulation on rat aortic stiffness and waveform parameters, 23rd Eur. Meet. Hypertens. Cardiovasc. Prot. (2013).
13. Z. Kouchaki, **G. Lindsay**, M. Butlin, J.K. Phillips, A.P. Avolio, Effect of denervation on viscoelastic properties of large arteries in polycystic kidney disease rats, ARTERY13. (2013).
14. **G. Lindsay**, K.D. Viegas, M. Butlin, A.P. Avolio, Sympathetic denervation decreases aortic compliance in rats, High Blood Press. Res. Counc. Aust. Meet. (2010).



# Animal Ethics Committee approvals

All studies presented in this thesis were approved by the Macquarie University Animal Ethics Committee (AEC). The final approval forms for each of these protocols can be found in Appendix C.

**AEC2010/003:** “The effect of sympathetic nerve input on large artery stiffness in conditions of normotension and hypertension”

**AEC2010/044:** “Large artery dimension, structure and stiffness in development of hypertension”

**AEC2011/044:** “Do stiff blood vessels or overactive nerves cause long-term high blood pressure in kidney disease?”

**AEC2012/002:** “Effect of acute baroreceptor stimulation on aortic haemodynamics”

# Table of contents

<i>Abstract</i>	<i>iii</i>
<i>Statement of originality</i>	<i>iv</i>
<i>Acknowledgments</i>	<i>v</i>
<i>List of Publications</i>	<i>vii</i>
<i>Animal Ethics Committee approvals</i>	<i>ix</i>
<i>List of figures</i>	<i>xv</i>
<i>Introduction</i>	<i>1</i>
<i>Literature Review Sympathetic tone and arterial stiffness</i>	<i>7</i>
<b>1.1 Anatomy and physiology</b>	<b>9</b>
1.1.1 Sympathetic outflow	9
Vasculature – small vessels	9
Vasculature - large vessels	10
Neural control of sympathetic nerve activity	14
<b>1.2 Large artery compliance</b>	<b>16</b>
<b>1.3 Smooth muscle function and large artery stiffness</b>	<b>18</b>
<b>1.4 Parameters of arterial stiffness</b>	<b>21</b>
<b>1.5 Sympathetic nerve activity and large artery stiffness in pathology</b>	<b>25</b>
<b>1.6 Large vessels and sympathetic tone</b>	<b>27</b>
<i>Methods Experimental techniques</i>	<i>31</i>
<b>1.7 Rat anaesthesia and homeostasis during surgery</b>	<b>32</b>
<b>1.8 Arterial stiffness measurement</b>	<b>33</b>

1.8.1 Pulse wave velocity measurement	33
1.8.2 Distensibility, compliance and diameter based measurements	35
1.8.3 Blood pressure parameters	41
<b>1.9 Sympathetic nerve recording</b>	<b>41</b>
<b>1.10 Blood pressure alteration</b>	<b>42</b>
1.10.1 Increasing blood pressure (phenylephrine)	42
1.10.2 Lowering blood pressure (sodium nitroprusside)	43
1.10.3 Effect of vasoactive agents on the aorta	43
<b>1.11 Sympathetic blockade</b>	<b>45</b>
<b>1.12 Post-processing and statistical analysis.</b>	<b>46</b>
1.12.1 Stiffness measurements	46
1.12.2 Blood pressure measurements over a continuum	47
1.12.3 Discrete blood pressure measurements	47
<b>1.13 Baroreceptor activity measurements</b>	<b>48</b>
<b>1.14 Power calculations</b>	<b>49</b>
<i>Effect of localised, unilateral sympathectomy on aortic stiffness in rats</i>	<b>50</b>
<b>1.15 Introduction</b>	<b>51</b>
<b>1.16 Methods</b>	<b>51</b>
1.16.1 Animals	51
1.16.2 Procedures	52
Pressure measurement and manipulation	52
Diameter measurements	52
1.16.3 Splanchnicectomy	52
<b>1.17 Data and Statistical analysis:</b>	<b>52</b>
<b>1.18 Results</b>	<b>53</b>
<b>1.19 Discussion</b>	<b>56</b>

<b>1.20 Conclusion</b>	<b>60</b>
<i>Effects of acute, chemically induced sympathectomy on aortic stiffness in the Wistar Kyoto rat</i>	<b>62</b>
<b>1.21 Introduction</b>	<b>63</b>
<b>1.22 Methods</b>	<b>63</b>
1.22.1 Animals	63
1.22.2 Procedures	64
1.22.3 Data and statistical analysis	64
<b>1.23 Results</b>	<b>64</b>
1.23.1 Cardiovascular parameters	64
1.23.2 Sympathetic nerve activity	69
<b>1.24 Discussion</b>	<b>71</b>
<b>1.25 Conclusion</b>	<b>75</b>
<i>Effect of sympathetic blockade on arterial stiffness and viscoelasticity in a rodent model of hypertension</i>	<b>77</b>
<b>1.26 Introduction</b>	<b>78</b>
<b>1.27 Methods</b>	<b>79</b>
1.27.1 Animals	79
1.27.2 Procedures	79
1.27.3 Data and statistical analysis	79
<b>1.28 Results</b>	<b>80</b>
1.28.1 Haemodynamic comparisons in strain at resting anaesthetized blood pressure	80
1.28.2 Pressure matched differences in haemodynamic parameters between WKY and SHR	81
MAP of 75 mmHg	81
MAP of 100 mmHg	87
MAP of 125 mmHg	91

MAP of 150 mmHg _____	91
1.28.3 Differences in baroreflex sensitivity between strains _____	92
<b>1.29 Discussion _____</b>	<b>93</b>
 <i>Effect of sympathetic blockade on the arterial stiffness of Lewis and Polycystic Kidney</i>	
<i>Disease rats _____</i>	<i>99</i>
 <b>1.30 Introduction _____</b>	 <b>100</b>
<b>1.31 Methods _____</b>	<b>101</b>
1.31.1 Animal preparation _____	101
1.31.2 Procedures _____	101
Pressure measurement and manipulation _____	101
1.31.3 Data and statistical analysis _____	102
<b>1.32 Results _____</b>	<b>103</b>
1.32.1 Haemodynamic differences between Lewis and LPK _____	103
MAP of 75mmHg (Table 7.1) _____	103
MAP of 100mmHg (Table 7.2) _____	110
MAP of 125mmHg (Table 7.3) _____	110
MAP of 150mmHg (Table 7.4) _____	111
1.32.2 Baroreceptor sensitivity _____	111
1.32.3 Step-wise linear regression between strains _____	112
1.32.4 Effect of sympathectomy on aortic haemodynamics within strains _____	114
MAP 75 mmHg (Table 7.1) _____	114
MAP 100 mmHg (Table 7.2) _____	114
MAP 125 mmHg (Table 7.3) _____	115
MAP 150 mmHg (Table 7.4) _____	115
1.32.5 Step-wise linear regression within strains _____	115
<b>1.33 Discussion _____</b>	<b>117</b>
1.33.1 Difference between strains _____	117
1.33.2 Sympathetic effects on arterial haemodynamics _____	121

1.34 Conclusions	126
<i>Conclusions</i>	127
1.35 Limitations	130
1.36 Future Work	131
1.37 List of Findings	132
<i>Appendix A Vascular properties in response to sympathetic blockade in hypertension: the effect of age</i>	134
A.1 Introduction	135
A.2 Methods	135
A.2.1 Animals	135
A.2.2 Procedures	136
A.2.3 Data and statistical analysis	136
A3. Results	136
A.3.1 Haemodynamic comparisons between strains and ages at resting anesthetized blood pressures	136
A.3.2 Pressure matched differences in haemodynamic parameters between WKY and SHR	137
A.4 Discussion	143
<i>Appendix B Aortic stiffness and pressure waveform parameters during baroreceptor field stimulation driven changes in sympathetic nerve activity</i>	145
B.1 Introduction	146
B.2 Methods	146
B.3 Results	148
B.4 Discussion	150
<i>Appendix C Animal Ethics Approval forms</i>	152
<i>References</i>	157

# List of figures

<i>Figure 2.1: The effect of various frequencies of sympathetic input on arteriolar tone. Higher frequencies of neurogenic input cause the release of greater amounts of nor-epinephrine, leading to vasoconstriction. (Rhoades and Pflanzner, 2003).</i>	13
<i>Figure 2.2: Sympathetic innervation of the vasculature emanates from different sections of the spinal column. Upper thoracic nerves control the ascending aorta, whilst lower thoracic and upper lumbar nerves control the abdominal aorta. (Netter, 2003)</i>	15
<i>Figure 2.3: The capacitance of large arteries. During systole, 60% of the stroke volume can be absorbed by the vessel wall. Following recoil during diastole, this blood is dissipated, creating an even flow throughout the cardiac cycle. (London and Guerin, 1999)</i>	16
<i>Figure 2.4: The compliance of an artery is determined by the slope of the tangent to the curve created as an artery is expanded through increasing pressure. This relationship between pressure and diameter is non-linear due to the properties of the arterial wall (Edited from London &amp; Guerin 1999).</i>	18
<i>Figure 2.5: The modified Maxwell model proposed by Bank et al, 1996. Elastin and collagen are connected in parallel with each other, whilst the contractile element of smooth muscle is also placed in series with collagen. As the smooth muscle is contracted, it recruits more collagen fibres which contribute to an increased elastic modulus (stiffness) of the vessel wall.</i>	20
<i>Figure 2.6: The modified Maxwell model proposed by Barra et al (1993). The contractile element (CE) is attached to the series elastic component (SEC), such that a contraction of the smooth muscle will recruit more elastin fibres, taking the strain away from the collagen fibres present in the parallel elastic component (PEC), thus reducing the Elastic modulus.</i>	20
<i>Figure 3.1: Illustration of the methodology for calculating PWV. Pressure transducers are placed at two sites along the aorta and the time taken (t) for a pressure pulse to pass from one transducer to the other is recorded.</i>	

These measurements are combined with the length between the catheters (L) to calculate PWV. (Image from Fitch et al, 2001)	35
Figure 3.2: Area in the curve (AIC) was calculated as the difference in distension between the systolic and diastolic phases of the arterial pulse (Equation 3.4). This hysteresis loop is indicative of the viscoelasticity of the aorta.	39
Figure 3.3: Example of the infusion of vasoactive drugs and the use of venous occlusion to reduce venous return for a passive reduction on arterial blood pressure.	44
Figure 3.4: PWV differences between the use of SNP and venous occlusion and PE and PE with venous occlusion. (Bottom) Concentration differences in the amount of drug used to achieve given blood pressures between the use of SNP and venous occlusion and PE and PE with venous occlusion.	46
Figure 4.1: Cutting the left splanchnic nerve produced a significant drop in blood pressure and a slight increase in cardiac contractility (PeakDP/dt) and pulse pressure (PP). This effect was transient as blood pressure soon returned to baseline values, presumably due to increase peripheral vascular smooth muscle recruitment by the remaining splanchnic nerve during baroreflex induced sympathoexcitation.	58
Table 5.1: Effect of sympathectomy on a range of haemodynamic variables. Sympathectomy produced a significant reduction in heart rate at mean arterial pressures (MAP) ranging from 75-125 mmHg. Following denervation, a significant increase in distensibility and compliance occurred at 100 mmHg as did PP. Significant increases in systolic and diastolic diameter occurred at 100mmHg. Significance is represented as: * $p < 0.05$ , ** $p < 0.01$ , *** $p < 0.001$ .	65
Figure 5.2: Change in sympathetic nerve activity (SNA) between control and denervated state at various mean arterial pressures (MAP). Maximal change in SNA occurred at 100 mmHg, and these values were significantly different between 125 mmHg and 150 mmHg. Statistical analysis were performed pairwise on the raw data of SNA between the control and denervated state.	69
Figure 6.1: Aortic distension curves between WKY and SHR before and after sympathetic denervation across a range of MAP's. Accompanying statistics are on the following page (Table 6.4).	86
Figure 6.2: Ratio of difference between the area under the distension curve before and after sympathetic denervation. No significant difference was observed between the strains at any MAP.	87
Figure 6.3: PWV of control WKY's and SHR's across a range of MAP's. No significant difference was observed between strains at any discrete MAP.	89



Figure 6.4: PWV comparison between WKY's before and after sympathetic denervation. A small but significant difference in PWV was observed at 100mmHg.	90
Figure 6.5: PWV comparison between SHR's before and after sympathetic denervation. No significant difference was observed at any discrete MAP.	90
Figure 6.6: Baroreceptor sensitivity of WKY rats and SHR. The SHR shows a higher set-point for which changes in blood pressure elicit change in SNA. However, both strains show the same sensitivity to changes in blood pressure.	93
Figure 7.1: Comparisons of PWV between Lewis and LPK rats and before and after hexamethonium across a range of MAPs. * denotes comparison following hexamethonium and # denotes comparison between strains. * $p < 0.05$ , ** $p < 0.01$ , *** $p < 0.001$ . # $p < 0.05$ , ## $p < 0.01$ , ### $p < 0.001$	103
Figure 7.2: Pressure-distension curves for Lewis and LPK rats before and after sympathetic denervation across a range of MAP's. See Table 7.5 for statistical differences.	109
Figure 7.3: Comparisons of ratio of difference in area under the distension curve before and after sympathetic denervation between strains and across a range of MAP's. * $p < 0.05$ , ** $p < 0.01$ , *** $p < 0.001$ .	110
Figure 7.4: Baroreceptor sensitivity between the Lewis and LPK. No significant difference was seen between these two strains.	112
Figure 7.5: (a) Pressure-diameter curve from the brachial artery of a human. Systole is characterized by an exponential increase in diameter at low blood pressures followed by a plateau at higher blood pressures. Image from Tardy & Meister, 1991. (b) Pressure-diameter curve from the abdominal aorta of the LPK rat. Systole is characterized by a small increase in diameter at low blood pressures and an exponential increase in diameter during late systole and early diastole.	120
Figure 7.6: Comparison of HR and $dP/dt(max)$ changes following injection of hexamethonium (A) and injection of phenylephrine (B). Following hexamethonium there is a significant and persistent decrease in both HR and $dP/dt(max)$ as the drug knocks out sympathetic activity. However, the phenylephrine induced changes in HR are small and transient and do not affect $dP/dt(max)$ .	125

# Introduction

Cardiovascular disease (CVD) continues to be the leading cause of non-communicable disease death in the world. In 2008 CVD accounted for 17 million deaths worldwide, 30% of all mortality, and is expected to be responsible for 23 million deaths annually in 2030 (World Health Organisation, 2013). In addition to the human cost of this disease is the economic cost that is needed to treat what are typically chronic symptoms of CVD. In Australia alone, the direct cost of CVD was \$7.6 billion in 2004, with a further \$6.6 billion in indirect costs. The total of \$14.2 billion accounted for 1.7% of gross domestic product (Access Economics, 2005).

Large artery stiffness is an independent risk factor for cardiovascular morbidity and mortality (Mitchell et al. 2010a). As the aorta stiffens, an increased load is placed upon the heart as more force is required to eject blood into the artery during systole (O'Rourke & Hashimoto 2007). Over time, this leads to left ventricular hypertrophy, which predisposes the heart to myocardial ischemia. In addition to this increased load, stiff arteries increase the pulse wave velocity (PWV) of the aortic pressure pulse which leads to early wave reflection, further increasing the magnitude of systole whilst reducing diastole, thereby increasing cardiac predisposition to ischemia (O'Rourke & Hashimoto 2007).

The impact of this resultant pathology arriving from increased large artery stiffness is made manifest in the number of epidemiological studies showing that increases in large artery

stiffness are predictive of cardiovascular events and all-cause mortality. This observation holds true for both the hypertensive population (Blacher et al. 1999, Laurent et al. 2001) and normal population as revealed by the Rotterdam study (Mattace-Raso et al. 2006), which showed that of a population of 2,835 subjects, arterial stiffness remained an independent predictor of coronary heart disease and stroke (Mitchell et al. 2010b). Thus, the clinical importance of arterial stiffness was recently recognised by including the measurement of PWV in the European Society of Hypertension Guideline for the Treatment of Hypertension (Mancia et al., 2007).

Increased arterial stiffness is associated with an increase in the amount collagen fibre density in the arterial wall in conjunction with fraying of the elastic lamellae, the functional wall element that provides the artery with its capacitive function. Interspersed between these passive fibres is smooth muscle, which is capable of contraction and relaxation in a similar manner to that of smaller arterioles. Previous research has shown that modulation of smooth muscle is able to alter the arterial stiffness of large arteries by adjusting the recruitment of the elastin and collagen fibres. The first evidence for this was provided by Dobrin and Rovick (Dobrin & Rovick, 1969), who showed that application of vasoconstrictors to the carotid arteries of dogs significantly altered the elastic modulus of the artery compared to when the smooth muscle was inactivated with potassium cyanide (KCN). These authors later proposed spring and dashpot models explaining the interaction between the active and passive elements of the artery (Dobrin & Canfield, 1977).

Later research by Bank et al (Bank et al. 1995; Bank et al. 1996) contradicted the results of Dobrin, showing that contraction and relaxation of human brachial artery smooth muscle produced an increase and decrease in brachial arterial stiffness respectively. These disparate results reflected the effect that different arterial wall constituents, namely the thicker

muscular wall of the brachial artery compared to the elastic wall of the carotid arteries, can have on the stiffness profile of the artery.

It is from this interest in the function of arterial smooth muscle that this present thesis began (Armentano et al. 2006, Bia et al. 2003a). *In vivo*, arterial smooth muscle tone is actively modulated via input from the sympathetic nerve fibres projecting through the arterial adventitial surface, the endothelium and circulating vasoreactive hormones (Segal 2005). The function of these inputs has been well established for the arterioles, namely regulation of mean blood pressure via control of total peripheral resistance and subsequently regulation of blood flow. However, it has not been established whether sympathetic input acutely alters large artery stiffness such as that of the aorta. Presently, there is much research being done to determine whether the endothelium can change aortic stiffness (Fitch et al. 2001, Hansen et al. 2013), yet comparatively little is being done regarding the effects of sympathetic nerve activity (SNA).

Similar to the results of studies involving smooth muscle activity and arterial stiffness (Weber et al. 1996), the effect of SNA on arterial stiffness is varied, it appears contingent on the type of artery being analysed (Delacrétaiz et al. 2001) and whether the alteration of SNA was chronic or acute, with some studies reporting spontaneous oscillations (Hayoz et al. 1993). For example, Bevan and Tsuru (Bevan & Tsuru 1981) showed that chronic removal of sympathetic tone to the rabbit ear produces a decrease in distensibility, whilst Mangoni et al (Mangoni et al. 1997) showed that acute chemical denervation produced increases in distensibility. To date, only two studies have attempted to assess the impact of SNA on aortic stiffness in humans (Lydakis et al. 2008, Sonesson et al. 1997), both of which used lower body negative pressure to stimulate SNA, yet were unable to produce any change in aortic stiffness.

This thesis investigates the effects of SNA on aortic stiffness in rats by means of acute sympathectomy. These studies utilise multiple parameters of arterial stiffness involving both the use of arterial pressure to determine PWV, as well as aortic diameter (via ultrasound), which, combined with arterial pressure, allows for assessment of large artery compliance. The details of these techniques are described in Chapter 3. The acuity of arterial stiffness assessment that these combined haemodynamic parameters offer is of high accuracy and yet has not been the practice of previous rodent research in this field. This may be due to the lack of fidelity in ultrasound at the time of early research in this field. Since then, ultrasound technology has been developed that is both able to resolve the rat aortic wall as well as track wall movement throughout the cardiac cycle.

The study presented in Chapter 4 involved the unilateral removal of sympathetic input to the abdominal aorta via cutting the left lesser splanchnic nerve. This produced no change in arterial stiffness. As unilateral denervation was insufficient to produce changes in arterial stiffness, sympathectomy was thereafter induced globally via the use of the nicotinic antagonist, hexamethonium (Hunter 1950, Mathias 1991).

Chapter 5 examines the effects of global, acute sympathectomy on the normotensive Wistar Kyoto (WKY) rat across a range of blood pressures. The results revealed that the removal of SNA produced a significant decrease in aortic stiffness at resting anaesthetised blood pressures (100mmHg) but not at high blood pressures. It was then hypothesized that if the animal had a higher resting SNA, the decrease in aortic stiffness following sympathectomy would be more pronounced. Therefore, the same protocol was applied to spontaneously hypertensive rats (SHR) (Chapter 6), which are known to display higher levels of SNA (Burgi et al. 2011, Judy & Farrell 1979). As observed in WKY, SHR displayed the most

significant decreases in aortic stiffness around 100mmHg, though these changes were less pronounced. The SHR also showed signs of vascular remodelling, as evidenced by reductions in aortic diameter at high blood pressures compared to their normotensive controls.

The denervation protocol was again used on the Lewis Polycystic Kidney (LPK) disease rat (Chapter 7), a rodent model known for its rapid development of hypertension, aortic calcification and increased baseline SNA (Harrison et al. 2010a). This study again showed that the decreases in arterial stiffness following sympathectomy occurred around resting anaesthetized blood pressures of both the LPK and its normotensive counterpart, the Lewis rat. However, it was also discovered that contributing to this decreased stiffness as measured by arterial compliance was, in part, through cardiac involvement as determined by heart rate and indices of cardiac contractility. These results revealed that not only does the direct sympathetic input into the arteries play a role in their stiffness profile, but so also does the rate at which these vessels are loaded and unloaded.

Detailed discussion of experimental results and implications of findings appear in the individual chapters, so there is no separate dedicated discussion chapter. However, Chapter 8 provides a summary of the findings in context of the stated aims of the thesis and draws conclusions regarding the overall function of SNA in determining arterial stiffness. Together, these studies have shown that alteration of the sympathetic input to large arteries is sufficient to change arterial stiffness. However, the magnitude of these changes does not exceed the influence of known contributors to large artery stiffness such as increased mean arterial pressure. It is therefore suggested that the changes in arterial stiffness mediated by SNA play at best a secondary functional role in actively modulating the function of the large arteries as capacitance vessels, although they can have a more prominent role in muscular conduit arteries that can modulate small vessel compliance and so peripheral wave reflection.

Moreover, whether the reductions seen in arterial stiffness are relevant with regard to the cardiovascular health of both the normal and hypertensive population has yet to be determined.

The Appendices contain data from experiments which are complementary to the experiments reported in Chapters 3-7. Appendix A describes a set of experiments assessing the effects of age in relation to SNA and large artery stiffness. Appendix B extends the effect of SNA to electric field activation of baroreceptors and to associated changes in vascular properties.

# Literature Review

## *Sympathetic tone and arterial stiffness*

### Summary

Anatomically, the rat abdominal aorta has a substantial proportion of smooth muscle and is innervated by sympathetic projections that act upon the  $\alpha$ -adrenergic receptors of smooth muscle in the aortic wall. The magnitude and even the directionality of the effect of these innervations upon vascular wall mechanics is highly varied in studies reported in the literature. This literature review details the various parameters used to quantify large artery stiffness, models of the mechanical interaction of the functional and structural components of the vessel wall, and the existing reported studies that investigate the effect of sympathetic activity upon the large arteries. There are no studies to date that investigate the effect of sympathetic nerve activity upon aortic stiffness, and this review reports on supporting evidence for a role of sympathetic activity, and poses the hypothesis that is addressed in the later chapters of this thesis.



The sympathetic nervous system is a branch of the autonomic nervous system primarily responsible for eliciting excitation responses in order to increase activity in the body (Guyenet 2006, Lambert 2001). It is associated with the flight or fight response, during which, after exposure to a threatening stimulus (African jungle cats are typically used as an example) there is a surge in sympathetic nerve activity (SNA) (Dotevall 1994). This activity causes vasoconstriction of the blood vessels in the visceral organs and an increase in heart rate and breathing rate among a host of other physiological changes. Together, these processes increase the amount of blood available to the muscles, therefore giving the animal the means to run from or fight the impending threat.

Far from being an antiquated vestige of more dangerous times, the sympathetic nervous system is actually constantly active, albeit at more basal levels. It ensures that we do not faint upon standing, that we can sweat in hot weather and that we are able to regulate the amount of light intake into our eyes via dilation or constriction of the pupils (Mano & Iwase 2003, Neuhuber & Schrödl 2011, Sundlöf & Wallin 1978) as well as number of other homeostatic functions. Indeed, one may still feel the sympathetic surge when exposed to modern perils which elicit the fight or flight response in everyday life (for example during sport or attention at critical moments).

The extent of innervation is vast, with sympathetic fibres terminating at all organs as well as every section of the vascular tree. This allows for a large degree of control of many homeostatic functions such as glucose balance and renal function as well as fine control of blood pressure via constricting or dilating blood vessels (Shields 1993).

## **1.1 Anatomy and physiology**

### **1.1.1 Sympathetic outflow**

Sympathetic nerves emanate from the first thoracic segment of the spinal column and descend to the third lumbar segment. From here the nerves either synapse at the paravertebral column that runs alongside the spine, or at prevertebral ganglia which are located between the paravertebral column and the organ of supply (Shields 1993). At this synapse, acetylcholine is released which communicates with the postganglionic neurons via nicotinic acetylcholine receptors. These are the same receptors activated during smoking, hence the name of the receptors after the discovery of their affinity for nicotine (Boehm & Huck 1997, Greene & Rein 1978). The post synaptic neurons then travel a long distance, relative to their parasympathetic counterparts, to their target organs. Upon arrival at their target organs, nor-epinephrine is released which activates adrenergic receptors, therefore causing the aforementioned effects (Greene & Rein 1978).

#### **Vasculature – small vessels**

Arterioles, in conjunction with cardiac output changes via the heart are the main effector organ for the immediate change of mean blood pressure. They consist primarily of a relatively thick layer of smooth muscle (compared to its size) which surrounds an endothelial surface. This large amount of smooth muscle allows the arteriole to modify its diameter (and therefore peripheral resistance) to a large extent, which is precisely why arterioles regulate blood pressure more so than any other blood vessel (Rhodes and Phlanzer, 2003). Descending into this smooth muscle layer is a dense coverage of sympathetic nerves. Arteriolar diameter is maintained via smooth muscle activation, the range of arteriolar

diameters is mediated by the frequency of sympathetic nervous system signals, circulating hormones and metabolic factors (Segal 2005).

### **Vasculature - large vessels**

The functionality of the large arteries as capacitance vessels is attributed to the internal structure of the arterial wall, which consists primarily of elastin, collagen and smooth muscle (Apter et al., 1966). These components are expressed differentially throughout the length of the arterial tree, with elastin being most prevalent within the ascending aorta, with gradually increasing vascular smooth muscle along the length of the aorta and toward the peripheral vasculature (Harkness et al. 1957a, Wolinsky & Glagov 1969). The components are further differentiated within the cross-sectional layers of the artery, of which there are three circumferential areas: the tunica intima (endothelium), tunica media and tunica adventitia.

The tunica intima consists primarily of a monolayer of epithelial cells that line the surface of the vascular system (Pasyk and Jakobczak, 2004). Collectively, the tunica intima acts as an organ used for the regulation of vessel tone, constriction and permeability of the vasculature. Through the release of vasodilators such as nitric oxide (NO) and endothelium derived hyperpolarizing factor (EDHF) and vasoconstrictors such as endothelin-1 and endoperoxides, homeostatic monitoring of blood pressure can occur.

The tunica media and adventitia provide the artery with the elasticity and strength needed to withstand high intraluminal pressures. At a young age, the arrangement of the elastin, collagen and smooth muscle within a structure such as the aorta is quite uniform (Karrer, 1961). The tunica media is arranged such that the smooth muscle cells are separated equally by intervening lengths of elastin, whilst the tunica adventitia consists primarily of collagen. The morphology of large arteries does however change with age, a phenomenon well

documented in the literature, not least because of its contribution to cardiovascular disease (Wissler and Robert, 1996). A primary observation in aging arteries is the increased deposition of collagen and degradation of elastin throughout the tunica media (Karrer 1961). The once uniform layers of smooth muscle cells and elastic lamellae become interspersed with collagen as the elastin fibres begin to fray (Milch 1965) .

Large arteries are themselves supplied with blood vessels (*vaso vasorum*) and nerves (*nervi vasorum*). These structures reside within the tunica adventitia and feed into the tunica media to ensure that the smooth muscles within the aortic wall are both innervated, provided with oxygen and able to remove metabolic wastes (Van Buren et al., 1996; Ritman and Lerman, 2007). The degree of innervation as well as the amount of smooth muscle cells within a region of aorta helps the aorta maintain the structural integrity (Fronek 1983, Kacem et al. 1997, 2006) and possibly stiffness of the vessel wall. Within the smooth muscle of arterioles, the frequency of the sympathetic input will dictate the calibre of the vessel (Rhodes and Phlanzer, 2003) (Figure 2.1). That is, at low frequencies, the arteriole becomes more dilated owing to the lack of norepinephrine being released onto the smooth muscle receptors. Gerova et al (Gerová et al. 1973) showed the effects of sympathetic nerve input on vessel calibre remained consistent in large arteries, though they lacked the same range of diameter change as arterioles. It was also observed that arterioles always exhibit some degree of basal neurogenic tone (Lee, 1989). It is assumed therefore, that the same principle of basal smooth muscle innervation applies within larger arteries, though this assumption has never been tested.

The aorta is primarily innervated by sympathetic input acting upon  $\alpha$ -adrenergic receptors of the smooth muscle (Kienecker and Knoche, 1978). These nerves emanate from different sections in the spinal column, with upper thoracic nerves controlling the ascending aorta and

nerves from the lower thoracic and upper lumbar controlling the vasoactivity of the descending and abdominal aorta (Figure 0.2).

### *Tonic control of arteriolar diameter*

Arteriole diameter is controlled by tonic release of norepinephrine.

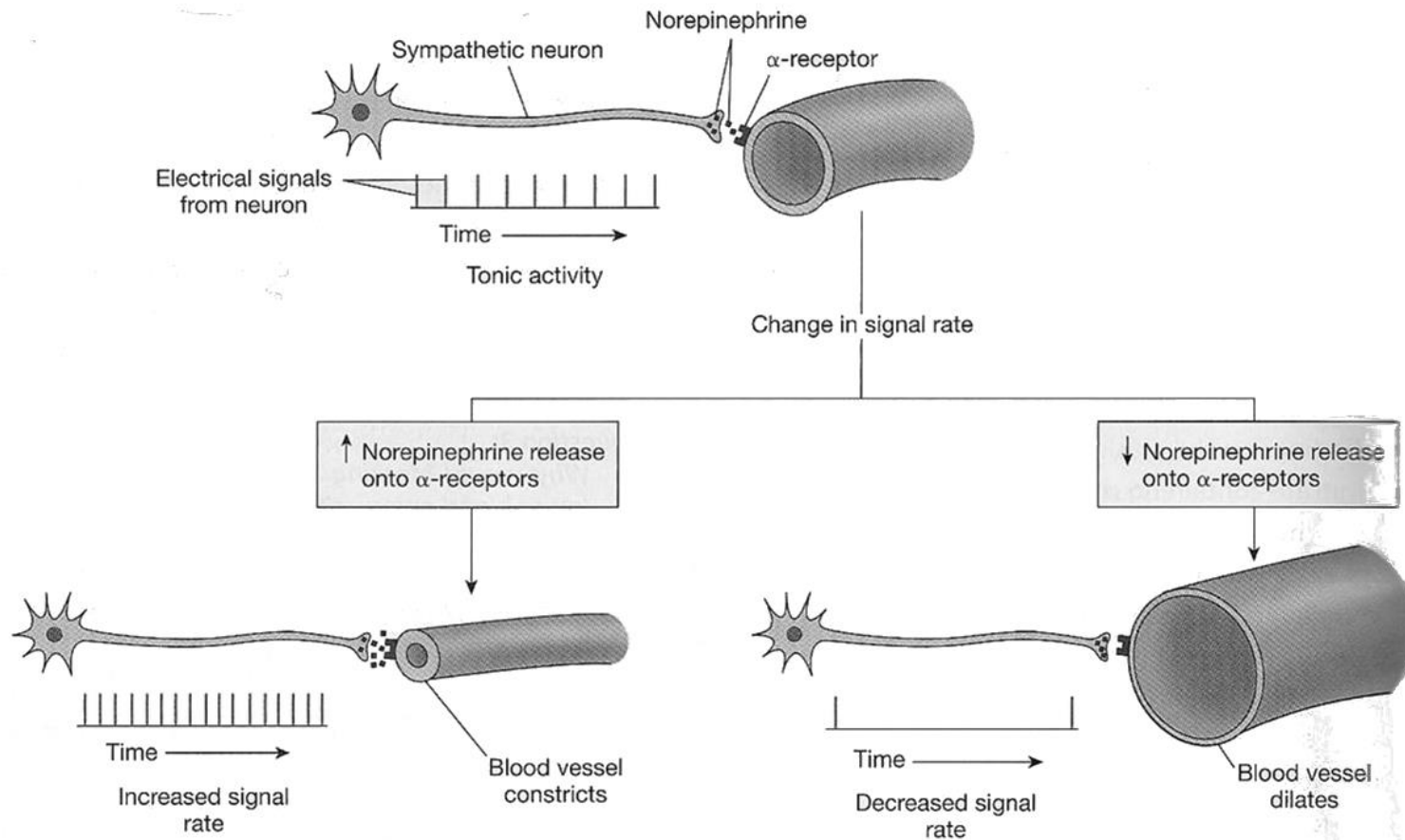


**Figure 0.1:** The effect of various frequencies of sympathetic input on arteriolar tone. Higher frequencies of neurogenic input cause the release of greater amounts of nor-epinephrine, leading to vasoconstriction. (Rhoades and Pflanzer, 2003).

Similar to the contents of the arterial wall, Kienecker showed that the degree of neurogenic innervation changes throughout the arterial tree, with small peripheral arteries having the greatest amount and the ascending aorta having the least, between which is a gradient of innervation (Kienecker & Knoche 1978a). This study also showed that an application of nor-adrenaline, an  $\alpha$ -adrenergic agonist was able to reduce the diameter of the small arteries and aorta of rabbits by 30% and 20% respectively. However, the functional effect of this adrenergic application in altering arterial stiffness was never measured. Generally, vascular remodelling to external stimuli is a hallmark of small and medium sized arteries (Schiffrin & Hayoz 1997).

### **Neural control of sympathetic nerve activity**

Activation of the sympathetic nervous system may be elicited by numerous regions of the brain (Guyenet 2006). The long term regulators of SNA are the rostral ventrolateral medulla, the spinal cord, the nucleus of the solitary tract and the hypothalamus. These structures receive inputs from peripheral barosensitive, thermosensitive, and glucosensitive neurons. Stretch sensitive receptors and their associated efferent neurons are thought to be the most important dictator of homeostatic cardiovascular function. Stretch receptors present in both the arteries (aortic arch and carotid sinus) and the lungs will cause a decrease in SNA when exposed to high arterial pressure or increased ventilation volumes respectively. Conversely, the typical barosensitive response to high blood pressure is deactivated during exercise owing to stretch sensitive receptors located in group III and IV muscle fibres of skeletal muscles which send centrally projecting afferent fibres to increase SNA (Sinoway & Li 2005). In certain individuals this inhibited baroreceptor response causes excessive hypertension, and is thought to be due to increased large artery stiffness (Schultz et al. 2013b). In addition, neurogenic activity also modulates endothelial function (Spieker 2002).

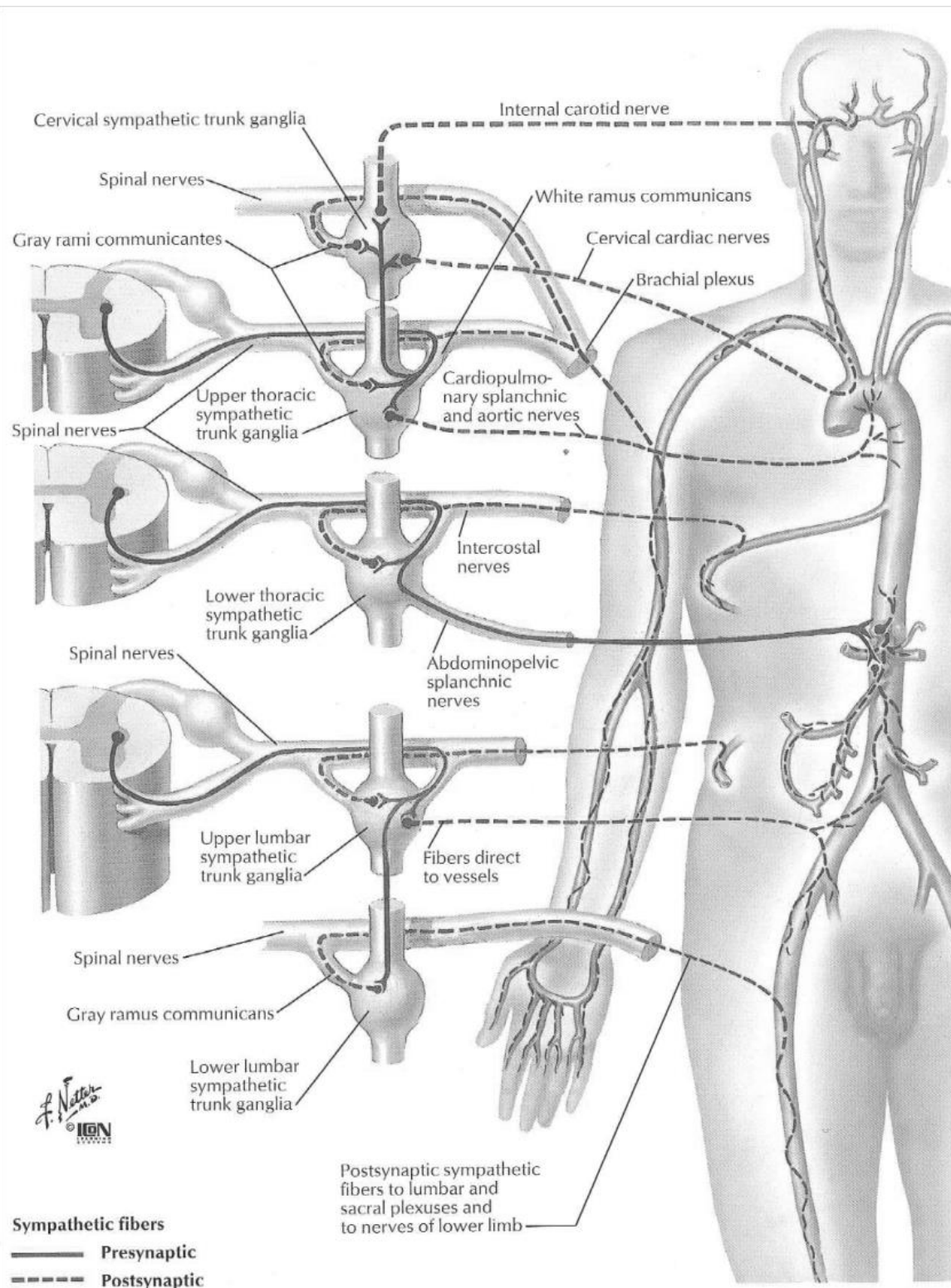


**Figure 0.2:** Sympathetic innervation of the vasculature emanates from different sections of the spinal column. Upper thoracic nerves control the ascending aorta, whilst lower thoracic and upper lumbar nerves control the abdominal aorta. (Netter, 2003)



## 1.2 Large artery compliance

Large arteries are the capacitance vessels of the arterial tree. Their compliant structure enables them to absorb up to 60% of the stroke volume by wall expansion during systole (Belz, 1995; London and Guerin, 1999). The elastic nature of the large arteries also allows them to recoil during diastole, thus evenly distributing blood throughout the cardiac cycle (see Figure 0.3). This property throughout the arterial tree transforms the pulsatile ejection of blood from the heart into a constant blood flow to the end organs, thus improving the efficiency of perfusion and blood supply to sites of metabolism. This action is analogous to that of *Windkessel* water pumps once used in fire fighting that converted a pulsatile pumping of water into a continuous flow of water at the fire hose end (Greenwald, 2002), and the lumped analysis of the arterial system is often referred to as a *Windkessel*.

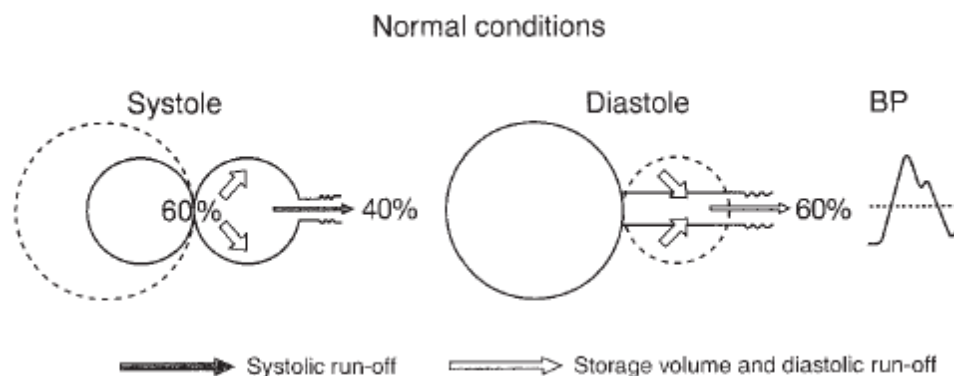


**Figure 0.3:** The capacitance of large arteries. During systole, 60% of the stroke volume can be absorbed by the vessel wall. Following recoil during diastole, this blood is dissipated, creating an even flow throughout the cardiac cycle. (London and Guerin, 1999)

Far from being inert tissue, large arteries are dynamically responsive organs, with the capacity to help regulate blood flow, blood pressure and cardiovascular function (Nichols et

al. 2011). This may be achieved rapidly (seconds to minutes) through the change of smooth muscle tone within the vessel wall, or slowly (months to years) through changes in the quantities and distribution of the proteins elastin and collagen (Pourmoghadam et al., 2002), the proteins that constitute the remaining structural properties of the vessel wall. Such changes in the artery are able to alter these haemodynamic properties, because they each change the capacitance of the vessel, thus altering the magnitude of the *Windkessel* function.

The degree of capacitance within an artery is defined mostly by the cross-sectional compliance within the vessel wall, as most of the dimensional change is in the radial direction compared to the tethered longitudinal direction (Krug et al. 2003). Since this thesis focuses primarily on the properties of the vessel wall, these terms will henceforth be used interchangeably. Thus the term ‘compliance’ will generally refer to ‘cross-sectional compliance’

The degree of arterial compliance changes non-linearly with distending pressure, owing to the presence of different materials in the vessel wall (London & Guerin, 1999). At low pressures, compliance is high. This is due to the presence of elastin fibres in the vessel wall, which exhibit elastic properties and are able to stretch, allowing an increase in blood volume to expand the artery wall with minimal pressure increase. As pressure increases, compliance decreases. This is because the increased pressure begins to load the stiffer collagen fibres in the vessel wall, thus the vessel becomes more rigid, and less able to accommodate additional blood volume within the vessel lumen.

Normally functioning arteries produce a typical pressure-diameter curve from which compliance can be calculated by the tangent to the curve (see Figure 0.4). Modification of the vessel wall however, will change the function of the vessel wall entirely. If a greater quantity

of collagen is added to the wall it will decrease the overall compliance of the vessel, resulting in a greater pressure increase for the same change in diameter (Romney and Lewanczuk, 2001). Wall mechanical properties can also be deduced from diameter/flow measurements (Hayoz 1995).

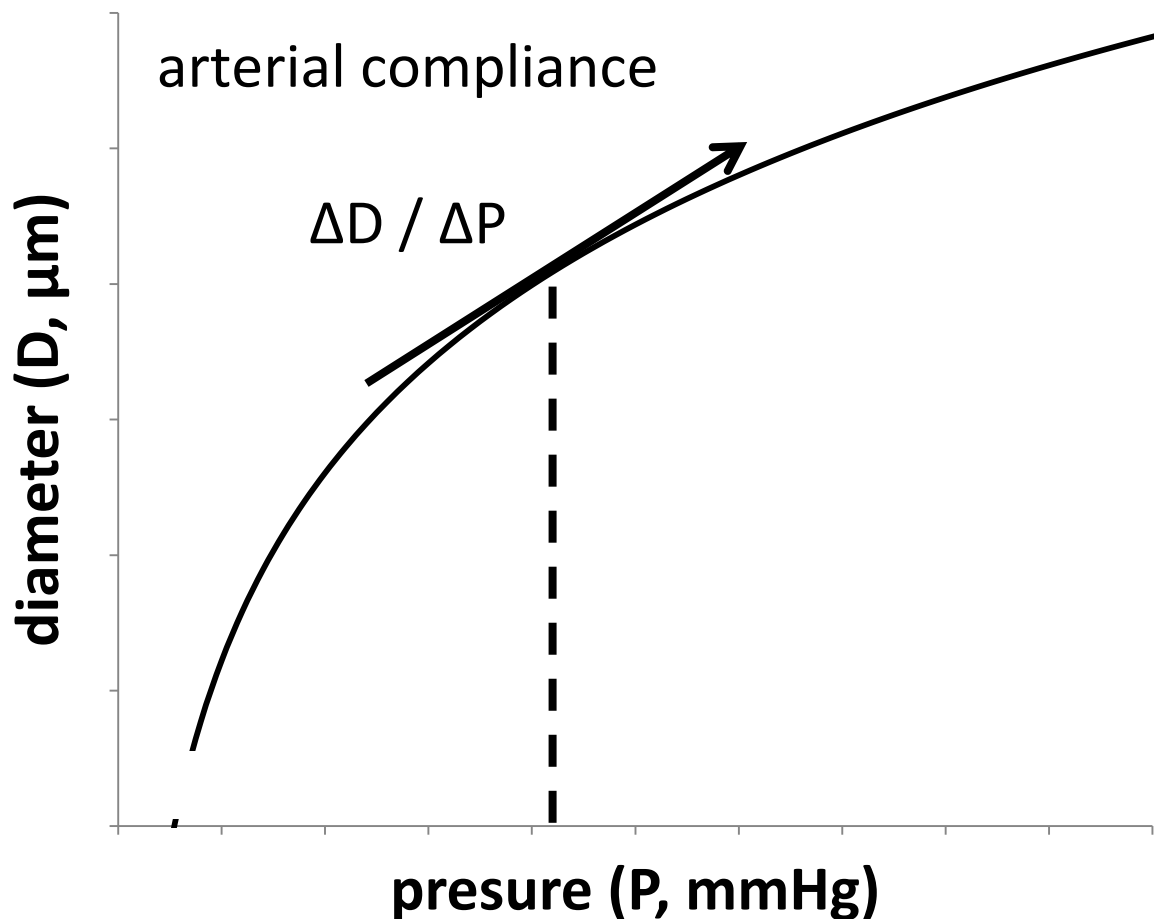


**Figure 0.4:** The compliance of an artery is determined by the slope of the tangent to the curve created as an artery is expanded through increasing pressure. This relationship between pressure and diameter is non-linear due to the properties of the arterial wall (Edited from London & Guerin 1999).

### 1.3 Smooth muscle function and large artery stiffness

Arterial stiffness is the inverse parameter of compliance. As arteries age or degrade due to ageing, environmental and other lifestyle factors (smoking, high cholesterol diets, lack of

exercise), their elastin fibres begin to fray and they increase the deposition of stiff materials such as collagen and fibronectin into the vessel wall (Kim et al. 2005a, Mitchell et al. 2003).

The effect of smooth muscle contraction and relaxation on arterial stiffness is controversial. Many studies have been conducted, both *in-vivo* and *ex-vivo* to determine whether smooth muscle plays a significant role in modulating aortic stiffness. Thus far, results have shown that smooth muscle contraction can produce an increase (Bank et al., 1995; Bank et al., 1996) or a decrease (Dobrin and Rovick, 1969; Barra et al., 1993) in aortic stiffness. The contention between the authors' conclusions stems from their assumptions of how the structural components within the vessel wall interact with each other (see Figure 0.5 and Figure 0.6).

If it is assumed that activation of smooth muscle draws upon elastin fibres (Figure 0.6), this would allow the vessel to increase its intraluminal pressure and maintain a lower wall stiffness compared to relaxed smooth muscle, since the recruited elastin would bear the load at pressures for which collagen would normally be recruited. However, if smooth muscle drew more upon collagen fibres (Figure 0.5), one would expect an increase in wall stiffness at all ranges of blood pressure, though the effect would be most apparent at lower blood pressures, since at high blood pressures collagen is already being loaded by the normal force of intraluminal pressure. It follows that at blood pressures within the normal physiological range, relaxation of smooth muscle would dramatically decrease the arterial stiffness if the smooth muscle recruited more collagen than elastin, whilst there would be little change if smooth muscle recruited more elastin than collagen. Finally, in both cases one would not expect to see large changes at low blood pressures when the smooth muscle is relaxed, since the elastin fibres are quite capable of bearing the load.

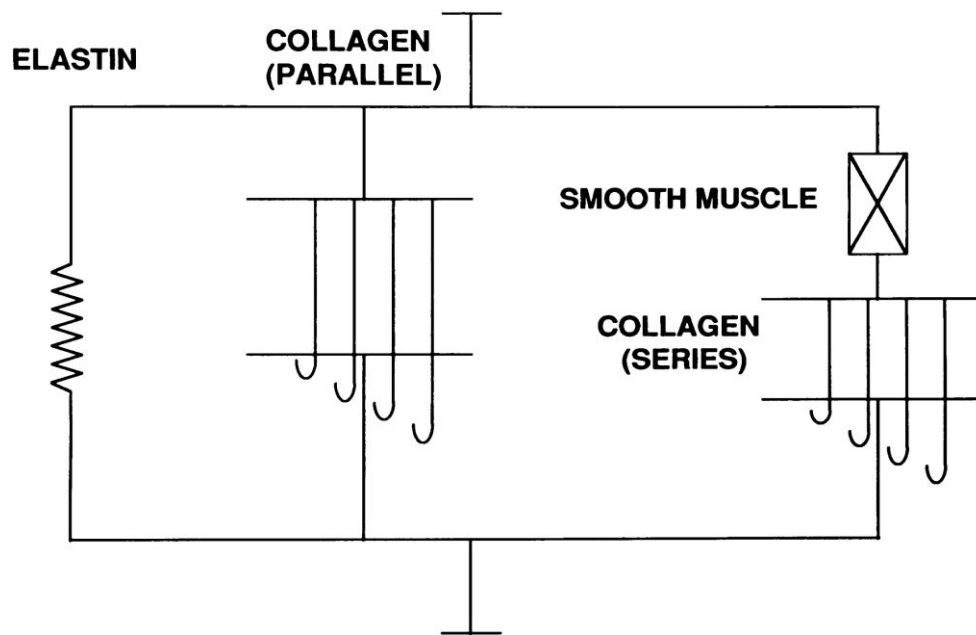


**Figure 0.5:** The modified Maxwell model proposed by Bank et al, 1996. Elastin and collagen are connected in parallel with each other, whilst the contractile element of smooth muscle is also placed in series with collagen. As the smooth muscle is contracted, it recruits more collagen fibres which contribute to an increased elastic modulus (stiffness) of the vessel wall.

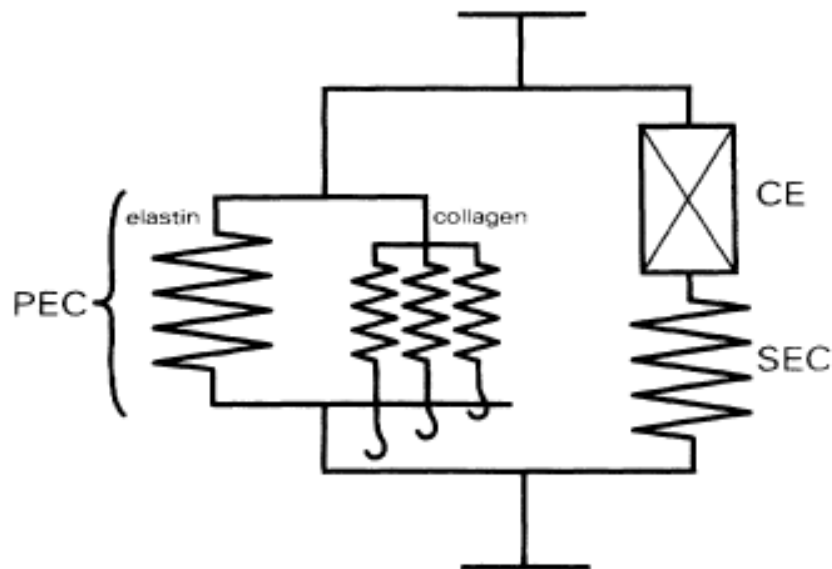


**Figure 0.6:** The modified Maxwell model proposed by Barra et al (1993). The contractile element (CE) is attached to the series elastic component (SEC), such that a contraction of the smooth muscle will recruit more elastin fibres, taking the strain away from the collagen fibres present in the parallel elastic component (PEC), thus reducing the Elastic modulus.

It is apparent from these previous studies by Bank et al (1995 and 1996), Dobrin and Rovick (1969) and Barra et al (1993) that different types of arterial beds and different animal models were used in each study. This is of significance since each of these arterial beds contain a different arterial wall composition. For example, whilst the aorta contains a small amount of smooth muscle, there is increased smooth muscle deposition as one moves toward the periphery of the arterial tree (Harkness et al. 1957b). Similarly, different species express different ratios of collagen, elastin and smooth muscle even within the same arterial bed (Wolinsky & Glagov 1969). This may have contributed to the differences in arterial function seen by these researchers upon alteration of smooth muscle tone. The animal model used in this thesis is the rat abdominal aorta. Compared to humans, the rat shows higher amounts of smooth muscle and more elastic lamellae per unit of wall thickness (Wolinsky & Glagov 1969). Therefore, care was taken when discussing the significance of the studies presented in the context of their relevance to humans.

## **1.4 Parameters of arterial stiffness**

A number of indices have been developed to quantify arterial stiffness. However, the computation of these indices is often influenced or confounded by additional haemodynamic factors such as heart rate, cardiac contractility or other limitations in signal acquisition and analysis, which makes calculating true arterial stiffness difficult.

Compliance measures the absolute diameter change for a given pressure step and assumes a fixed vessel length (Equation 3.2, 0), (O'Rourke et al. 2002) to define. In non-invasive human studies, researchers typically used aortic measurements of diameter coupled with brachial measurements of pressure, disregarding any effects of pulse amplification from

central to peripheral arteries (Liao et al. 1999) leading to inaccurate compliance estimation especially where there are significant changes in heart rate (Avolio et al. 2013).

Often measurements of compliance also do not account for changes in diastolic diameter. This becomes significant when examining changes in compliance following treatments that alter the tone of the arterial wall. This is resolved in large part by expressing the relationship of pressure and diameter in terms of distensibility (Equation 3.3, 0), which normalizes the compliance term for diastolic diameter. This parameter is considered to be the inverse of the elastic modulus and therefore a much more accurate descriptor of arterial stiffness (Glasser & Arnett 1998, Mangell et al. 1996). To illustrate the difference between distensibility and compliance: one may gain increased compliance by increasing the resting diameter of the vessel, but this does not necessarily translate to an increase in distensibility (Van Bortel et al. 1995). Angiotensin converting enzyme inhibitors do not alter the resting diameter of the vessel, and lead to an increase in compliance by altering the wall distensibility (Kool et al. 1993) whereas isosorbide dinitrate increases compliance by altering the resting diameter of the vessel wall (Kool et al. 1995)

An additional parameter is that of arterial distension (Equation 3.4, 0). This measures the percentage change in arterial diameter throughout the cardiac cycle. When combined with arterial pressure, this parameter is effectively calculating arterial stiffness at multiple points during systole and diastole. This is an improvement over distensibility alone, which only calculates stiffness as a function of the difference between diastole and systole and therefore assumes a linear relationship between changes in blood pressure and changes in arterial diameter (Leone et al. 2008). Furthermore, this measurement allows for normalisation of diameter measurements, which is useful when there are variations in aortic diameter sizes between subjects.

A method of *in-vivo* assessment of arterial stiffness is the measurement of the arterial pulse wave velocity (PWV). This method of arterial stiffness assessment is currently the “gold-standard” for non-invasive, large artery stiffness measurement in humans (Wilkinson et al. 1998). PWV is the speed at which the pulse created by cardiac contraction travels through the wall of the blood vessel. The use of PWV to indicate stiffness is well established throughout the literature (Blacher et al. 1999, Laurent et al. 2001) and is used as a measure of arterial stiffness because it is minimally affected by cardiac factors, although it is highly dependent on mean arterial pressure (Avolio et al. 1983). PWV is related to the Young’s modulus ( $E$ ) of the vessel wall the Moens-Korteweg equation (Equation 2.1), which utilises Newton’s equation for wave speed in a material, with the equation for bulk modulus substituted for volumetric strain (Nichols et al. 2011).

$$PWV = \sqrt{\frac{E_{inc} \cdot h}{2 \cdot \rho \cdot r}} \quad \text{Equation 2.1}$$

As can be seen in the Moens-Korteweg equation, PWV is also influenced by the dimensions of the artery in terms of radius ( $r$ ) and wall thickness ( $h$ ). Therefore, in values of PWV, one must ensure that the  $h/r$  ratio remains relatively constant if any change is to be attributed to stiffness ( $E$ ). However, the  $E_{inc}$  (incremental elastic modulus) is the major determinant for PWV, particularly in relatively thin walled vessels such as the aorta, in which the  $h/r$  ratio is relatively constant. This can be seen in the case of increasing blood pressure, which will increase PWV (Avolio et al. 1983), despite the fact that  $h$  is decreasing and  $r$  is increasing. According to the Moens-Korteweg equation this  $h/r$  change decreases PWV. As it does not,  $E$  is assumed to primarily dictate PWV.



Augmentation index (AIx) is another clinical measure often used as a parameter associated with arterial stiffness, requiring measurement of a single pressure waveform. AIx measures the degree to which the peak of a measured pressure wave is over and above the incident pressure. It has been traditionally held that this augmentation was mostly a result of reflected pressure waves from the complex branching of the arterial system, with stiff arteries increasing the speed and amplitude of wave reflection, leading to a greater and earlier augmentation of the pressure wave. A competing model of the vasculature uses a *windkessel*, reservoir, or compliance function that acts across the whole large artery vasculature, independent of location. This estimated *windkessel* effect is subtracted from the pulse waveform and subsequent analysis conducted using either Fourier or wavelet analysis. Studies using this modelling approach demonstrate that it is the *windkessel*, not wave reflection, that provides the greatest contribution to the AIx. (Davies et al. 2010, Schultz et al. 2013a). However, the model, perhaps in its infancy, has met with criticism including that it is a combination of both a zero dimensional component (the *windkessel*) with one dimensional parameters (Hughes et al. 2012, Mynard et al. 2012). Additionally, the *windkessel* parameters, which are defined as being independent of wave effects, have been shown to be dependent upon wave propagation (Mynard 2013). AIx is primarily calculated as in Equation 2.2, where  $P_s$  is systolic pressure,  $P_d$  the diastolic pressure and  $P_i$  is the inflection point in the pressure waveform. These values are gathered via the pressure waveform, wherein the inflection point can be identified as the point which coincides with the first positive to negative crossing of the fourth derivative of pressure (Nichols et al. 2011). Further confounding the use of AIx as a stiffness parameter is its reliance upon the transit time of the reflected wave and the time of arrival of this reflected wave during the pressure pulse, it is thus a heart rate dependent measurement. A slower heart rate will cause the reflected wave to arrive closer to systole thus increasing the AIx, whilst a higher heart rate will cause it to

arrive during diastole, nominally termed a negative AIx. This technical shortcoming of this particular measurement becomes evident when evaluating the arterial stiffness of the elderly, particularly those with higher heart rates and therefore, their AIx is reduced despite increased arterial stiffness (McEniery et al. 2005).

$$AIx = \frac{P_s - P_i}{P_s - P_d} \quad \text{Equation 0.2}$$

## **1.5 Sympathetic nerve activity and large artery stiffness in pathology**

There is growing evidence to suggest that increased SNA is associated with the development of hypertension and thereby cardiovascular disease. Studies in conscious humans have measured increases in muscle sympathetic nerve activity (mSNA) in patients with hypertension (Matsukawa et al. 1993). Further, Greenwood et al (Greenwood et al. 2001) showed an association between increased mSNA and left ventricular hypertrophy. This observation was made within essential hypertensive patients matched for blood pressure. Therefore, it is likely that hypertension resulting from increased SNA is both a result of increased vascular tone as well as the trophic effects of sympathetically derived circulating hormones on the myocardium such as catecholamines, angiotensin II and insulin like growth factor 1 (Malpas 2010). However, new evidence suggests there may be a central mechanism for increase in blood pressure arising from increased SNA. Spontaneously hypertensive rats (SHR) have increased activity in the anterior hypothalamic area of the brain as well as

increased release of acetylcholine in the rostral ventral lateral medulla, both of which contribute to the hypertension seen in these animals (Kubo et al. 2002)

It has been shown that obstructive sleep apnoea has an independent effect on arterial stiffness (Doonan et al. 2011). Patients suffering sleep apnoea undergo periods of hypoxia during sleep. This may be due to obstruction of the airway due to relaxation and collapse of soft tissue surrounding the throat or due to dysfunction in the respiratory centres of the brain (Eastwood et al. 2010). During these periods of asphyxiation there are dramatic cardiovascular, respiratory, neural and humoral changes, not least of which is a marked increase in SNA (Smith et al. 1996). Increased levels of carbon dioxide (hypercapnia) and decreased oxygen (hypoxemia) activate chemoreceptors, triggering increased SNA. Inspiration would normally help to suppress the increase in SNA resulting from chemoactivation. However, apnoeic events only occur during post expiratory events, this period of respiration results in an increase in SNA (even in healthy people) due to lack of inhibition of the sympathetic reflex via thoracic stretch receptors and is sustained throughout the apnoeic event (Phillips & Somers 2000). Thus the increase in SNA resulting from apnoea is two-fold: chemo activation and stretch receptor inactivity.

These increases in SNA continue throughout the duration of the apnoeic event and result in a dramatic surge in blood pressure at the end of each apnoeic event, and returns to normal values upon the resumption of normal breathing. Throughout the apnoeic event, blood pressure steadily decreases (despite the aforementioned surge in SNA); this may be due to the bradycardia that occurs during apnoea or carbon dioxide and hypoxemia induced vasodilation (Phillips & Somers 2000). It has been observed that prior to the post apnoeic hypertension (late apnoea), there is a significant increase in arterial stiffness, as measured by the AIx of the radial arterial pulse (Jelic et al. 2002) compared to resting blood pressures. These changes

occurred despite a reduction in blood pressure and without any change in heart rate between the awake period and during the late apnoeic period. These data suggest that the surge in SNA was able to increase large artery stiffness. However, AIx is not considered as robust a measure of local large artery stiffness as aortic PWV, since it is affected by the summation of the wave reflections from the distal arterial tree including the peripheral, muscular arteries (Nichols et al. 2011). Further, the increases in stiffness seen may also be due to endothelial dysfunction arising from intermittent hypoxia (Feng et al. 2012)

Further evidence for the association between increased SNA and arterial stiffness comes from smoking. Smoking increases SNA both acutely (Narkiewicz et al. 1998) and chronically (Hering et al. 2010) as well as increasing PWV. Both acute and chronic increases in PWV are independent of blood pressure (Kim et al. 2005b). Acutely, smoking introduces nicotine into the blood stream causing activation of the sympathetic chain ganglia, thereby increasing blood pressure via direct vasoconstriction and increasing circulating catecholamines. The increase in PWV seen following smoking is not likely a result, of direct sympathetic innervation of arterioles, since baroreceptors quickly counter the increase in blood pressure resulting from smoking with sympathoinhibition. Indeed, this was made evident by Narkiewicz et al (Narkiewicz et al. 1998), who needed the use of vasodilatory substances concurrently with smoking to reveal the sympathoexcitatory effects of smoking. Instead, the acute effects of smoking on PWV are likely to be complex and involve multiple vascular systems including endothelial and renal function.

## **1.6 Large vessels and sympathetic tone**

These aforementioned studies have in part led to the justification for a study that seeks to definitively quantify the effect of SNA on large artery stiffness. Heretofore, there has been

little research on this topic, which has perhaps been considered sufficiently explained within the field of smooth muscle tone on large artery stiffness. However, there is a certain specificity that has yet to be attained, a specificity whose importance is made evident in the growing literature of cardiovascular diseases which present with elevated SNA as well as increased arterial stiffness. Thus, a study which quantifies the contribution of SNA to arterial stiffness will allow future researchers to account for this additional factor when assessing arterial stiffness.

Among the first studies to assess the role sympathetic nerves have on arterial mechanics was by Gerova et al (1973). In this study, the researchers stimulated the efferent connections to the canine abdominal aorta via bilateral stimulation of the sympathetic chain ganglia at the level of LG1-LG2. This produced a decrease in abdominal aortic diameter, with the greatest change occurring at the iliac bifurcation (10% change in diameter) and the least at the level of the renal artery (3%). However, this study did not determine whether these changes in arterial diameter affected wall stiffness.

A later study by Joannides et al (1995) demonstrated that alteration of sympathetic tone to the human radial artery was sufficient to induce significant changes in both the incremental elastic modulus and compliance. Specifically, they demonstrated that increasing SNA via cold pressor stimulus leads to an increase in compliance and a decrease in the incremental modulus. However, they recognised that this resulted from a decrease in midwall stress as a result of the size of the arterial wall thickening, thus decreasing the radius/wall thickness ratio of the vessel. Since stress is directly related to the incremental modulus (Dobrin & Rovick 1969) and arterial compliance is related to the inverse of the incremental modulus (Bader, 1967), this helped to explain these results. Joannides et al (1995) went on to suggest that the smooth muscle contraction may also unload collagen fibres in favour of elastin fibres,

therefore also contributing to the lowered compliance during the cold pressor test. Interestingly, a study conducted one year earlier by Boutouyrie et al (1994), on the same artery showed a decrease in compliance following cold pressor test.

Boutouyrie et al (1994) used exactly the same ultrasound device and blood pressure monitoring device (plethysmograph) and the same stimulus to induce and increase in sympathetic activity over the exact same amount of time (2 minutes). Moreover, both studies examined compliance using the same formula and at the same mean arterial pressure (100mmHg). Inexplicably, Joannides et al (1995) did not reference the study by Boutouyrie et al (1994) and so does not account for the differences in results. It is therefore difficult to speculate what caused the differences in results. One potential explanation lies in the lack of change seen in the internal arterial diameter during cold pressor stimulation in the study by Boutouyrie et al (1994) whereas Joannides did see a change. Therefore, unlike Joannides et al (1995), the stress of the load was not borne by the increase in wall thickness for the subjects in the Boutouyrie et al (1994) study. Instead, the increase in SNA produced arterial diameter and wall thickness independent changes in smooth muscle tone which increased recruitment of stiff collagen fibres leading to an increase in stiffness. Unfortunately, Boutouyrie et al (1994) did not examine changes in wall thickness, so these assertions cannot be verified. Such a differential response may have occurred due to differences in the responses of the subjects to the cold pressor test. Another study by Lafleche et al (1998) using a more elastic artery (carotid) and the same cold pressor test protocol had findings similar to that of Boutouyrie et al (1994), in that distensibility decreased following an increase in SNA.

Only a few studies have sought to assess the effects of sympathetic activity on central arterial stiffness. Lydakis et al (2008) showed that increased sympathetic activation induced by lower body negative pressure was not sufficient to cause any change in arterial stiffness. However,

this study used largely surrogate measures of stiffness, central pressure and SNA in the form of AIx, wave transform function and renal vascular resistance index. New data suggests that AIx is not significantly related to regional large artery stiffness and should not be regarded as indicative of systemic arterial stiffness, instead it is more accurately a marker for left ventricular afterload (Climie et al. 2013). These results seen by Lydakis et al (2008) were also seen by Sonesson et al (1997), wherein sympathetic stimulation via lower body negative pressure did not alter the mechanical properties of the aorta as assessed by pressure-diameter curves.

Thus, it can be seen that there is sufficient evidence to suggest that modification of SNA can acutely alter large artery stiffness provided that the vessel has both sufficient vascular smooth muscle and sympathetic inputs. It is for this reason that the rat abdominal aorta was chosen as a representative arterial segment for this thesis since it exhibits both the function of a capacitance vessel and as well as enough sympathetic innervation and muscular tone to allow modification of arterial diameter (Gerová et al. 1973). Since previous studies were unsuccessful in modifying large artery stiffness by means of stimulating SNA (Lydakis et al. 2008, Sonesson et al. 1997), the studies in this thesis employed the removal of SNA to determine its effect on arterial stiffness. In order to determine whether increased SNA contributes to arterial stiffness in the hypertensive condition, two hypertensive rodent models were also used and compared with their normotensive counterparts.

# Methods

## *Experimental techniques*

### Summary

This chapter outlines and discusses the methods that are employed in the studies across many of the chapters within this thesis. These methods include :

- (i) basic animal surgical preparation and anaesthesia,
- (ii) aortic blood pressure and diameter measurement
- (iii) calculation of parameters of aortic wall mechanics including pulse wave velocity, distension, distensibility, compliance and viscoelasticity
- (iv) sympathetic nerve activity recording and quantification
- (v) acute manipulation of blood pressure for assessing the above parameters across a full range of physiological blood pressures
- (vi) systemic sympathetic blockade through administration of hexamethonium
- (vii) baroreceptor activity assessment.

The chapter also evaluates the use of vasoactive agents for the acute manipulation of blood pressure and the subsequent effect these vasoactive agents have on the vessel being investigate, the abdominal aorta.

The work on the effect of vasoactive agents upon aortic stiffness was the subject of a conference abstract presented in 2012 (Butlin et al. 2012).



## **1.7 Rat anaesthesia and homeostasis during surgery**

Anaesthesia was induced via intraperitoneal injection of urethane (10% w/v in 0.9% physiological saline at 1.3 g/kg, ethyl carbamate, Sigma-Aldrich Pty. Ltd., Australia, saline NaCl, Baxter Healthcare, Australia). Urethane provides long periods of surgical anaesthesia with a large therapeutic window, with minimal cardiorespiratory depression (Field et al., 1993). The effects of urethane on SNA have previously been studied and have been shown to initially produce a decrease in SNA, but return to basal levels of activity after one hour (Matsukawa & Ninomiya 1989). This time-period in which the effects of urethane on SNA were present, occurred before the period for which data was collected for analysis. Therefore, the chosen anaesthetic, urethane, would not have effected SNA levels in the data presented in this thesis. Anaesthesia was maintained with intravenous injection of urethane (0.2 g/kg in saline) as required by monitoring responsiveness to a pain reflex. Testing of the pain reflex was conducted by pinching the paw of the rat and checking for a leg retraction. Wakefulness was also determined by corneal touch reflex.

Temperature was measured using a rectal thermometer with an automatically adjusting heat mat (Harvard Instruments) maintaining the measured temperature at 37°C. All animals were paralyzed with pancuronium bromide (0.02 mg/kg/hour, iv). Animals were given a tracheotomy and mechanically ventilated via a tracheal tube with oxygen enriched air. Ventilation was adjusted to achieve an expired CO<sub>2</sub> percentage of 4-5%. This was generally attained with a rate of 80 cycles per minute at a tidal volume of 4-5 ml. Paralysis was induced to prevent the animal from competing with the respirator and in so doing cause irregular breathing patterns which may lead to irregular cardiovascular activity. Pancuronium bromide does also have a mild vagolytic effect which leads to a slightly increased heart rate, but this was not considered to be sufficient to cause significant changes in the aortic stiffness

parameters assessed in these studies. There is some evidence from obstructive sleep apnoea (OSA) studies that show positive pressure ventilation can lead to decreases in blood pressure and arterial stiffness in patients with existing OSA (Drager et al. 2007, Shiina et al. 2010). However, these decreases are compared to the disease state, so it cannot be determined whether such decreases would be seen in cases where OSA was not originally present.

ECG leads were placed subcutaneously in a lead I configuration to allow monitoring of heart rate. Temperature, ECG and CO<sub>2</sub> concentration data were recorded with an analogue to digital data acquisition system and associated software (CED 1401, Spike 2, Cambridge Electronic Design, United Kingdom). Intravenous drugs were delivered via cannulae in the left femoral artery (0.9 mm outer diameter, polyvinyl chloride, Silastic, Midland, Michigan).

## **1.8 Arterial stiffness measurement**

### **1.8.1 Pulse wave velocity measurement**

Throughout the work presented in this thesis, pulse wave velocity (PWV) was calculated using the foot-to-foot method. This involves the measurement of two pressure wave signals at two points along the length of the aorta. Two high fidelity pressure sensing catheters (1.6F; Scisence, Canada) were introduced into the aorta via the carotid and femoral artery and left to reside at the proximal and distal ends of the abdominal aorta. Identification of these areas was made primarily via the shape of the pressure waveform and later via ultrasonographic confirmation. The catheters were held in place via sutures at the carotid and femoral insertion sites. Blood pressure was recorded at a sampling rate of 2 kHz using an analogue to digital data acquisition system and associated software (CED 1401, Spike 2, Cambridge Electronic Design, United Kingdom). In order to calculate PWV (Equation 3.1), a distance measurement (d) of the pulse path length was required. This was acquired post-mortem by measuring the

distance between the pressure sensing tips of the catheters with a length of wetted suture placed along the aorta between the two sensors, and measurement of that suture.

The transit time ( $tt$ ) was measured between the feet of the pressure waves from the proximal and distal pressure sensors. PWV was then calculated:

$$PWV = d / tt \quad \text{Equation 0.1}$$

Due to the small size of the catheters used in these experiments, they pose no risk of significantly altering blood flow in the aorta. The mean diameter of a rat aorta at the level where the proximal catheter is placed (descending aorta), was 1.4mm whereas the catheter was only 0.63mm. The diameter of the area that is conducting blood with the catheter is not simply the aortic diameter minus the catheter diameter. In order to attain this effective diameter, first, one must determine the effective area of the aorta with the catheter in place. This is equal to the area of the aorta without the catheter subtracted by the area of the catheter. The effective diameter is then defined as the diameter of the effective area. In the case of these studies, there was a reduction in effective area of 20.3% and a reduction in effective diameter of 10.7%

The foot, not the peak, of the pressure wave is used because it is considered to be free from the influence of wave reflections and thus constructive or destructive interference (Fitch et al., 2001). The foot of the pressure wave can be defined by the peak of the second derivative of the pressure wave, indicating the maximum change in slope of the pressure wave, that is, the very beginning of the systolic upstroke (Figure 0.1).

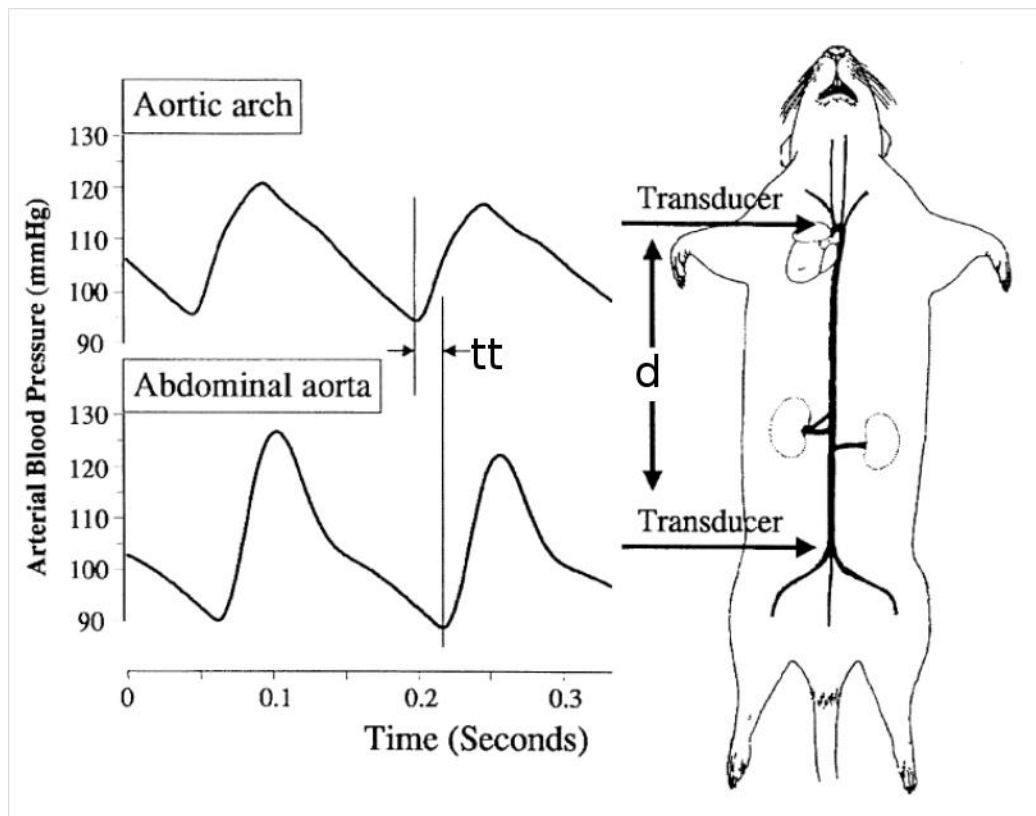


**Figure 0.1:** Illustration of the methodology for calculating PWV. Pressure transducers are placed at two sites along the aorta and the time taken ( $tt$ ) for a pressure pulse to pass from one transducer to the other is recorded. These measurements are combined with the length between the catheters ( $d$ ) to calculate PWV (Equation 3.1, Image from Fitch et al, 2001).

### 1.8.2 Distensibility, compliance and diameter based measurements

In addition to PWV, arterial stiffness may also be calculated using the *in-vivo* strain response (vessel diameter) to the applied stress (blood pressure) at a single site, such as the aorta. The abdominal aorta, between the two pressure catheters, was imaged using an ultrasonic probe (7.2 Mhz, 40 mm window), which was placed on the right side of the animal and imaged in brightness mode (B-mode), positioned to clearly visualise the proximal and distal aortic wall (Figure 3.2). The clearly imaged section of the vessel was windowed by the operator, and the frequency signal within this window was processed by vessel wall tracking software (Art.Lab, Esaote, Netherlands) in real time to measure aortic diameter. The signals were acquired at a sampling rate of 60 Hz. Pressure and diameter measurements were processed

offline using MatLab (Mathworks) to upsampled both signals to 2 kHz. Pressure data was then calibrated using the data from the Spike recordings. Blood pressure and diameter signals were then time shifted to align their diastolic feet to allow for generation of pressure-diameter curves.

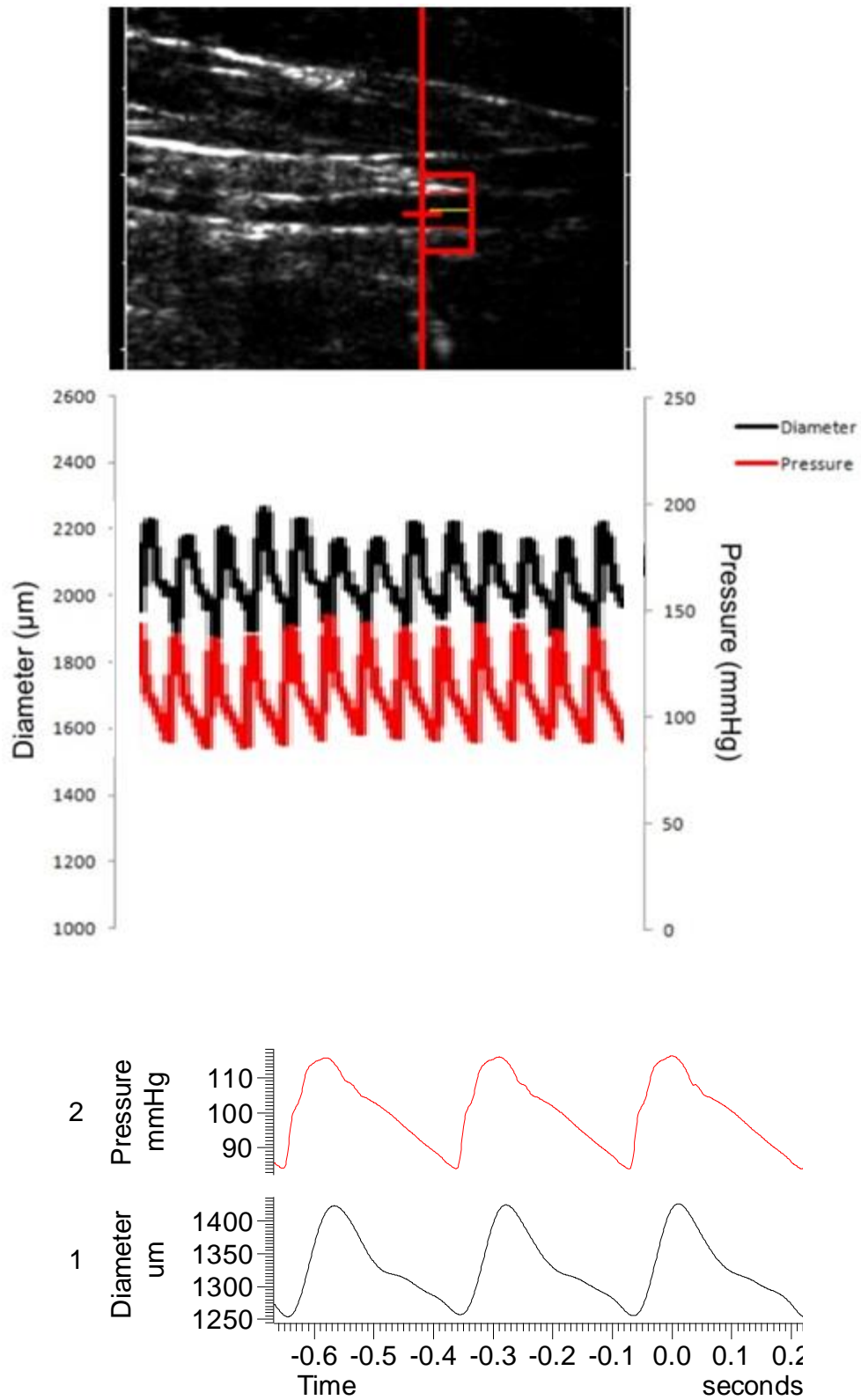


**Figure 3.2** Ultrasound image of the abdominal aorta and vessel wall tracking software (Art.Lab) and the resultant diameter and pressure (after calibration) waveforms. Waveforms were sampled at 2 kHz. Bottom panel; ensemble averaged waveforms of pressure (top) and diameter (bottom).

Compliance (Equation 3.2) and distensibility (Equation 3.3) were calculated using these diameter measurements, coupled with aortic pressure taken from the proximal intravascular pressure sensor.

$$C = \frac{\Delta D}{\Delta P} \quad \text{Equation 0.2}$$

$$\text{distensibility} = \frac{\Delta D}{\Delta P \cdot D_d} \quad \text{Equation 0.3}$$

where C is compliance,  $\Delta D$  is the difference between systolic and diastolic diameter,  $\Delta P$  is the difference between systolic and diastolic pressure and  $D_d$  is diastolic diameter.

Viscoelasticity may be measured *ex-vivo* by placing an arterial ring in a tensile tester and stretching the segment to attain the stress-strain curve of the vessel with respect to time. However, with the use of aortic wall tracking technology outlined above, one can also measure viscoelasticity *in-vivo* by coupling aortic diameter measurements with aortic pressure measurements, thus measuring strain and stress respectively. When plotted on separate axes, a hysteresis loop is formed between the ascending systolic curve and the descending diastolic curve. The area in this curve (AIC) was used to calculate viscoelasticity (Figure 0., Equation 0.4). A large loop indicates an increase in viscoelasticity of the vessel and is due to a phase delay between the pressure and diameter waveforms. An increased

phase delay occurs as the vessel becomes stiffer, since it takes more energy to begin distending the blood vessel resulting in an exponential looking systolic phase.

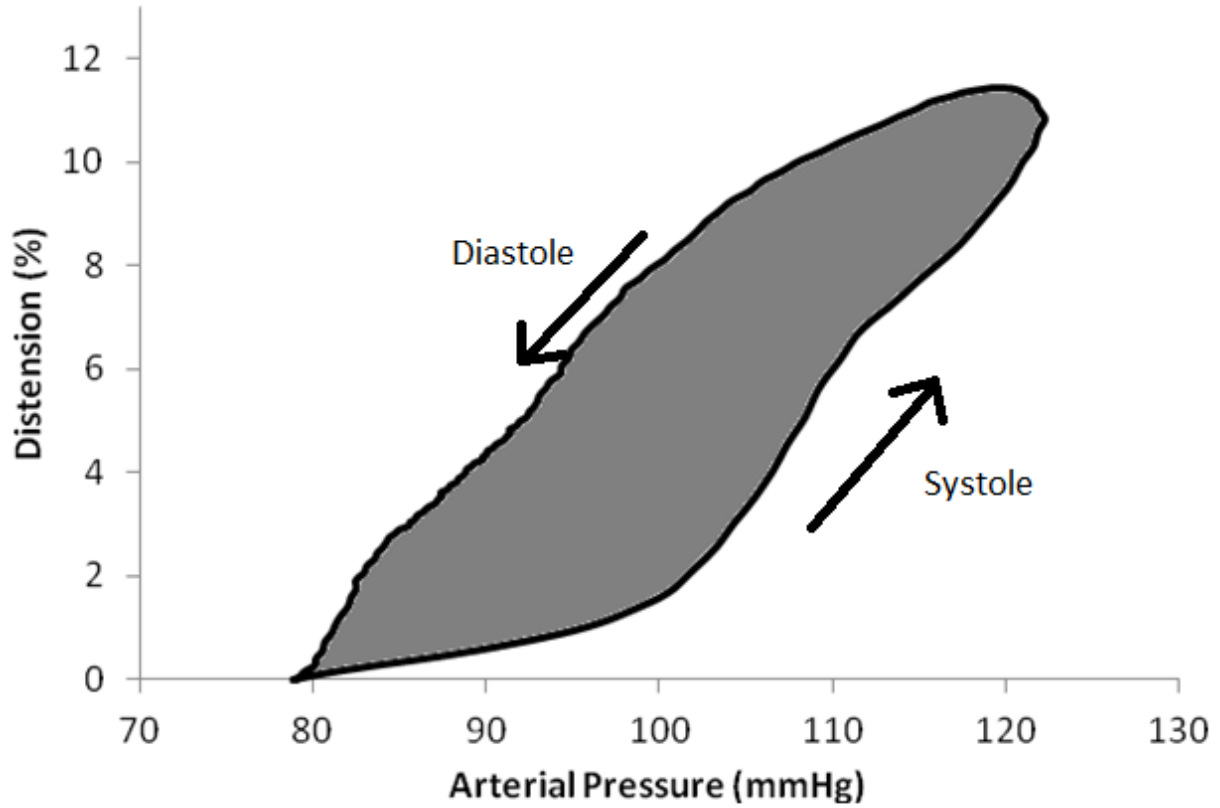


**Figure 0.3:** Area in the curve (AIC) was calculated as the difference in distension between the systolic and diastolic phases of the arterial pulse (Equation 0.4). This hysteresis loop is indicative of the viscoelasticity of the aorta.

$$AIC = \left[ \int_{P_s}^{P_d} distension(P).dP \right]_{diastole} - \left[ \int_{P_s}^{P_d} distension(P).dP \right]_{systole} \quad \text{Equation 0.4}$$

There are many different types of stiffness measurements derived from diameter and pressure measurements including compliance, distensibility and distension (Equation 0.5). As stated in Chapter 2, the subtle distinctions between these measurements become important when



assessing the effects of a treatment that may alter the diastolic diameter of the artery. This applies specifically to the experiments presented in this thesis because whilst the measurements are taken from the same site along the aorta, the introduction of sympatholytic or sympathoexcitatory drugs has the potential to change the resting diameters of the vessel, either by reducing heart rate or by global blood vessel dilation.

$$distension (\%) = \frac{(D - D_d)}{D_d} \times 100 \quad \text{Equation 0.5}$$

From the Moens-Korteweg equation (Equation 3.6), PWV depends on the elastic modulus of the wall material ( $E$ ) and the vessel geometry (radius  $r$  and wall thickness,  $h$ ) as well as the density of blood ( $\rho$ ). Thus, measurements of vessel geometry enables a better determination of the effect a given treatment on the material stiffness ( $E$ ) of the vessel. Although accurate measurements of diameters can be obtained, the wall tracking technology used in the present experiments is unable to resolve wall thickness measurements. This is because the required frequency of the ultrasound is too low. The 7.2 MHz frequency used, measuring at a depth of 35mm (2288 pixels) has a resultant resolution of 15 $\mu$ m/pixel. Given that the thickness of the rat abdominal aortic wall is approximately 100  $\mu$ m (Mello et al. 2004), only changes exceeding a 15% change in wall thickness could accurately be detected. Notwithstanding the limitation in measurement of wall thickness, diameter measurements enable determination of overall wall compliance effects, which supplement the PWV measurements.

$$PWV = \sqrt{\frac{E_{inc} \cdot h}{2 \cdot \rho \cdot r}} \quad \text{Equation 0.6}$$

### 1.8.3 Blood pressure parameters

To better identify the factors contributing to increased arterial stiffness, additional parameters were extracted from the blood pressure waveform using a custom designed script in Spike software. Pulse pressure (PP) is the difference between the systolic peak and diastolic foot of the pressure pulse. Large fluctuations in this variable can contribute significantly to measurements such as compliance (Equation 3.2) and distensibility (Equation 3.3). A surrogate for cardiac contractility was determined from the maximum value of the first derivative of the pressure pulse (dP/dt(max)) (Chan et al. 1984a, Hamlin & del Rio 2012). As a vascular parameter it represents the rate of change in blood pressure throughout the cardiac cycle and describes the dynamic loading of the vessel wall.

## 1.9 Sympathetic nerve recording

Throughout the experiments presented in this thesis, sympathetic outflow was quantified using recordings made from the Greater Splanchnic nerve. This nerve originates from T5-T9 and synapses at the coeliac ganglia, which innervates the viscera. This nerve contributes significantly to the control of blood pressure, since 25% of total blood volume is contained in the splanchnic vasculature (Kandlikar & Fink 2011).

The left splanchnic nerve was exposed via a flank incision and dissected free from connective tissue. Distinct from the typical splanchnic nerve recording, the rats in experiments presented in this thesis had their left splanchnic intact. This was to ensure that sympathetic tone was

still being provided to the aortic plexus, which itself branches from the coeliac ganglia, the first ganglia that the splanchnic nerve terminates into.

The splanchnic nerve was attached to a bipolar electrode and the cavity was filled with paraffin oil to insulate the electrodes, attached to the nerve, from the surrounding body. Recorded nerve activity was amplified and passed through a band pass filter (10-1000 Hz) using a CWE bioamplifier and acquired at 2 kHz using a data acquisition system (CED 1401 and Spike software, Cambridge Electronic Design, United Kingdom).

## **1.10 Blood pressure alteration**

Blood pressure was altered using intravenous phenylephrine (PE) and sodium nitroprusside (SNP). This was done to observe the changes in all measured parameters over a full range of physiological blood pressure. In addition to this, it was used to compare parameters at a matched blood pressure where strains or treatments resulted in different resting blood pressures. Predefined mean arterial pressures to reflect low, moderate and high blood pressures were chosen at which to capture aortic diameters: 75 mmHg, 100 mmHg, 125 mmHg and 150 mmHg.

### **1.10.1 Increasing blood pressure (phenylephrine)**

PE is a  $\alpha_1$ adrenergic receptor agonist used in the treatment of hypotension (Cooper and Mowbray, 2004). Through its action on the  $\alpha_1$ adrenergic receptors of the arteriolar smooth muscle, PE causes vasoconstriction, leading to an increase in total peripheral resistance, thus increasing blood pressure. Blood pressure was raised in animals by injecting an intravenous bolus of PE (15  $\mu$ g/kg). This concentration consistently achieved a 50-60mmHg increase in

blood pressure and was sufficient to assess the changes in arterial stiffness over a range of blood pressures.

### **1.10.2 Lowering blood pressure (sodium nitroprusside)**

SNP is a potent vasodilator that affects the smooth muscle lining the walls of the vascular system. This occurs as SNP liberates NO molecules, which bind to the haeme groups of guanylate cyclase receptors. This leads to the activation of cyclic guanosine monophosphate (cGMP), which causes a cascade of cGMP dependent protein kinases (PKG) to become activated. These PKG's interact with a multitude of cellular proteins such as ion channels and pumps, receptors and enzymes in order to decrease the amount of intracellular  $\text{Ca}^{2+}$  (Carvajal et al., 2000). Blood pressure was lowered in animals by injecting an intravenous bolus of SNP (15µg/kg). This concentration consistently achieved a 40-50 mmHg decrease in blood pressure and was sufficient to assess the changes in arterial stiffness over a range of blood pressures.

### **1.10.3 Effect of vasoactive agents on the aorta**

A pilot study was conducted to determine whether the vasoactive drugs used to manipulate blood pressure were also interacting with the smooth muscle of the aorta. Arterial stiffness was measured in 6 male Sprague Dawley rats (12 weeks old) by means of PWV. To determine whether SNP influenced aortic stiffness, SNP was first infused into the animal (30 µg/kg/min) to lower blood pressure. After the animals blood pressure returned to baseline, the inferior vena cava was occluded to reduce blood pressure by means of reducing venous return (Figure 0.).

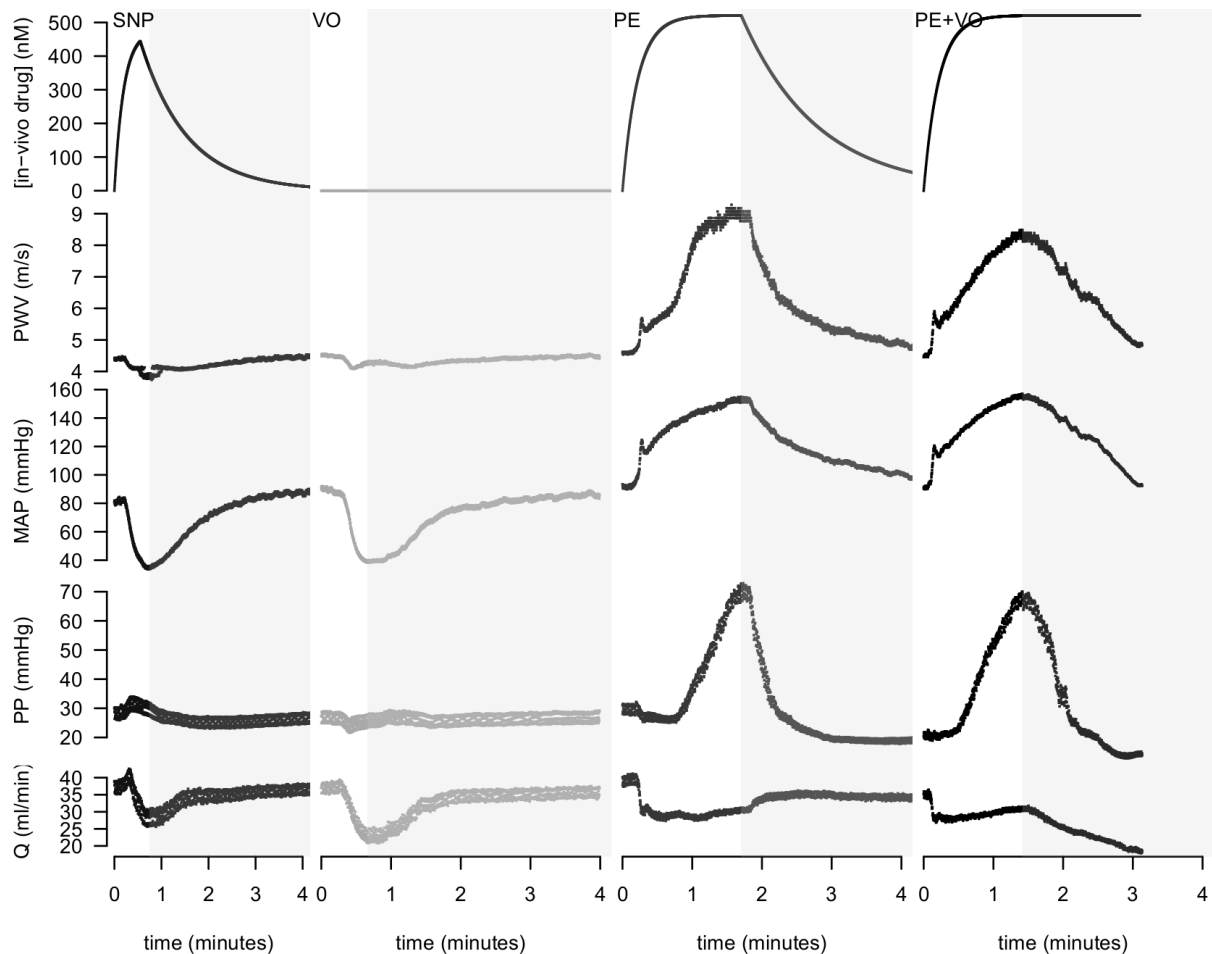


**Figure 0.4:** Example of the infusion of vasoactive drugs and the use of venous occlusion to reduce venous return for a passive reduction of arterial blood pressure. VO= venous occlusion, Q= blood flow (ml/min).

To determine the effects of PE on arterial tone, PE was first infused ( $30\mu\text{g/kg/min}$ ) to increase BP and then infusion was ceased to allow BP to return to baseline BP. PE was again infused ( $30\mu\text{g/kg/min}$ ), however BP was reduced via venous occlusion whilst PE was continuously being infused (Figure 0.). Both SNP and PE were compared against their alternative means of altering BP during the return to baseline component of pressure manipulation. As such, it was possible to compare whether the residual SNP that is being actively broken down as BP returns to baseline is having any effect on arterial stiffness. Similarly, it was also possible to compare whether a greater amount of PE in the arterial system is able to alter arterial stiffness compared to a smaller amount.

The results showed that there was no significant difference between the SNP and venous occlusion ( $p=0.24$ ) and a small but significant increase in PWV (3% increase) with PE and venous occlusion compared to PE alone at blood pressures around 100 mmHg ( $p<0.05$ ) (Figure 0.). It was at these blood pressures that the greatest difference in concentration of PE was present in the aorta of the two experimental conditions. These results show that very high concentrations of PE can interact with aortic smooth muscle to induce changes in arterial stiffness. A possible reason for the lack of effect of SNP on large vessels may be due to the kinetics of drug uptake by the aortic wall or the lower concentrations required to reach low blood pressures. Given the small and practically negligible drug interaction with arterial stiffness, these drugs were used throughout this thesis; they were necessary in both matching blood pressures between strains of rat and following experimental protocols which permanently altered blood pressure. Moreover, the concentrations used in all studies were significantly less than those used in this pilot study, hence the actual effect would be even less than the small effects noted in these pilot studies. However, these results were still considered in the discussions of the studies presented in this thesis.

## **1.11 Sympathetic blockade**

Hexamethonium is a nicotinic acetylcholine receptor antagonist that acts upon the sympathetic chain ganglia to reduce sympathetic nerve activity (Hunter, 1950). This drug does not interact with muscarinic acetylcholine receptors and thus does not affect parasympathetic activity. In the experiments presented in Chapters 5, 6 and 7, this drug is used to induce global sympathetic blockade allowing for comparisons of stiffness between intact and denervated arteries. Hexamethonium was injected at a concentration of 20 mg/kg. This concentration produced absolute blockade (as determined by the lack of change in SNA following PE challenge) for sustained periods of time (over 3 hours).

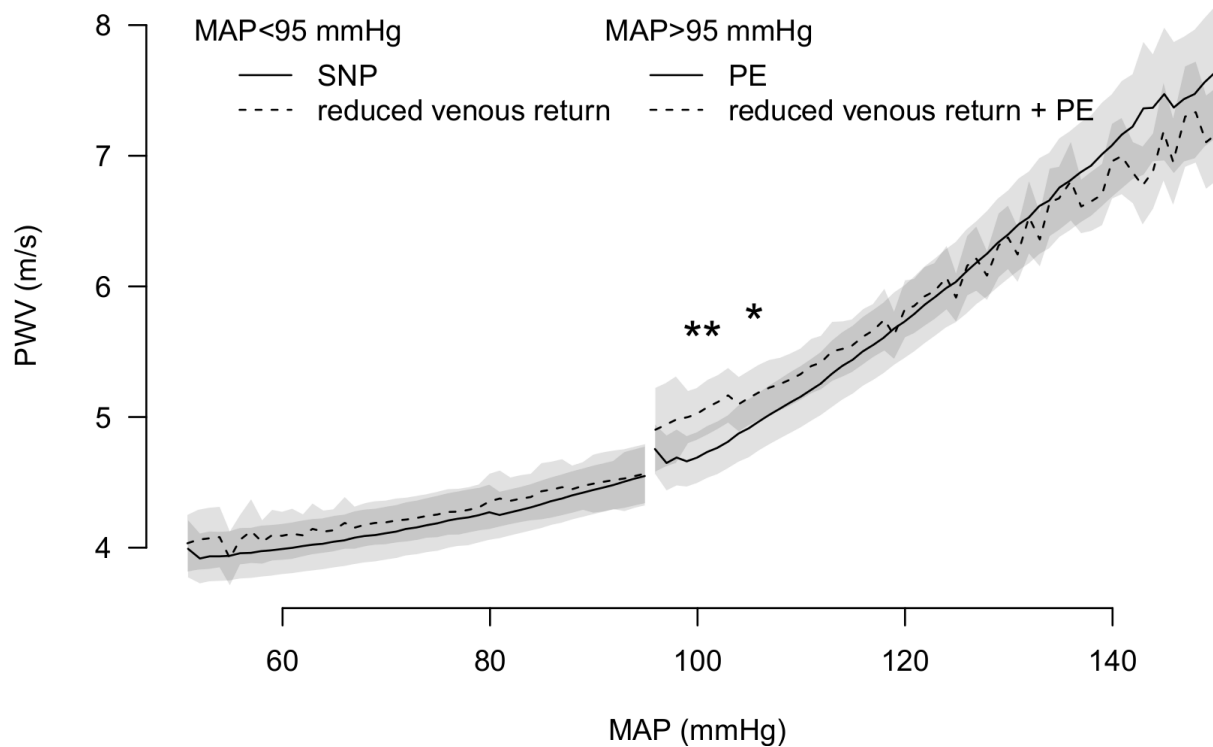


Figure 0.5: PWV differences between the use of SNP and venous occlusion (VO) also PE and PE with venous occlusion. Significant differences between the blood pressure altering methods were observed for PE infusion at MAP below 110 mmHg. Shaded area designates 95% confidence limits.

## 1.12 Post-processing and statistical analysis.

### 1.12.1 Stiffness measurements

The data acquired in these studies fell into two distinct types: continuous and discrete blood pressure. All values that did not require diameter measurements to be calculated (such as PWV) were continuous. However, since the ultrasound required complex acquisition and processing, distinct blood pressure values were chosen at which diameter based measurements would be recorded. This required two types of statistical analysis to be made.

### **1.12.2 Blood pressure measurements over a continuum**

Mean arterial blood pressure measurements were split into 5 mmHg bins ranging from 50-180 mmHg, the upper and lower limits depending on the strain of rat used in the given study. For example, a normotensive rat would achieve mean arterial blood pressures ranging from 160-50mmHg depending on the type of vasoactive agent used, whilst a hypertensive rat could reach mean arterial pressures of 180-75mmHg. The majority of these data were acquired by deconstruction of the pressure pulse such as deriving the second derivative of the pressure pulse to acquire the minima of the diastolic foot required to determine transit time and thereby PWV. These data were taken during the period of time following injection of the aforementioned vasoactive drugs and therefore represents a passive return to baseline values. For these data, pairwise comparison was used between the control and treatment condition at all the bins of blood pressure. These results were Bonferoni corrected for repeated measures across the entire range of blood pressures being assessed in a given analysis. This correction prevented the introduction of type 1 statistical errors into the analysis. Pairwise comparison was only used when the animals were acting as their own controls such as before and after the use of hexamethonium. Comparisons between strains were unpaired. Data are presented as mean  $\pm$  standard deviation when comparisons are made between strains (i.e. non-paired analysis) and mean  $\pm$  standard error when comparing differences when the animal was acting as their own control (i.e. pair-wise analysis).

### **1.12.3 Discrete blood pressure measurements**

Data that relied upon diameter recordings were either singular measurements at a discrete blood pressure, such as compliance or distensibility, or were based around the pressure-distension loops made when these two parameters were merged. Singular measurements were again compared via pairwise analysis with rat strains and unpaired between strains. However,



linear regression of the systolic upstroke was used to compare the pressure-distension curves of different aortic conditions (such as innervated and denervated). Distension values were first broken down into 5 mmHg bins and separated into their systolic and diastolic phase. To ensure the pressure-distension data could be statistically compared via linear regression, the data needed to be transformed from its native polynomial shape. This was done via a square-root transformation on all the pressure-distension curves. This involved calculating the square root of each distension value at each 5 mmHg bin. These pressure bins were again used to calculate the viscoelasticity of the aorta by means of measuring the AIC. Systolic distension values were subtracted from the diastolic distension values at each 5mmHg bin. These values were summed and multiplied by 5 mmHg to calculate the AIC.

### 1.13 Baroreceptor activity measurements

Baroreceptor sensitivity was compared between strains of rat by measuring the change in SNA as blood pressure was being changed. SNA was first rectified and averaged (time constant 1s). SNA was normalized by setting the level of SNA following hexamethonium to 0% and resting SNA at 100%. SNA and BP values were acquired immediately following injection of either SNP or PE, the so called active phase of induced blood pressure change. These data were then compiled to form a baroreceptor function curve with SNA placed on the Y axis and MAP on the X axis. Nonlinear regression analysis was used to fit a four parameter sigmoid logistic function curve to this curve (GraphPad Prism v5, as per Equation 3.7).

$$y = P1 + \left[ \frac{P2 - P1}{1 + 10^{\{P3-x\}P4}} \right] \quad \text{Equation 0.7}$$

Where  $y$  is SNA,  $x$  is MAP,  $P1$  is the bottom plateau,  $P2$  is the top plateau,  $P3$  is halfway between the top and bottom plateau and  $P4$  is the steepness of the curve. The first derivative of the logistic function curve was used to calculate maximal gain.

## **1.14 Power calculations**

Previous studies from our group have shown that the average PWV, at 100 mmHg is 4.0 m/s in normotensive rats with a standard deviation of 0.5 m/s. To detect a change in PWV equal to 0.5 m/s and achieve a significance with 95% confidence ( $p < 0.05$ ) at 80% power, a sample size of 8 was required for each of the strains of rat assessed throughout this thesis.

# **Effect of localised, unilateral sympathectomy on aortic stiffness in rats**

## **Summary**

To investigate the effect of sympathetic nerve activity on abdominal aortic wall mechanics, measures of aortic wall stiffness and compliance were evaluated before and following severing of the right splanchnic nerve that projects to the abdominal aorta in Wistar Kyoto rats (n=10). There was no difference in any of the measured haemodynamic parameters following the localised, unilateral sympathectomy at low, resting, or high physiological mean arterial pressures. However, a large variability between rats in response to the splanchnicectomy was observed. The results indicate that either there is insufficient smooth muscle response to sympathetic innervations to the abdominal aorta to effect a change in abdominal aortic wall mechanics, or, alternatively, that there is a compensatory sympathetic response to the splanchnicectomy, and that this response was received by the aorta via the intact left splanchnic nerve. These findings informed the development of further experiments to test these two possibilities. These experiments are presented in the subsequent chapters.

## **1.15 Introduction**

It is well established that sympathetic input to arteriolar smooth muscle is responsible for the maintenance of mean arterial blood pressure by controlling small vessel calibre and therefore peripheral resistance (Guyenet 2006). However, the extent to which sympathetic input regulates large artery smooth muscle cell tone is less well established. As in small arteries, sympathetic fibres project onto the smooth muscle cells in the wall of large arteries, albeit not as densely. These projections terminate at  $\alpha_1$ -adrenergic receptors and therefore have the potential to regulate smooth muscle tone (Kienecker & Knoche 1978b). It is the hypothesis of the present study that changes in the level of sympathetic activity will modify the tone of aortic smooth muscle, differentially loading the passive structural material components of the vessel (collagen and elastin), leading to changes in the capacitive and haemodynamic properties of the aorta. Such effects were assessed by unilateral sympathetic denervation at the level of the splanchnic nerve and subsequent measurement of arterial stiffness via pulse wave velocity (PWV) and arterial diameter based metrics of stiffness.

## **1.16 Methods**

### **1.16.1 Animals**

All male Wistar Kyoto (WKY) rats (n=10, 15 $\pm$ 4 weeks of age, 300 $\pm$ 50 g, Animal Resource Centre Perth) were anaesthetized and monitored as described in Chapter 3, Section 3.1.

## **1.16.2 Procedures**

### **Pressure measurement and manipulation**

All animals were instrumented and blood pressure was measured as stated in Chapter 3, Sections 3.3 and 3.4.

### **Diameter measurements**

Diameter measurements were made as described in Chapter 3, Section 3.2.

## **1.16.3 Splanchnicectomy**

Control (splanchnic nerve intact) measurements of diameter were made before surgical cut down of the nerve but after exposure of the splanchnic nerve. To expose the splanchnic nerve, a dorsal incision was made left of the midline and between the base of the ribs and the pelvis. Electrocautery was then used to remove the latissimus dorsi and expose the underlying nerves. The splanchnic nerve was dissected and sutures were placed around it. The left splanchnic nerve was then severed and diameter and pressure measurements were repeated at baseline, low and high blood pressures induced by sodium nitroprusside and phenylephrine infusion respectively.

## **1.17 Data and Statistical analysis:**

Arterial stiffness data were analysed as described in Chapter 3, Section 3.4.

## 1.18 Results

Following the cutting of the left splanchnic nerve innervating the abdominal aorta at baseline anaesthetised mean arterial pressures (MAP) ( $92\pm 5$  mmHg), there was a trend towards an increase in aortic compliance, however this was not statistically significant ( $p=0.059$ , Table 0.1). There were also no significant differences between any of the other arterial stiffness parameters measured at low (Table 4.3), baseline (Table 0.1) or high (Table 0.3) values of MAP. There were no significant differences in other haemodynamic parameters measured within any of the MAP's. This indicates that the lack of response seen following unilateral denervation is not due to a significant difference in factors such as distending pressure.

**Table 0.1:** Comparison of haemodynamic values at anaesthetized baseline blood pressure before and after unilateral splanchnicectomy. N=10, data are presented as mean  $\pm$  SEM

	Control	Unilateral splanchnicectomy	p-value
Systolic pressure (mmHg)	121 $\pm$ 6	121 $\pm$ 5	NS
Diastolic pressure (mmHg)	77 $\pm$ 6	78 $\pm$ 5	NS
MAP (mmHg)	92 $\pm$ 6	92 $\pm$ 5	NS
Systolic diameter ( $\mu$ m)	1448 $\pm$ 168	1496 $\pm$ 182	NS
Diastolic diameter ( $\mu$ m)	1236 $\pm$ 142	1259 $\pm$ 157	NS
Pulse pressure (mmHg)	44 $\pm$ 2	43 $\pm$ 2	NS
Diameter change ( $\mu$ m)	212 $\pm$ 32	237 $\pm$ 36	NS
Compliance (mm/mmHg)	4.93 $\pm$ 0.79	5.56 $\pm$ 0.80	NS
Distensibility ( $\times 10^{-3}$ mmHg $^{-1}$ )	3.95 $\pm$ 0.39	4.46 $\pm$ 0.39	NS
PWV (m/s)	2.95 $\pm$ 0.31	3.07 $\pm$ 0.34	NS

**Table 0.2:** Comparison of haemodynamic values at high blood pressure before and after unilateral splanchnicectomy. N=6, data are presented as mean  $\pm$  SEM

	<b>Control</b>	<b>Unilateral splanchnicectomy</b>	<b>p-value</b>
Systolic pressure (mmHg)	170 $\pm$ 4	168 $\pm$ 3	NS
Diastolic pressure (mmHg)	113 $\pm$ 1	109 $\pm$ 4	NS
MAP (mmHg)	132 $\pm$ 1	128 $\pm$ 3	NS
Systolic diameter ( $\mu$ m)	1945 $\pm$ 170	1919 $\pm$ 178	NS
Diastolic diameter ( $\mu$ m)	1746 $\pm$ 144	1724 $\pm$ 173	NS
Pulse pressure (mmHg)	57 $\pm$ 4	58 $\pm$ 4	NS
Diameter change ( $\mu$ m)	199 $\pm$ 30	195 $\pm$ 29	NS
Compliance (mm/mmHg)	3.51 $\pm$ 0.46	3.29 $\pm$ 0.40	NS
Distensibility ( $\times 10^{-3}$ mmHg $^{-1}$ )	1.97 $\pm$ 0.11	1.97 $\pm$ 0.27	NS
PWV (m/s)	3.64 $\pm$ 0.52	3.76 $\pm$ 0.49	NS

**Table 0.3:** Comparison of haemodynamic values at low blood pressure before and after unilateral splanchnicectomy. N=3, data are presented as mean  $\pm$  SEM

	<b>Control</b>	<b>Unilateral splanchnicectomy</b>	<b>p-value</b>
Systolic pressure (mmHg)	72 $\pm$ 7	66 $\pm$ 4	NS
Diastolic pressure (mmHg)	44 $\pm$ 5	44 $\pm$ 4	NS
MAP (mmHg)	54 $\pm$ 6	52 $\pm$ 4	NS
Systolic diameter ( $\mu$ m)	1537 $\pm$ 243	1522 $\pm$ 217	NS
Diastolic diameter ( $\mu$ m)	1374 $\pm$ 221	1286 $\pm$ 109	NS
Pulse pressure (mmHg)	27 $\pm$ 2	22 $\pm$ 1	NS
Diameter change ( $\mu$ m)	163 $\pm$ 24	236 $\pm$ 108	NS
Compliance (mm/mmHg)	5.91 $\pm$ 1.02	10.51 $\pm$ 4.50	NS
Distensibility ( $\times 10^{-3}$ mmHg $^{-1}$ )	4.14 $\pm$ 0.42	2.77 $\pm$ 0.56	NS
PWV (m/s)	2.26 $\pm$ 0.20	2.27 $\pm$ 0.26	NS

**Table 0.4:** Comparison of nerve intact haemodynamic values across a range of MAPs. \*indicates comparison between baseline and high blood pressure, † indicates comparison between low and baseline blood pressure, ‡ indicates comparison between low and high blood pressure. \*p<0.05, \*\*p<0.01, \*\*\*p<0.001. ‡p<0.05, ‡‡p<0.01, ‡‡‡p<0.001.

	Low blood pressure	Baseline blood pressure	High blood pressure
Systolic pressure (mmHg)	72±7†	121±6***	170± 4‡‡‡
Diastolic pressure (mmHg)	44±5	77±6***	113± 1‡‡‡
MAP (mmHg)	54±6†	92±6***	132± 1‡‡‡
Systolic diameter (µm)	1537±243	1448±168**	1945± 170
Diastolic diameter (µm)	1374±221††	1236±142**	1746± 144
Pulse pressure (mmHg)	27 ±2†	44±2**	57± 4‡‡
Diameter change (µm)	163±24	212±32	199± 30
Compliance (mm/mmHg)	5.91± 1.02	4.93±0.79*	3.51± 0.46‡
Distensibility (x10 <sup>-3</sup> mmHg <sup>-1</sup> )	4.14±0.42	3.95±0.39**	1.97± 0.11‡‡‡
PWV (m/s)	2.26± 0.20†	2.95±0.31*	3.64± 0.52

Expected significant differences in arterial stiffness were found between control anesthetized baseline blood pressure and high blood pressures, with reductions in compliance and distensibility (P<0.05 and P<0.01 respectively) and a significant increases in PWV (P<0.05) (Table 4.4). There was less difference between baseline anesthetized pressures and lower blood pressures, with only PWV being significantly reduced (P<0.05). As expected, there were significant differences in arterial stiffness between the low and high blood pressure ranges. Interestingly, there were only significant differences in arterial diameters between baseline and high blood pressures. All of these changes in stiffness were associated with significant changes in MAP.



## 1.19 Discussion

The magnitude of the role of sympathetic inputs to smooth muscle in the large arteries has remained largely unknown in terms of quantifiable effects. Previous studies have shown that chronic denervation can result in structural and functional changes in the aortic wall (Bevan & Tsuru 1981), whereas more recent studies have shown an association between sympathetic nerve activity and increases in aortic stiffness (Casey et al. 2011, Świerblewska et al. 2010). The present study sought to determine whether acutely removing sympathetic activity was sufficient to alter the haemodynamic properties of the aortic wall.

Practically, it was not possible to perform bilateral denervation, as this would not allow for an accurate and reproducible measurement of diameter, since it would involve movement and re-placement of the ultrasound probe. Furthermore, a previous study by (Gerova et al. 1973) showed that each side of the projecting sympathetic nerves contributes 50% towards aortic tone, therefore leaving sufficient scope for detection of effects using unilateral denervation.

Unilateral splanchnicectomy resulted in no significant difference in any measured parameter from the control, fully innervated state. These results suggest that there is insufficient sympathetic input into the abdominal aorta to produce any significant changes in aortic stiffness. Similar findings have been shown in studies that have measured aortic stiffness following sympathetic activation via exercise and lower body negative pressure (Lydakis et al. 2008, Sonesson et al. 1997). The proposed outcome of sympathetic denervation has also been studied using smooth muscle relaxants, and this study also showed no changes in aortic stiffness (Barra et al. 1993).

A possible reason for the lack of change in aortic stiffness is the relatively small amount of smooth muscle and/or sympathetic innervation in the aorta compared to resistance vessels. Indeed Kieneker and Knoche (1978) showed that whilst sympathetic innervation of the aorta is present, it is sparse. This means that there may be insufficient capacity for the sympathetic nervous system to activate smooth muscle to produce functional changes in aortic stiffness.

The lack of response to sympathectomy may also be in part due to the fact that only half of the sympathetic innervation was removed from the aorta. The abdominal aorta is supplied with sympathetic projections from both the left and right splanchnic nerve. In the present experiment the right splanchnic nerve was still intact, therefore allowing some tonic input to remain in the smooth muscle. Furthermore, cutting the left splanchnic nerve produced a transient reduction in blood pressure, most likely due to the removal of innervation to resistance vessels in the mesenteries, which are a downstream effector site from the same nerve that innervates the aorta. Following this reduction, blood pressure soon returned to baseline values (Figure 0.1). Such a rapid return to baseline would need to be generated by an increase in SNA leading to an increase in HR, venous return, cardiac contractility (as estimated by  $dP/dt(max)$ ) and peripheral resistance. Some evidence for this can be seen in Figure 4.1, as  $dP/dt(max)$  increases following the cutting of the nerve. An increase in peripheral resistance would need to be mediated by an increase in activity to the remaining right splanchnic nerve to the mesenteries. This right splanchnic nerve compensation may have also increased its tonic input into the abdominal aorta, resulting in no difference in aortic stiffness between the control and splanchnicectomy.

A bilateral sympathectomy, requiring surgical cut-down on both sides of the aorta, would have made it impossible to use ultrasound to record abdominal aortic diameters. Surgery to cut the nerve, would involve displacement of the ultrasound probe. It would not be possible

to replace the ultrasound probe in the exact position as the control measurement as there were no reference objects in the frame, other than the aorta itself. Therefore, quantitative measurement of the diameter before and after denervation could only be made if the ultrasound probe was not moved.

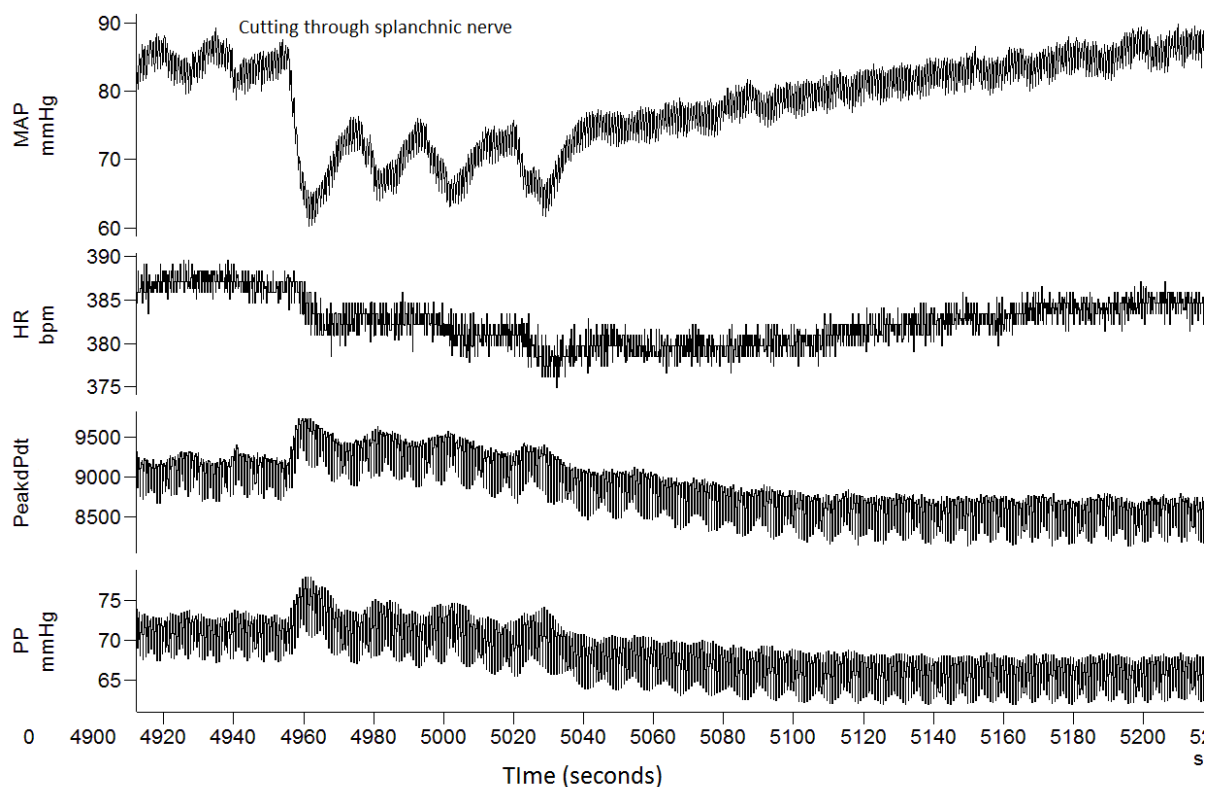


**Figure 0.1:** Cutting the left splanchnic nerve produced a significant drop in blood pressure and a slight increase in cardiac contractility (PeakDP/dt) and pulse pressure (PP). This effect was transient as blood pressure soon returned to baseline values, presumably due to increase peripheral vascular smooth muscle recruitment by the remaining splanchnic nerve during baroreflex induced sympathoexcitation.

One confounding factor was the degree of variability in the measured haemodynamic parameters following splanchnicectomy. In some animals, stiffness parameters were decreased and in others they were increased. This was not associated with any consistently changing haemodynamic parameter, such as blood pressure or diameter, which may account for this variability. Instead it is possible that the sympathetic denervation and subsequent drop in blood pressure may have triggered a cascade of autonomic changes akin to neurogenic shock (Dumont et al. 2001) accounting for this variation. Further confounding this analysis

were the disparate and small sample sizes used in some of the pressure ranges assessed in this study (ie N=3 in the low blood pressure range). As stated in section 3.8, a sample size of 8 was required to detect changes in PWV equal to 0.5m/s with a sigma of 0.5 and a power of 80%. It is entirely conceivable that with a greater sample size, the slight trends seen in, for example, compliance at low blood pressures may prove to be different.

Although there was a large degree of variability in the response to splanchnicectomy, the expected changes in stiffness parameters with changes in pressure were present and consistent. As MAP increased from baseline to a high blood pressure (average MAP increase of 38 mmHg) there was an associated reduction in compliance and distensibility with an increase in PWV. There was a lesser effect with blood pressure lowering of 39 mmHg from baseline MAP, with only PWV showing differences between blood pressures. This may have been due to an interaction of sodium nitroprusside (SNP) with the vessel wall causing vasodilation. Evidence for this is the increase in diastolic diameter at low blood pressures compared to baseline blood pressures. However, direct comparison between SNP lowering of blood pressure and vasodilator independent lowering of blood pressure demonstrated that SNP did not affect aortic PWV (Section 3.4.3)

Previous studies have shown that in the human brachial artery, the maximum increases in compliance and decrease in PWV achieved by complete vasodilation using nitroglycerine is 90% and 33% respectively (Bank, 1999; Laurent, 1992). The human brachial artery however contains relatively large amounts of smooth muscle (Humphrey & Na 2002) and is well supplied with sympathetic input compared to the aorta of small rodents (Kienecker & Knoche 1978a). The present study therefore illustrates the significant effects of arterial morphology on stiffness measurements and may be used as an example of the confounding effects when

making inferences about the effects of vasoactive substances on medium sized peripheral arteries to those of large central conduit arteries.

This is the first study to date that has measured the effect of splanchnicectomy on aortic PWV as a surrogate measure of arterial stiffness. The present study did not find changes in PWV. However, few studies have been able to detect changes in PWV in response to acute changes in physiological parameters that were independent of changes in blood pressure (Tan et al. 2012a, Vlachopoulos et al. 2006). Typically, significant and sustained changes in PWV are found with changes in the content of the aortic wall (O'Rourke & Hashimoto, 2007).

The limiting factor in this study was the incomplete removal of sympathetic tone from the abdominal aorta. As such, the experiments outlined in the following chapters employ the use of the sympathetic blocking drug, hexamethonium, ensuring removal of sympathetic activity. In addition, this method ensures that the ultrasound probe is not moved during the denervation process therefore it does not change the site of the aorta from which diameter is being measured during the control and denervation periods.

## **1.20 Conclusion**

The main finding of this study was that unilateral splanchnicectomy was not able to produce a significant change in abdominal aortic stiffness. After removing sympathetic input to the aorta via the left splanchnic nerve, there was no measurable change in arterial stiffness as assessed by compliance, distensibility or PWV. This lack of effect may be due to a number of factors: (i) insufficient smooth muscle response to evoke a local change in stiffness; (ii) a lack of the dense sympathetic innervations and activity in the abdominal aorta required to cause significant changes in smooth muscle tone; (iii) compensation of sympathetic activity

from the right splanchnic nerve following left splanchnicectomy, which increased smooth muscle tone in the absence of the left splanchnic nerve. However, given the low sample sizes in many of the pressure ranges assessed in this chapter, this must be taken as a very tentative finding and certainly one that may not hold if the sample sizes were increased. The remaining chapters in this thesis report on experiments designed to investigate the role of sympathetic activity of arterial stiffness by sympathetic inhibition and also to assess which of these three possible mechanisms is likely explanation for the findings of unilateral denervation.

# **Effects of acute, chemically induced sympathectomy on aortic stiffness in the Wistar Kyoto rat**

## **Summary**

Following the results reported in Chapter 4, a method of complete sympathetic blockade was used to eliminate any possible compensatory mechanisms as may have been observed in the experiments involving unilateral denervation (Chapter 4). Complete sympathetic blockade was induced in Wistar Kyoto rats (n=16) by an intravenous bolus of the nicotinic acetylcholine receptor antagonist, hexamethonium. Sympathetic activity and aortic pressure and diameter were measured before and following administration of hexamethonium across a range of physiological blood pressures. It was confirmed that hexamethonium administration caused a significant reduction in sympathetic activity from baseline levels and that this significantly decrease arterial stiffness as measured by pulse wave velocity, compliance, and distensibility. The magnitude of the effect was dependent on the level of mean arterial pressure, with the change in PWV with sympathetic blockade being greatest at lower mean arterial pressures. This is most likely due to the fact that sympathetic activity in the control condition (before sympathetic blockade) was much greater than at higher blood pressures, due to the baroreceptor feedback mechanism in response to blood pressure changes. Therefore, the relative magnitude of change in sympathetic nerve activity was greatest at lower pressures, and subsequently the largest changes in aortic stiffness parameters were observed within this pressure range. This study confirms the hypothesis that sympathetic nerve activity has a functional role in the regulation of smooth muscle tone and arterial stiffness in the abdominal aorta of rodents

## **1.21 Introduction**

Previously, unilateral splanchnicectomy (Chapter 4) was used to elucidate the effects of SNA on arterial stiffness. This produced no change in stiffness, which was postulated to be due to a compensatory response of the remaining sympathetic input into the aorta, or alternatively, due to a lack of either sympathetic innervations or smooth muscle control in the aorta to cause an acute change in stiffness. However, this lack of effect may have also been due to the small sample size used in the study.

The present study assesses the effect of acute chemical blockade of the sympathetic chain ganglia with hexamethonium and measuring the changes in arterial stiffness. Unlike the previous intervention (Chapter 4), hexamethonium completely removes sympathetically mediated tone in all vascular beds (see Chapter 3, Section 3.5). Such a technique demonstrates unequivocally how arterial stiffness changes in the presence and absence of sympathetic tone. These measurements are taken over a range of mean arterial pressures (MAP), to determine the pressure dependant effects of SNA on arterial stiffness. Furthermore, this study uses multiple means of determining arterial stiffness through the use of both blood pressure and aortic diameter recordings. These data will improve the determination of factors contributing to changes in arterial stiffness.

## **1.22 Methods**

### **1.22.1 Animals**

All male Wistar Kyoto rats (n=16, 15±5 weeks of age, 300±50 g, Animal Resource Centre Perth) were anaesthetized and monitored as described in Chapter 3, Section 3.1.



### **1.22.2 Procedures**

All animals were instrumented and blood pressure was measured as stated in Chapter 3, Sections 3.3 and 3.4.

Diameter measurements were made as described in Chapter 3, Section 3.2.

Sympathetic nerve recordings were made as described in Chapter 3, Section 3.3

### **1.22.3 Data and statistical analysis**

Arterial stiffness data were analysed as described in Chapter 3, Section 3.4. SNA was compared via pairwise t-test before and after hexamethonium. In addition, the percentage difference of SNA change following hexamethonium was compared between blood pressures with a Students t-test.

## **1.23 Results**

### **1.23.1 Cardiovascular parameters**

Aortic distension was significantly increased following sympathetic blockade as determined by linear regression. These increases in distension were present at MAPs of 75, 100 and 125 mmHg and decreased in magnitude as pressure increased ( $p < 0.001$  for all, Figure 5.1, Table 5.2). The same trend was seen in the compliance measurements, with significant increases seen at 75, 100 and 125 mmHg (Table 5.1).

**Table 0.1:** Effect of sympathectomy on a range of haemodynamic variables. Comparisons were made between control and denervated conditions at each discrete blood pressure using paired t-tests. Sympathectomy produced a significant reduction in heart rate at mean arterial pressures (MAP) ranging from 75-125 mmHg. Following denervation, a significant increase in distensibility and compliance occurred at 100 mmHg as did PP. Significant increases in systolic and diastolic diameter occurred at 100mmHg. Data is presented as Mean  $\pm$  SEM. Significance is represented as: \* $p < 0.05$ , \*\* $p < 0.01$ , \*\*\* $p < 0.001$ .

MAP	75 mmHg		100 mmHg		125 mmHg		150 mmHg	
	WKY	WKY	WKY	WKY	WKY	WKY	WKY	WKY
	Control	Denervated	Control	Denervated	Control	Denervated	Control	Denervated
Systolic (mmHg)	93 $\pm$ 1	96 $\pm$ 1	123 $\pm$ 1	125 $\pm$ 2	155 $\pm$ 3	153 $\pm$ 3	182 $\pm$ 2	182 $\pm$ 2
Diastolic (mmHg)	57 $\pm$ 1	55 $\pm$ 1	81 $\pm$ 1	79 $\pm$ 1	107 $\pm$ 2	105 $\pm$ 2	124 $\pm$ 2	121 $\pm$ 2
Systolic Diameter ( $\mu$ m)	1466 $\pm$ 74	1548 $\pm$ 83	1594 $\pm$ 99	1769 $\pm$ 91**	1934 $\pm$ 95	1937 $\pm$ 92	2059 $\pm$ 101	2045 $\pm$ 103
Diastolic Diameter ( $\mu$ m)	1291 $\pm$ 69	1303 $\pm$ 77	1399 $\pm$ 89	1514 $\pm$ 79*	1772 $\pm$ 87	1742 $\pm$ 87	1919 $\pm$ 100	1918 $\pm$ 103
$\Delta$ Diameter ( $\mu$ m)	174 $\pm$ 14	245 $\pm$ 22**	194 $\pm$ 18	255 $\pm$ 24*	154 $\pm$ 20	184 $\pm$ 20**	139 $\pm$ 26	127 $\pm$ 15
PP (mmHg)	36 $\pm$ 2	39 $\pm$ 2	40 $\pm$ 2	45 $\pm$ 2*	47 $\pm$ 2	48 $\pm$ 2	61 $\pm$ 3	62 $\pm$ 2
Heart rate (bpm)	404 $\pm$ 9	337 $\pm$ 11***	392 $\pm$ 6	342 $\pm$ 6***	365 $\pm$ 8	344 $\pm$ 6**	351 $\pm$ 11	348 $\pm$ 7
dP/dt(max) (mmHg/s)	4977 $\pm$ 489	4398 $\pm$ 446	4489 $\pm$ 362	4196 $\pm$ 289	3816 $\pm$ 314	3540 $\pm$ 317	3712 $\pm$ 373	3510 $\pm$ 223
Compliance (mm/mmHg)	4.70 $\pm$ 0.27	6.72 $\pm$ 0.93*	4.39 $\pm$ 0.36	5.32 $\pm$ 0.47**	3.30 $\pm$ 0.39	3.75 $\pm$ 0.40**	2.21 $\pm$ 0.37	2.08 $\pm$ 0.30
Distensibility ( $\times 10^{-3}$ (mmHg $^{-1}$ ))	3.74 $\pm$ 0.24	5.46 $\pm$ 1.00	3.20 $\pm$ 0.24	3.63 $\pm$ 0.22*	2.09 $\pm$ 0.23	2.32 $\pm$ 0.27	1.20 $\pm$ 0.21	1.11 $\pm$ 0.16
AIC (%.mmHg)	178 $\pm$ 25	204 $\pm$ 26	249 $\pm$ 28	277 $\pm$ 36	139 $\pm$ 22	166 $\pm$ 28	106 $\pm$ 22	111 $\pm$ 23

Aortic systolic and diastolic diameters were increased at 100 mmHg following sympathetic blockade ( $p<0.01$ ,  $p<0.05$  respectively, Table 5.1), whilst there was a significant increase in the difference between diameters at 75, 100 and 125 mmHg ( $p<0.01$ ,  $p<0.05$ ,  $p<0.01$  respectively). There was a high degree of variability of the response of diastolic diameter to denervation at 75 and 125 mmHg (75 mmHg:  $11\pm138$  mmHg; 125mmHg:  $-29\pm98$  mmHg).

There was a small but significant reduction in PWV at blood pressures ranging from 90-140 mmHg (90 mmHg: 3.9%,  $p<0.05$ ; 95 mmHg: 3.13%,  $p<0.001$ ; 100 mmHg: 2.8%,  $p<0.001$ ; 105 mmHg: 2.4%,  $p<0.05$ ; 110 mmHg: 2.9%,  $p<0.01$ ; 115 mmHg: 2.6%,  $p<0.01$ ; 120 mmHg: 2.3%,  $p<0.05$ ; 125 mmHg: 2.4%,  $p<0.05$ ; 130 mmHg: 2.6%,  $p<0.05$ ; 135mmHg: 2.7%,  $p<0.05$ ; 140 mmHg: 0.3%,  $p<0.05$ , Figure 0.1).

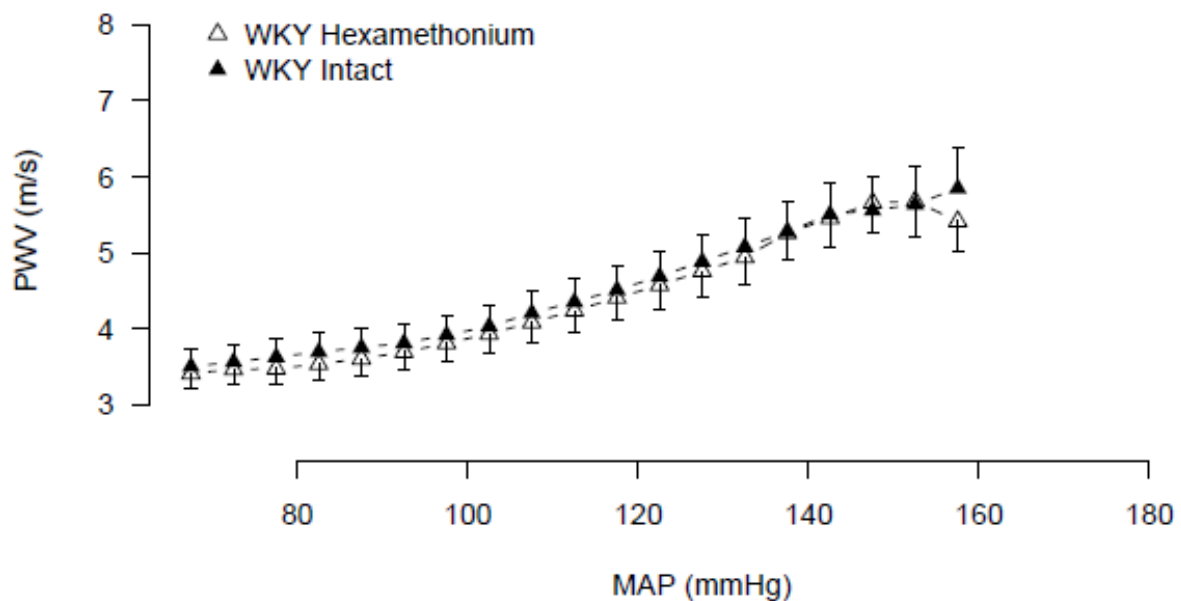


**Figure 0.1:** Pulse wave velocity values (PWV) showed small but significant reductions following denervation at MAP's ranging from 90 mmHg to 140 mmHg. Comparisons were made between control and hexamethonium at each blood pressure value following Bonferroni correction for repeated measures across the range of blood pressures. Values are presented as mean  $\pm$  SEM.

Distensibility was increased following hexamethonium injection only at the MAP of 100 mmHg. This was accompanied by a significant increase in PP ( $p<0.05$ , Figure 0.1), which, coupled with the decrease in PWV, would be expected to cause a reduction in distensibility. At 75 mmHg and 125 mmHg there was a high degree of variability of the response in distensibility to denervation (75 mmHg:  $1.7 \times 10^{-3} \pm 3.5 \times 10^{-3} \text{ mmHg}^{-1}$ ; 125 mmHg:  $2.4 \times 10^{-4} \pm 6.5 \times 10^{-4} \text{ mmHg}^{-1}$ ).

There was a significant reduction in heart rate at MAPs of 75, 100 and 125 mmHg following sympathetic denervation ( $p<0.0001$ ,  $p<0.0001$ ,  $p<0.01$  respectively) but not at 150 mmHg (Figure 0.2). This was not accompanied with a decrease in  $dP/dt(\text{max})$  at any MAP. There was also no significant difference in AIC at any MAP following denervation.

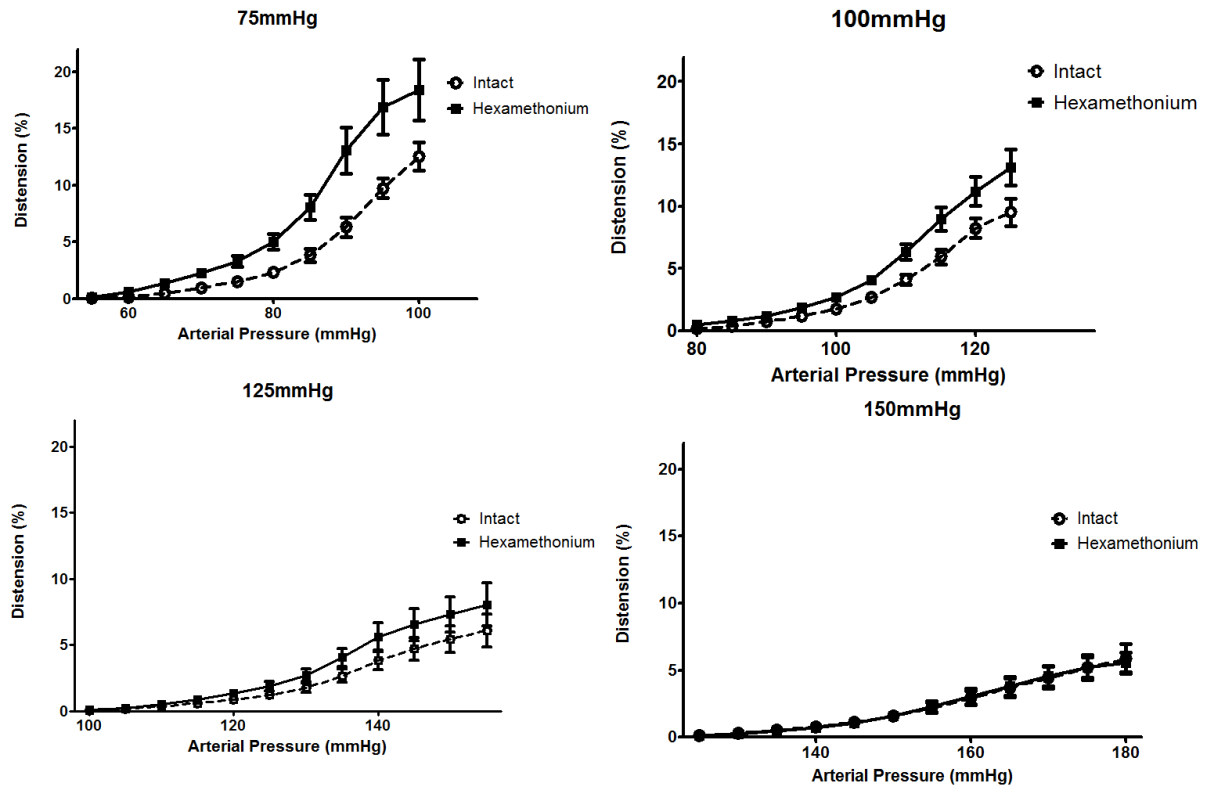


**Figure 0.2:** Effect of sympathetic denervation on distension at different mean arterial pressures (MAP). Comparisons were made between control and denervation using linear regression on the above curves transformed using a square root transform. As MAP increased, both distension and the difference between control and denervation decreases. Values of linear regression are shown in table 5.2.

**Table 5.2** Linear regression data taken from pressure-distension curves in figure 5.2. Statistical significance indicated with: \*\* $p < 0.01$ , \*\*\* $p < 0.001$ .

MAP (mmHg)	control		denervated	
	slope ( $\times 10^{-2} \%$ .mmHg)	intercept	slope ( $\times 10^{-2} \%$ .mmHg)	intercept
75	$7.7 \pm 0.4$	$-4.4 \pm 0.3$	$9.17 \pm 0.4^{**}$	$-4.9 \pm 0.4$
100	$6.5 \pm 0.2$	$-4.9 \pm 0.2$	$7.08 \pm 0.2$	$-5.3 \pm 0.3^{***}$
125	$4.6 \pm 0.2$	$-4.1 \pm 0.4$	$5.18 \pm 0.2$	$-4.6 \pm 0.4^{***}$
150	$4.2 \pm 0.2$	$-4.4 \pm 0.4$	$3.57 \pm 0.2$	$-4.5 \pm 0.4$

### 1.23.2 Sympathetic nerve activity

There was a significant reduction in SNA at all blood pressure levels following hexamethonium (75mmHg: intact:  $19.87 \pm 4.77 \mu\text{V}$ , denervation:  $9.9 \pm 1.80 \mu\text{V}$ ,  $p < 0.05$ ; 100mmHg: intact:  $21.45 \pm 3.36 \mu\text{V}$ , denervation:  $13.44 \pm 2.65 \mu\text{V}$ ,  $p < 0.001$ ; 125mmHg: intact:  $13.84 \pm 2.33 \mu\text{V}$ , denervation:  $10.52 \pm 1.38 \mu\text{V}$ ,  $p < 0.05$ ; 150mmHg: intact:  $11.85 \mu\text{V} \pm 1.71$ , denervation:  $10.82 \pm 1.61 \mu\text{V}$ ,  $p < 0.01$ ). There were also significant differences in SNA between blood pressures, with SNA at 100 mmHg being significantly higher than 125 mmHg (55%,  $p < 0.05$ ) and 150 mmHg (81%,  $p < 0.05$ ) (Figure 0.). An example comparison of the difference in SNA before and after hexamethonium can be seen in Figure 5.4.

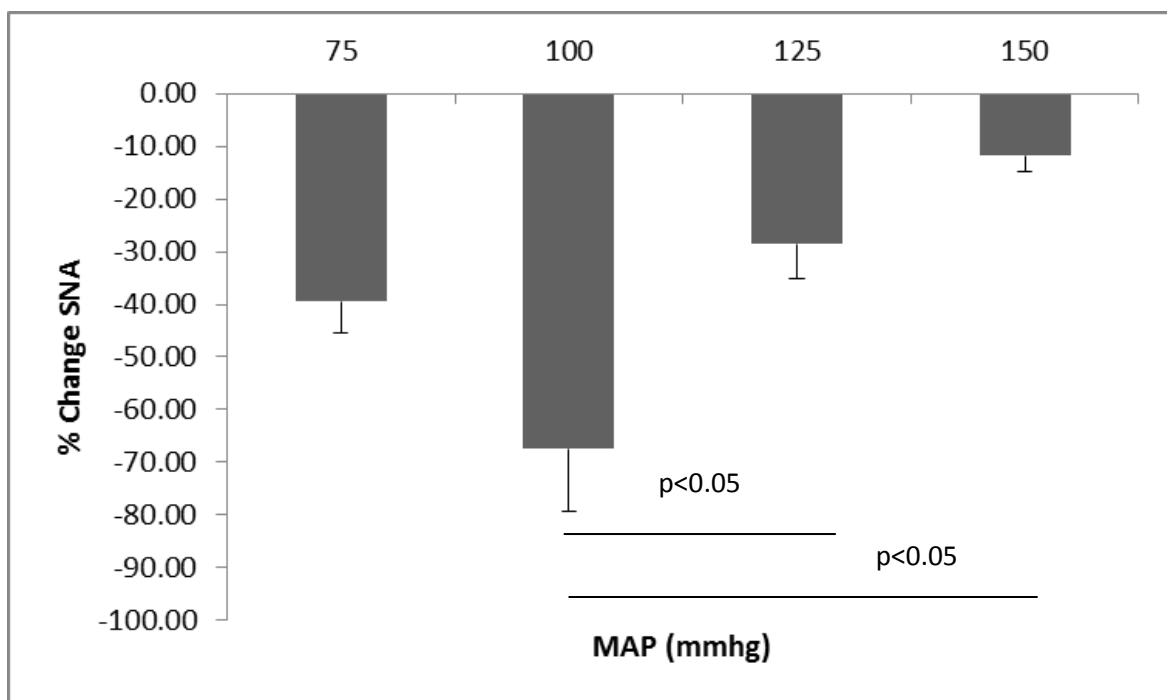


**Figure 0.3:** Change in sympathetic nerve activity (SNA) between control and denervated state at various mean arterial pressures (MAP). Maximal change in SNA occurred at 100 mmHg, and these values were significantly different between 125 mmHg and 150 mmHg. Statistical analysis were performed pairwise on the raw data of SNA between the control and denervated state.

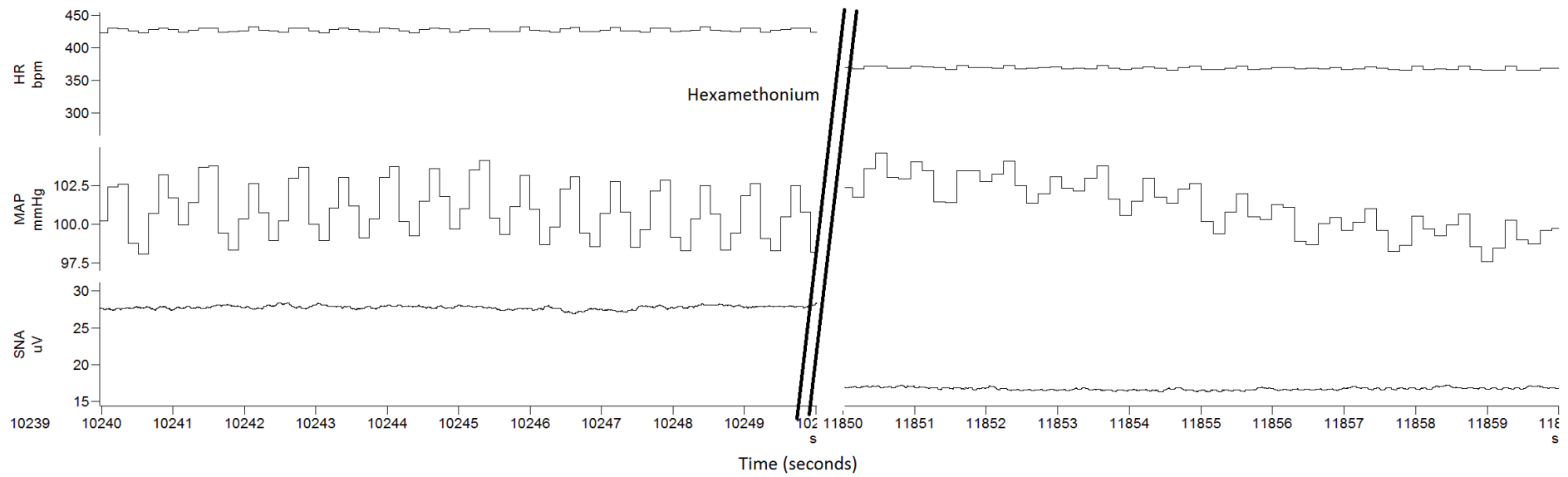


**Figure 5.4:** Comparison of SNA and HR following sympathetic denervation at matched MAP. MAP was matched using phenylephrine to compensate for the drop in MAP with hexamethonium. Hexamethonium produced a significant reduction in both heart rate and SNA.

## 1.24 Discussion

This study shows that sympathetic denervation is able to produce a significant decrease in aortic stiffness. This effect is most prominent at low blood pressures and decreases as blood pressure increases. These findings were confirmed using data derived from both PWV and measurements of aortic diameter and pressure. The lack of contribution from other associated viscoelastic factors such as AIC implies that these changes are solely due to changes in aortic smooth muscle tone.

The quantification of the effect of smooth muscle tone on arterial stiffness has long been a point of contention in vascular haemodynamics. Previous studies have shown that decreases in smooth muscle tone are able to produce a decrease (Bank et al. 1995), increase (Rovick & Dobrin 1969) or no change (Barra et al. 1993) in arterial stiffness. Possible reasons for these differences could be due to the investigators using different arteries for their experiments (human brachial, canine carotid ex-vivo and canine thoracic respectively), all of which have different arterial wall composition as well as performing their experiments at different blood pressure ranges. The present study has demonstrated that the blood pressure at which stiffness recordings are taken is important, mainly due to the nonlinear elastic properties of the arterial wall material (Danpinid et al. 2010)

The present study sought to quantify the effect of SNA on aortic stiffness across a range of mean blood pressures, using a variety of different stiffness measuring techniques. This study utilised a novel application of the echotracking device Art.Lab, which was able to detect and measure changes in aortic diameter simultaneously with changes in aortic pressure in rats. This enabled greater insight into the factors that contribute to the changes in arterial stiffness,



not simply determining if aortic stiffness had increased or decreased in response to denervation.

PWV was reduced in the MAP range of 90-140 mmHg following sympathetic denervation. This effect was diminished as MAP was increased. At 90 mmHg PWV was reduced by 3.9% whilst at 140 mmHg PWV was reduced by 0.3%. This change may reflect the pressure dependency of the arterial wall. As blood pressure is increased, a greater load is placed on the collagen within the arterial wall causing increased stiffness (Bank et al. 1996). Such increases in stiffness due to the passive elements in the arterial wall leaves little to no capacity for the smooth muscle to cause any changes in arterial stiffness.

Alternatively, the reduction of effect on PWV at higher pressures may also be due to the decreased difference in SNA between the control and denervated animal at high blood pressure. Increasing blood pressure via phenylephrine causes sympathoinhibition in the control state via the baroreceptor mechanism, reaching levels similar to that of the hexamethonium state. Conversely, animals treated with hexamethonium do not further reduce their SNA when given phenylephrine as SNA has been completely removed. Therefore, the SNA and subsequently the smooth muscle tone may be similar at high pressures between these two conditions thus accounting for the small difference in PWV. However, not all changes seen in PWV are attributable to SNA, since it was shown at 75mmHg that there was a smaller change in SNA, yet a greater increase in compliance and the pressure-distension curve. This may indicate that at low MAP's aortic smooth muscle only requires small modifications in tone to be able to alter the interaction between elastin and collagen to produce changes in arterial stiffness.

Distensibility was only significantly increased at 100 mmHg following denervation. At this pressure there was also a significant increase in PP and a significant increase in diastolic diameter. These changes are in apparent contradiction to each other, as an increase in PP, coupled with a decrease in PWV and increase in diastolic diameter, would cause a reduction in distensibility. The conclusion, therefore, is that at a MAP of 100 mmHg, the differences between the systolic and diastolic diameter following hexamethonium were so significant that they compensated for the increase in PP to produce an increase in distensibility. Indeed, whilst significant differences were also seen between systolic and diastolic diameter following denervation at 75 and 125 mmHg MAP, it was only at 100 mmHg that there was a significant increase in systolic diameter, thus highlighting this MAP as particularly sensitive to changes in arterial tone. There were no significant differences in systolic or diastolic blood pressure at any of the defined MAP's meaning that all the changes seen are purely a function of change in the arterial wall and not due to extraneous effects of different distending pressures between control and sympathetic denervation.

Consistent with the increases in the differences between systolic and diastolic diameters at the MAP of 75, 100 and 125 mmHg were also increases in compliance. These results align well with the changes seen in PWV, since both are metrics of wall stiffness, with compliance being a parameter of stress and strain, and PWV being derived from the differences in wave speed in materials of different stiffness. One reason why these increases in compliance did not translate to an increase in distensibility, despite the lack of change in diastolic diameter and PP at 75 and 125mmHg, is the degree of variability in response in diastolic diameter to sympathetic denervation. There was no consistent directionality of response in diastolic diameter at these MAP's and since the diastolic diameter is an input to distensibility, a high variability also occurred in this metric.

Pressure-distension curves were generated to investigate whether a difference in aortic stiffness could be identified throughout the cardiac cycle using data derived from ultrasound measurement of vessel diameter. To compensate for differences in diastolic diameters between animals, all the diameter data were first normalized into a measurement of distension, which measured change in diameter as a percentage difference from the resting diastolic diameter. Distension values were then taken during the period of systolic pressure increase and plotted against pressure. The magnitude of the slope of the resultant line was equivalent to compliance, the inverse of stiffness. Similarly, changes in the y intercept between treatments were also considered increases in compliance, only they did not have a common origin of pressure.

Significant increases in the pressure-distension curves occurred at 75, 100 and 125 mmHg, consistent with changes seen in PWV and compliance. These data also demonstrate the pressure-dependent nature of arterial stiffness measurements. The greatest increases in pressure-distension following denervation were observed at 75 and 100 mmHg, whereas the peak distension begins to converge at 125 and 150mmHg between the control and denervated condition. A potential confounding factor for distension measurements was an interaction with  $dP/dt(max)$ .  $dP/dt(max)$  can be seen as an approximation for an index of cardiac contractility in the absence of left ventricular pressure measurements. Cardiac contractility has previously been shown to be associated with arterial stiffness (Palmieri et al. 2004). However, a mechanism was not proposed. If there is a significant change in cardiac contractility, the rate at which the arterial wall is loaded differs, that is, there is a change in the dynamic loading of the wall components throughout the cardiac cycle, particularly in the early phase. If the vessel is loaded quickly, the collagen within the artery wall is recruited making the vessel stiff, if the vessel is loaded slowly the elastic fibres are recruited first

making the vessel less stiff. In the present study, there was no significant change in  $dP/dt(\max)$  following sympathetic denervation, though there was a downward trend in  $dP/dt(\max)$ . It is not known if an improved measurement of cardiac contractility (eg left ventricular pressure measurement) may have given a significant result, although the defining parameter for dynamic wall loading would still be  $dP/dt(\max)$ . Also correlated to changes in  $dP/dt(\max)$  is heart rate which was also significantly reduced in this study. Whilst the contribution of heart rate to changes in stiffness was not included in this analysis, it was completed in chapter 7 of this thesis.

There was also no significant difference in AIC at any level of blood pressure. AIC is a metric for viscoelasticity of the vessel wall (Vayssettes-Courchay et al. 2011a). If there is a large difference between the distension of systole and that of diastole, AIC will be increased. This may occur due to changes in smooth muscle tone, however there is a strong influence of both heart rate and  $dP/dt(\max)$  on this parameter. Heart rate influences the time of diastole, with shorter heart rates allowing more time during diastole, which then allows the distension during diastole to remain increased for a longer period of time, thus resulting in an increased AIC. Increased  $dP/dt(\max)$  increases AIC for the aforementioned reason, namely reducing distension during systole. Therefore, a potential reason why no change is observed in AIC is that the increased distension during systole (causing a reduction in AIC) following sympathetic denervation is countered by the decreased heart rate effect, which maintains a higher distension throughout diastole.

## **1.25 Conclusion**

These data show that there is a small but significant effect of sympathetic driven smooth muscle tone on aortic stiffness. Removing sympathetic tone produces a decrease in aortic

stiffness that can be measured both by PWV and by arterial stiffness parameters derived from pressure and diameter measurements. These differences are more apparent at lower pressures, and this is most likely linked to the natural withdrawal of SNA at high pressures through the baroreceptor mechanism. Sympathetic blockade significantly increased abdominal aortic distension and this effect was also greatest at lower pressures.

This study is the first to investigate and confirm the role of SNA in the regulation of smooth muscle in the abdominal aorta of normotensive rats and its role in the determination of pressure-dependent arterial stiffness. The findings demonstrate that this SNA input has a functional role as quantified by aortic stiffness parameters.

# **Effect of sympathetic blockade on arterial stiffness and viscoelasticity in a rodent model of hypertension**

## **Summary**

Sympathetic nerve activity (SNA) has a functional role in the regulation of abdominal aortic wall mechanics in the normotensive rat (Chapter 5). Hypertension is often associated with increased SNA, and therefore the magnitude of the effect of basal SNA on aortic wall mechanics is hypothesised to be greater in hypertension. The experiments presented in this chapter investigate aortic wall mechanics in the Spontaneously Hypertensive Rat (SHR, n=27) and compares these findings to the normotensive control strain, the Wistar Kyoto rat (WKY, n=16). In both strains, abdominal aortic pressure and diameter were measured before and following sympathetic blockade by administration of hexamethonium. Systemic sympathetic blockade decreased abdominal aortic stiffness as measured by PWV in both WKY and SHR at mean arterial pressures lower than 150 mmHg. The response in compliance was more variable, with increases in compliance in WKY rats and decreases in compliance at some mean pressures for the SHR. There were no changes in parameters of viscoelasticity, although changes in the pressure-distension curves were observed. These results show that removing SNA is able to reduce aortic stiffness at normal blood pressures, but has no effect at high blood pressures.

## 1.26 Introduction

Chapter 5 showed that the removal of SNA in a normotensive rodent model resulted in a significant reduction in arterial stiffness between a MAP of 90 and 140mmHg. Increased SNA is a major contributor to the development of acute hypertension due to the associated increase vasoconstriction in peripheral arterioles (Esler 2000) and chronic (resistant) hypertension through interaction with renal function (Krum et al. 2009, Osborn et al. 1997). Such increases in hypertension lead to a degeneration of the capacitive function of the aorta, as the sustained and increased distending forces cause elastin in the arterial wall to fray and lose its function, due to possible effect of mechanical fatigue (O'Rourke & Hashimoto 2007). The increase in arterial stiffness in turn increases hypertension by increasing the speed of wave reflection, thus augmenting the arterial pressure pulse as well as by increasing the external load on the heart as a pump (O'Rourke & Hashimoto 2007). Increased arterial stiffness with age further causes increased hypertension via blunting the baroreceptor sensitivity in the carotid arteries, thereby leading to higher basal SNA (Ng et al. 1993, Okada et al. 2011).

A rodent model known for its increased SNA is the spontaneously hypertensive rat (SHR). SHR develop increased blood pressure and SNA as they age (Judy & Farrell 1979) and increases in SNA have been shown to be associated with increased PWV (Cosson et al. 2007). The Cosson study, estimated SNA using heart rate variability and associated this with PWV. The studies presented in this thesis measure SNA from the splanchnic nerve and thus provide a more robust association between PWV and SNA. This present study also quantifies the real contribution of SNA to abdominal aortic PWV by measuring aortic stiffness before and following complete removal of SNA by sympathetic blockade. Given that the previous chapter showed that removal of sympathetic tone reduced arterial stiffness (in normotensive

rats), it is hypothesized that the increases in aortic stiffness seen in the SHR are due, in part, to a causal relationship with increased sympathetic tone that develops in the SHR with age. The present study utilizes sympathetic blockade to assess the contribution of SNA to arterial stiffness at pressure matched blood pressures in both normotensive (data from the Chapter 5) and hypertensive rats. This study utilises multi-modal means of arterial stiffness assessment, using data derived from pressure signals (PWV) and diameter data (pressure-distension, distensibility, compliance and viscoelasticity) to quantify the factors contributing to arterial stiffness.

## **1.27 Methods**

### **1.27.1 Animals**

Male Wistar Kyoto (WKY) rats (n=16 aged 15±5 weeks) and SHR's (n=27 aged 15±5 weeks) (Animal Resource Centre, Perth, Australia) were anaesthetized and monitored as described in Chapter 3, Section 3.1.

### **1.27.2 Procedures**

All animals were instrumented and blood pressure was measured as described in Chapter 3, Sections 3.3 and 3.4. Diameter measurements were made as described in Chapter 3, Section 3.2. Sympathetic nerve recordings were made as described in Chapter 3, Section 3.3

### **1.27.3 Data and statistical analysis**

Arterial stiffness data were analysed as per section 3.4.

In addition, both strains were compared at their resting anaesthetized blood pressure at each age group. Comparisons were made using unpaired Students t-tests. Further, the ratio of area



difference under the ascending pressure-distension curve before and after sympathetic denervation was compared both between pressure ranges and between strains. These comparisons were made using unpaired Students t-tests. Results are presented as mean±standard deviation, unless otherwise stated.

Although animals were studied across a small age range ( $15\pm 5$  weeks), all analysis is presented as an average across that age range (10 to 20 weeks). (For a breakdown of the age effect within this age range, see Appendix A).

## **1.28 Results**

### **1.28.1 Haemodynamic comparisons in strain at resting anaesthetized blood pressure**

Resting anaesthetized MAP was greater in the SHR compared to the WKY (SHR:  $136\pm 16$  mmHg vs WKY:  $97\pm 13$  mmHg,  $p<0.001$ , Table 6.1). Systolic pressure was also higher in SHR (SHR:  $166\pm 18$  mmHg vs WKY:  $117\pm 17$  mmHg,  $p<0.001$ , Table 6.1) as was diastolic pressure (SHR:  $112\pm 15$  mmHg vs WKY:  $79\pm 14$  mmHg,  $p<0.001$ , Table 6.1) and pulse pressure (SHR:  $53\pm 7$  mmHg vs WKY:  $38\pm 8$  mmHg,  $p<0.001$ , Table 6.1). Increase in blood pressure was accompanied by an increase in PWV (SHR:  $7.03\pm 1.98$  m/s vs WKY:  $4.49\pm 1.04$  m/s,  $p<0.001$ , Table 6.1). There was no difference in heart rate or  $dP/dt(\max)$  between strains.

**Table 0.1:** Baseline haemodynamic values for both SHR and WKY. Comparisons were made between SHR and WKY for each parameter. Significant differences between WKY and SHR are indicated with \* $p<0.05$ , \*\* $p<0.01$ , \*\*\* $p<0.001$ .

	WKY	SHR
MAP (mmHg)	97±14	136±16***
HR (BPM)	405±25	401±23
Systolic Pressure (mmHg)	117±17	166±18***
Diastolic Pressure (mmHg)	79±14	112±15***
Pulse Pressure (mmHg)	38±8	53±7***
Systolic Diameter (µm)	1594±410	1695±309
Diastolic Diameter (µm)	1400±368	1561±276
dP/dt(max) (mmHg/s)	4409±1719	4167±1171
PWV (m/s)	4.49±1.04	7.03±1.98***

### 1.28.2 Pressure matched differences in haemodynamic parameters between WKY and SHR

#### MAP of 75 mmHg

At a MAP of 75 mmHg, heart rate was decreased within both strains following denervation, but there were no differences between strains (WKY control: 400±27 bpm; WKY denervated: 337±38 bpm,  $p<0.001$ , SHR control: 387±27 bpm; SHR denervated: 338±25 bpm,  $p<0.001$ , Table 6.2 and Table 6.3). The dP/dt(max) was higher in the control WKY compared to that of the control SHR (WKY: 5215±1402 mmHg/s; SHR: 3693±1503 mmHg/s,  $p<0.05$ ). There was no significant change in PWV between the control WKY and denervated WKY (WKY control: 3.56±0.23 m/s; WKY denervated: 3.46±0.21 m/s, Figure 0.4) nor difference between the control SHR and denervated SHR (SHR control: 3.88±0.75 m/s; SHR denervated: 3.95±0.79 m/s, Figure 0.5) and no difference between strains (Figure 0.3). However, there was a reduction in compliance in the SHR following denervation (SHR control: 5.07±2.00

mm/mmHg, SHR denervated:  $4.36 \pm 1.76$  mm/mmHg,  $p < 0.05$ ) There was a significant difference in pressure-distension (as determined by y-intercept) between the control WKY and SHR ( $p < 0.01$ ) (Figure 0.1, Table 0.4) as well as a significant difference in pressure-distension following denervation in both strains of rat (WKY:  $p < 0.01$ ; SHR:  $p < 0.001$ ). This was associated with an increase in compliance in the WKY following hexamethonium compared to the SHR following hexamethonium (WKY denervated:  $5.94 \pm 2.32$  mm/mmHg; SHR denervated:  $4.36 \pm 1.76$  mm/mmHg,  $p < 0.05$ , Table 6.2 and Table 6.3) There was no difference in AIC between strains (WKY control:  $178 \pm 79$  % .mmHg; SHR control:  $117 \pm 73$  % .mmHg) or within strains (WKY hex:  $204 \pm 83$  % .mmHg; SHR hex:  $151 \pm 115$  % .mmHg). There was also no significant difference between the ratio of area difference between the control ascending pressure-distension curve and the denervated ascending pressure-distension curve between strains (Figure 0.2).

**Table 0.2:** Haemodynamic values at all pressure ranges for control (intact) vessels. Haemodynamic comparisons were made between strains at each discrete MAP. For comparison to the sympathetic blockade state (Table 6.3) \*p<0.05, \*\*p<0.01, \*\*\*p<0.001. For comparison between strains †p<0.05, ††p<0.01, †††p<0.001. Data presented as Mean ± SD

	75mmHg		100mmHg		125mmHg		150mmHg	
	WKY	SHR	WKY	SHR	WKY	SHR	WKY	SHR
<b>Intact</b>								
Systolic (mmHg)	93±4	92±7**	123±6	123±6	154±12	157±8	182±6	180±9
Diastolic (mmHg)	56±1	58±5	80±4	82±5*	106±8	104±4	123±6	125±8
Systolic Diameter (µm)	1444±76	1449±47*	1584±82**	1414±84	1954±97††	1329±136††	2027±99†	1692±64†
Diastolic Diameter (µm)	1267±69	1270±42**	1377±71*	1263±73	1761±82††	1205±120††	1885±95†	1559±61†
Δ Diameter (µm)	177±21**	179±13	193±20*	142±21	162±19**	122±27**	143±19	133±12
PP (mmHg)	36±7	36±6***	41±9*	41±7***	48±8	55±9*	63±9	57±6*
Heart rate (bpm)	400±27***	387±27***	394±23***	373±32***	366±34	386±20**	351±41	383±35***
dP/dt(max) (mmHg/s)	5215±1402†	3693±1503†	4483±1239†	3285±952*†	3995±1055	4539±2137	3918±1170	3910±896
Compliance (mm/mmHg)	4.58±1.16	5.07±2.00*	4.29±1.55**	3.32±1.21*	3.29±1.70**	2.20±0.46	1.25±0.77	1.50±0.47
Distensibility (x10 <sup>-3</sup> /mmHg)	3.80±0.91	3.89±1.19	3.20±1.03*	2.62±0.91	2.01±0.93	1.80±0.33	3.80±0.91	3.89±1.19
PWV (m/s)	3.56±1.00	3.88±0.75	3.92±1.11*	4.48±0.85*	4.69±1.49*	5.11±0.94	5.56±1.93	5.84±1.11
AIC (%.mmHg)	178±79	117±72	250±113	120±106	139±89	142±148	106±78	107±73

**Table 0.3:** Haemodynamic values at all pressure ranges for denervated vessels. Haemodynamic comparisons were made between treatments at each discrete MAP. For comparison during sympathetic blockade (Table 6.2) \*p<0.05, \*\*p<0.01, \*\*\*p<0.001. For comparison between strains †p<0.05, ††p<0.01, †††p<0.001. Data presented as Mean ± SD

	75mmHg		100mmHg		125mmHg		150mmHg	
	WKY	SHR	WKY	SHR	WKY	SHR	WKY	SHR
<b>Denervated</b>								
Systolic (mmHg)	96±4	98±6**	126±6	129±6	153±12	157±8	181±5	180±9
Diastolic (mmHg)	55±2	56±6	78±5	77±6*	104±9	98±3	120±5	122±6
Systolic Diameter (µm)	1558±76	1404±47*	1744±82**†	1396±84†	1918±97††	1396±136††	2018±99†	1706±64†
Diastolic Diameter (µm)	1301±69	1210±42**	1498±71*	1237±73	1730±82††	1248±125††	1891±95†	1567±61†
Δ Diameter (µm)	258±21**	194±13	254±20*	152±21	196±19**	148±27**	128±19	139±12
PP (mmHg)	39±8	45±10***	45±8*	54±9***	49±6†††	65±5*†††	61±7	59±7*
Heart rate (bpm)	337±38***	338±25***	342±23***	323±31***	344±26	332±7**	346±27	337±32***
dP/dt(max) (mmHg/s)	4507±1436	3435±1433	4266±1159	3948±1042*	3670±1145	5010±1017	3561±818	3576±615
Compliance (mm/mmHg)	5.94±2.32†	4.36±1.76*†	5.29±2.06**†††	2.76±0.96*†††	3.74±1.77**	2.25±0.66	2.07±1.17	2.53±1.02
Distensibility (x10 <sup>-3</sup> /mmHg)	4.61±2.03	3.53±1.17	3.64±0.9*1†††	2.22±0.68†††	2.34±1.14	1.82±0.53	1.14±0.57	1.48±0.33
PWV (m/s)	3.46±0.90	3.95±0.79	3.81±1.07*	4.43±0.86*	4.57±1.38*	5.14±0.94	5.66±1.74	5.98±1.08
AIC (%.mmHg)	204±83	151±114	277±142	136±86	166±112	144±103	111±82	70±66

**Table 0.4:** Comparisons of pressure-distension data. Linear regression was used on the square root transformed pressure-distension curves (Figure 0.1). Comparisons were made both between strains and following sympathetic blockade at each discrete MAP. For comparison between control and sympathetic blockade \*p<0.05, \*\*p<0.01, \*\*\*p<0.001. For comparison between strains †p<0.05, ††p<0.01, †††p<0.001. Data presented as Mean ± SD

MAP (mmHg)	WKY				SHR			
	control		denervated		control		denervated	
	slope (x 10 <sup>-2</sup> %.mmHg)	intercept (x 10 <sup>-2</sup> %.mmHg)	slope (x 10 <sup>-2</sup> %.mmHg)	intercept (x 10 <sup>-2</sup> %.mmHg)	slope (x 10 <sup>-2</sup> %.mmHg)	intercept (x 10 <sup>-2</sup> %.mmHg)	slope (x 10 <sup>-2</sup> %.mmHg)	intercept (x 10 <sup>-2</sup> %.mmHg)
75	7.7±0.4	22.5±9.1	9.17±0.4 **	35.9±9.2	7.69±0.3	45.7±5.7 †††	6.8±0.2	43.7±0.5
100	6.5±0.2	22.2±6.0	7.08±0.2	34.4±6.5***	6.1±0.3	41.4±7.1	5.6±0.2	35.8±0.6 *
125	4.6±0.2	25.3±6.2	5.18±0.2	29.3±7.4***	4.3±0.3	39.6±1.0	4.6±0.1	35.8±0.6
150	4.2±0.2	29.2±7.0	3.57±0.2 *	29.0±6.7	4.1±0.1	32.8±4.1	4.2±0.1	46.4±0.3. ***

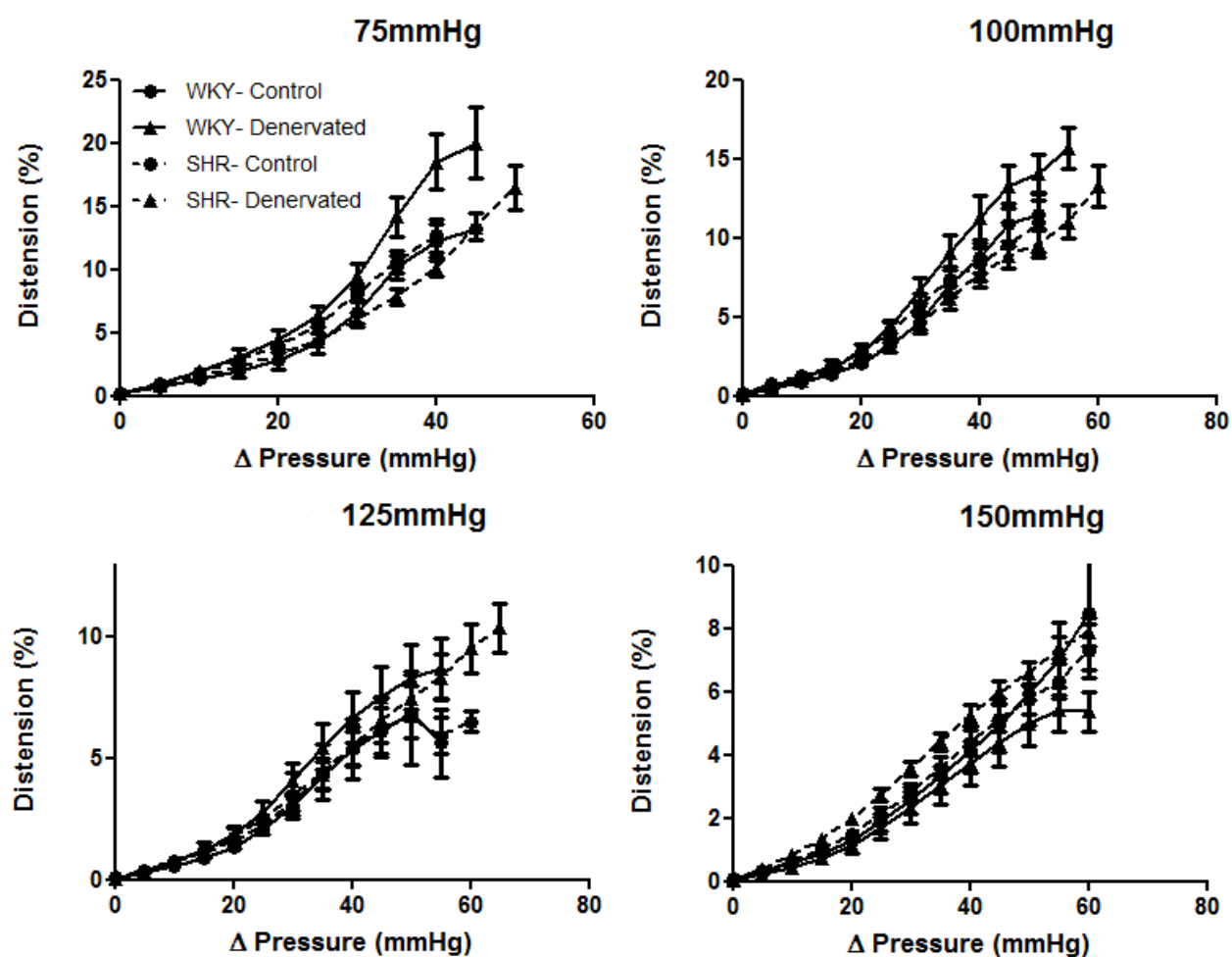


**Figure 0.1:** Aortic pressure-distension curves for WKY and SHR before and during sympathetic blockade across a range of MAP's. Data presented as Mean  $\pm$  SD. Accompanying statistics and comparisons are in Table 0.4.

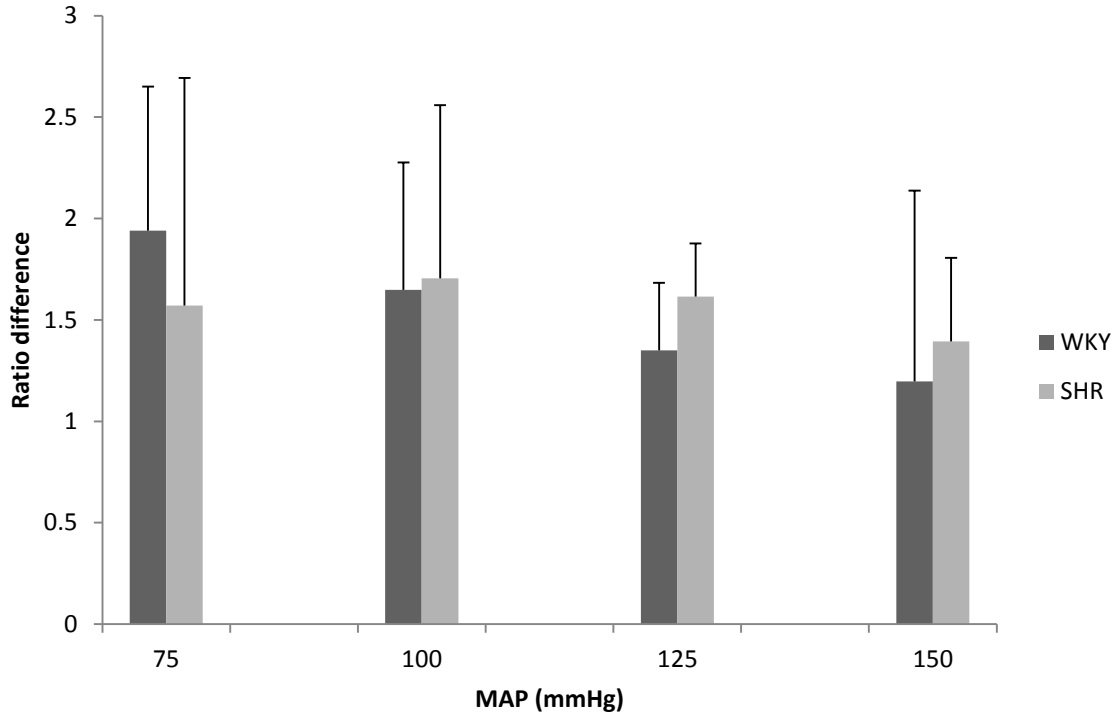


**Figure 0.2:** Ratio of difference between the area under the systolic pressure-distension curve before and during sympathetic blockade. Comparisons were made between strain at each discrete MAP. No significant difference was observed between the strains at any MAP.

### MAP of 100 mmHg

At a MAP of 100 mmHg, the heart rate was again decreased within both strains with denervation, but there was no difference between strains (WKY control:  $394 \pm 23$  bpm; WKY denervated:  $342 \pm 23$  bpm,  $p < 0.001$ , SHR control:  $373 \pm 32$  bpm; SHR denervated:  $323 \pm 31$  bpm,  $p < 0.001$ , Table 6.2 and Table 6.3). The  $dP/dt(\max)$  was higher in the control WKY compared to that of the control SHR (WKY:  $4483 \pm 1239$  mmHg/s; SHR:  $3285 \pm 952$  mmHg/s;  $P < 0.05$ ). Distensibility was greater in the denervated WKY compared to the denervated SHR (WKY denervated:  $3.64 \times 10^{-3} \pm 0.91 \times 10^{-3}$  mmHg $^{-1}$ ; SHR denervated:  $2.22 \times 10^{-3} \pm 0.68 \times 10^{-3}$  mmHg $^{-1}$ ;  $p < 0.01$ ) as was compliance (WKY denervated:  $5.29 \pm 2.06$  mm/mmHg; SHR denervated:  $2.76 \pm 0.96$  mm/mmHg;  $p < 0.01$ ). PWV was significantly decreased between the



control WKY and denervated WKY (control:  $3.92 \pm 0.25$  m/s; denervated:  $3.81 \pm 0.24$  m/s;  $p < 0.05$ , Figure 0.4) whilst there was no difference with denervation in the SHR (Figure 6.5) or between strains (Figure 0.3). There was no significant difference in pressure-distension curves between the control WKY and SHR (Table 0.4). The denervated WKY showed a significant increase in pressure-distension from the control ( $p < 0.001$ ) as did the SHR ( $p < 0.05$ , Table 0.4). There was no difference in AIC between strains (WKY control:  $250 \pm 113$  %. $\text{mmHg}$ ; SHR control:  $121 \pm 106$  %. $\text{mmHg}$ ) or within strains following denervation (WKY hex:  $277 \pm 142$  %. $\text{mmHg}$ ; SHR hex:  $135 \pm 86$  %. $\text{mmHg}$ ). There was also no significant difference between the ratio of area difference between the control ascending pressure-distension curve and the denervated ascending pressure-distension curve between strains (Figure 0.2).

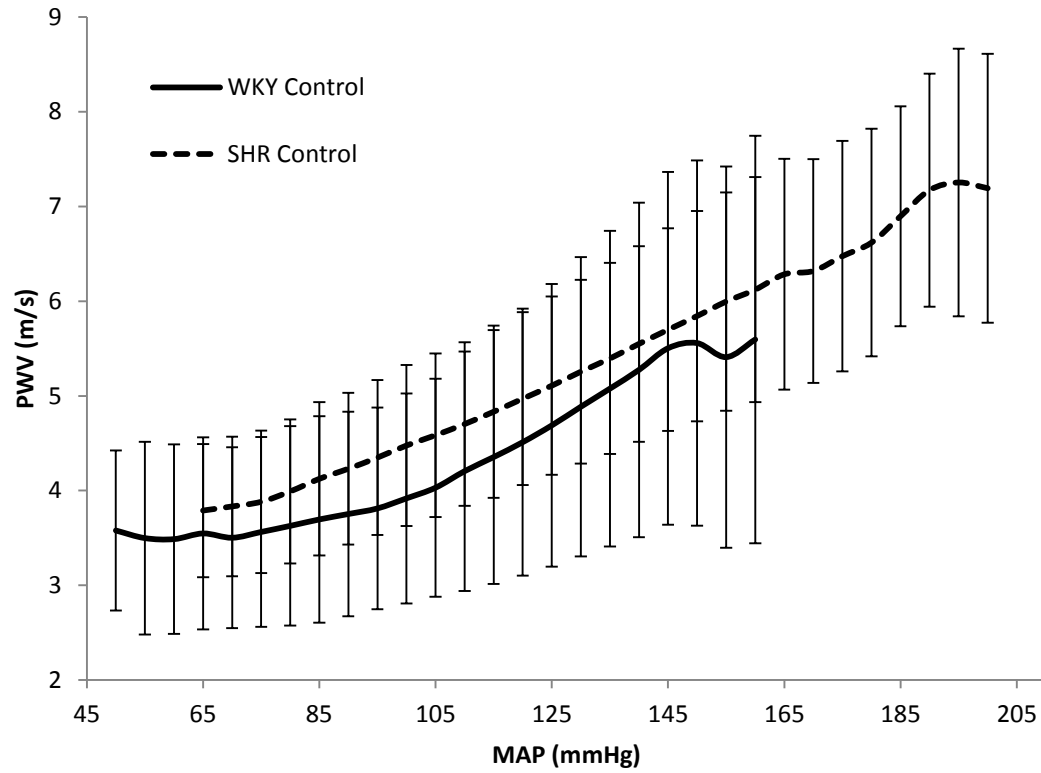


**Figure 0.3:** PWV comparison of control WKY's and SHR's across a range of MAP's before sympathetic blockade. Comparisons were made using an unpaired t test with Bonferroni correction for repeated measures at each blood pressure value shown. No significant difference was observed between strains at any discrete MAP. Data presented as Mean  $\pm$  SD

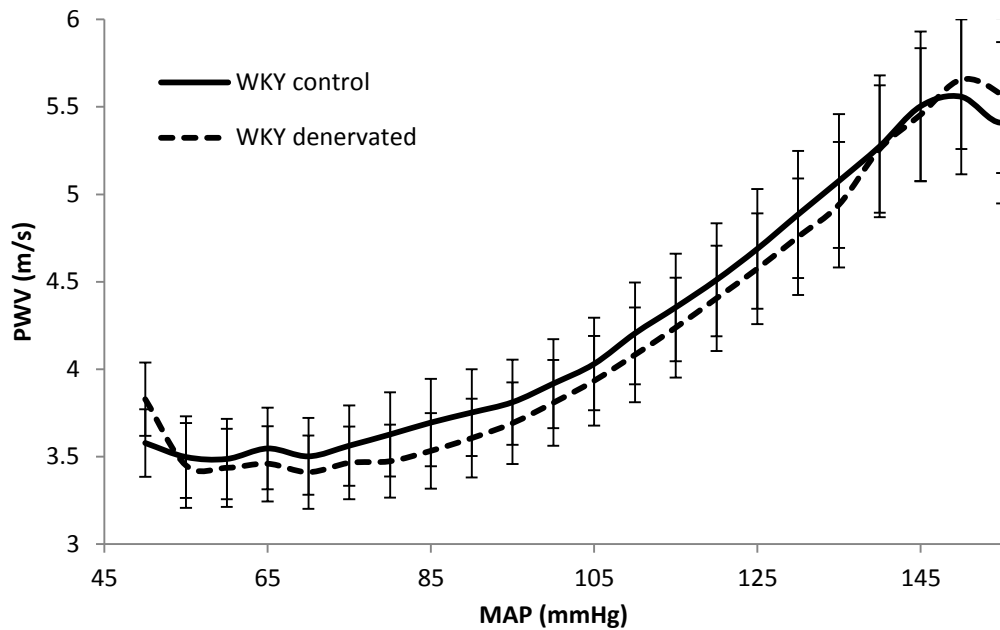


**Figure 0.4:** Pairwise PWV comparison between WKY's before and during sympathetic blockade. Comparisons were made using a paired t test with Bonferroni correction for repeated measures at each blood pressure value shown. A small but significant decrease in PWV was observed at MAP's ranging from 90-140mmHg. Data presented as Mean  $\pm$  SE

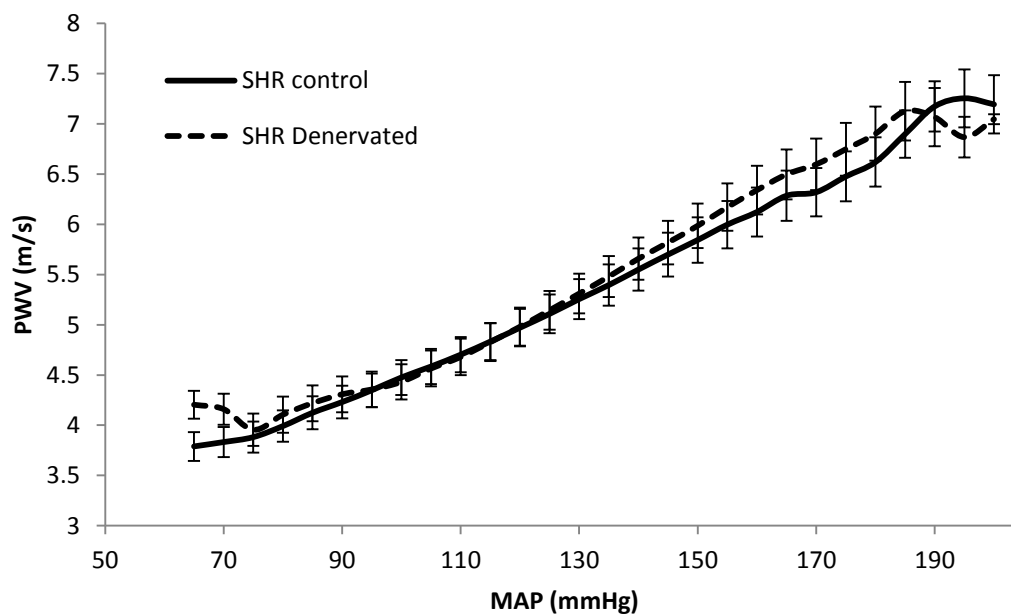


**Figure 0.5:** Pairwise PWV comparison between SHR's before and during sympathetic blockade. Comparisons were made using a paired t test with Bonferroni correction for repeated measures at each blood pressure value shown. A small but significant decrease in PWV was observed at a MAP of 100mmHg. Data presented as Mean  $\pm$  SE

### **MAP of 125 mmHg**

At a MAP of 125 mmHg, PP (mmHg) in the denervated WKY was less than that of the denervated SHR (denervated WKY:  $49 \pm 6$  mmHg; denervated SHR:  $65 \pm 5$  mmHg) and there was a significant reduction in HR between the control SHR and denervated SHR (SHR control:  $386 \pm 20$  bpm; SHR denervated:  $332 \pm 7$  bpm;  $p < 0.01$ , Table 6.2 and Table 6.3). The WKY showed a significantly higher systolic and diastolic diameter compared to the SHR, both before and after denervation (Table 6.2 and Table 6.3). There was no significant difference in pressure-distension between the intact WKY and SHR. There was however a significant difference in pressure-distension following denervation in the WKY ( $p < 0.001$ , Table 0.4). There was no difference in AIC between strains (WKY control:  $139 \pm 89$  % .mmHg; SHR control:  $142 \pm 148$  % .mmHg) or within strains (WKY hex:  $166 \pm 112$  % .mmHg; SHR hex:  $144 \pm 103$  % .mmHg). There was a slight trend towards the SHR ratio of area difference between the control ascending pressure-distension curve and the denervated ascending pressure-distension curve being greater than that of the WKY, but it was not significant ( $p = 0.07$ ) (Figure 0.2).

### **MAP of 150 mmHg**

At a MAP of 150 mmHg, there was a significant reduction in the HR of the SHR before and after denervation (SHR control:  $383 \pm 35$  bpm; SHR denervated:  $337 \pm 32$  bpm;  $p < 0.001$ ; Table 6.2 and Table 6.3). There was also a significant increase in both systolic and diastolic diameter in the WKY compared to the SHR both before and after denervation (Table 6.2 and Table 6.3). There was no significant difference in pressure-distension between the control WKY and SHR or following denervation in the WKY (Table 0.4). However, there was a significant increase in pressure-distension following denervation in the SHR ( $p < 0.001$ , Table 6.4). This was not associated with any change in PWV for the SHR (Figure 6.5). There was

also no difference in AIC between strains (WKY control:  $106 \pm 78$  %. $\text{mmHg}$ ; SHR control:  $107 \pm 73$  %. $\text{mmHg}$ ) or within strains (WKY denervated:  $111 \pm 82$  %. $\text{mmHg}$ ; SHR denervated:  $77 \pm 66$  %. $\text{mmHg}$ ). There was no significant difference between the ratio of area difference between the control ascending pressure-distension curve and the denervated ascending pressure-distension curve between strains (Figure 0.2).

### **1.28.3 Differences in baroreflex sensitivity between strains**

Baroreflex sensitivity between WKY and SHR was assessed via induced changes in blood pressure via the use of PE and SNP ( $n = 19$  SHR,  $n = 8$  WKY). Comparisons of baroreflex sensitivity were not made after hexamethonium due to sympathetic blockade inhibiting the baroreceptor output pathway. There was a significantly higher MAP50 seen for the SHR compared to the WKY reflecting a higher resting BP of the SHR (Figure 0.2, WKY:  $119 \pm 17$   $\text{mmHg}$ ; SHR:  $164 \pm 27$ ,  $p < 0.01$ ). There was, however, no significant difference in the gain between strains (WKY:  $2.42 \pm 0.7$  %/ $\text{mmHg}$ ; SHR:  $1.96 \pm 0.86$  %/ $\text{mmHg}$ ;  $p = 0.22$ )

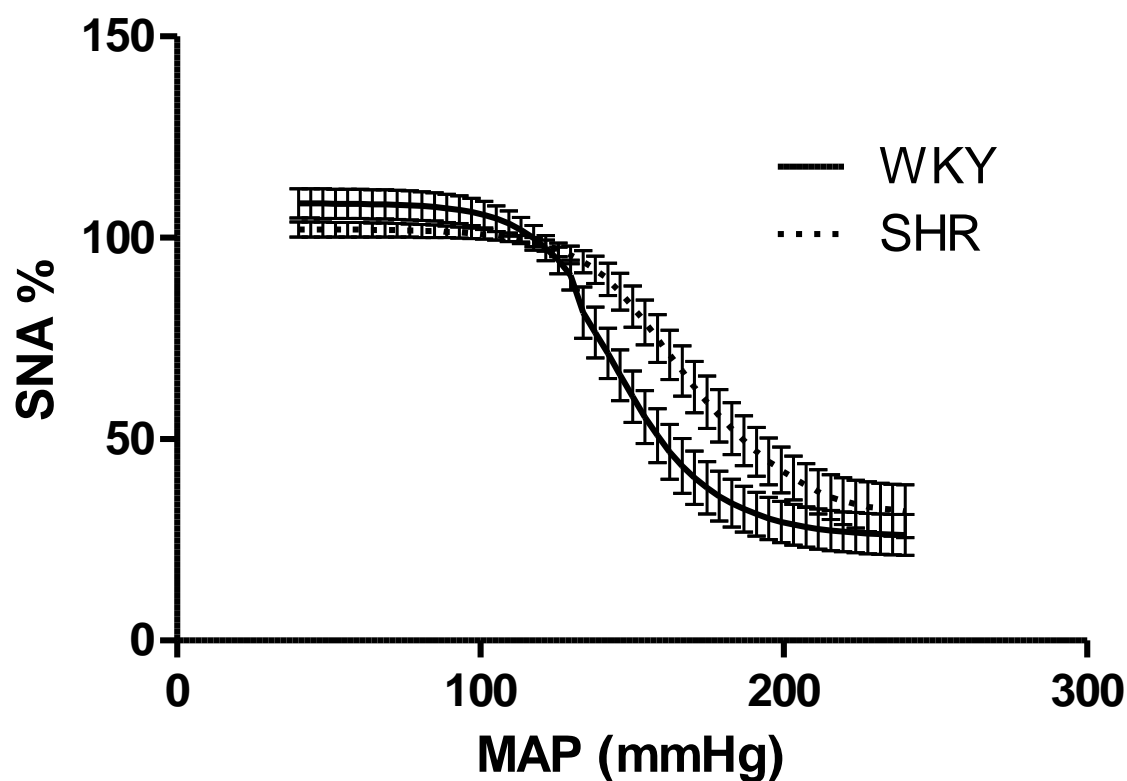


**Figure 0.6:** Baroreceptor sensitivity of WKY rats and SHR. The SHR showed a higher set-point for which changes in blood pressure elicit change in SNA. However, both strains displayed the same sensitivity to changes in blood pressure.

## 1.29 Discussion

This study shows that the SHR and the WKY display different aortic stiffness at various levels of MAP as well as different responses to sympathetic denervation. Specifically, the greatest decreases in arterial stiffness following sympathetic denervation are achieved at MAP's similar to the normal level of blood pressure of the given animal group ( $97 \pm 14$  mmHg for WKY's and  $136 \pm 16$  mmHg for SHR's). This suggests an arterial remodelling effect around the normal blood pressure of the animal.

Chronic exposure to elevated arterial pressure has been shown to lead to endothelial damage and vascular wall remodelling in rodent studies (Prado & Rossi 2006). Remodelling involves an increase in the elastin-collagen ratio (Najjar et al. 2005, O'Rourke & Nichols 2005) and increased integrin and fibronectin deposition (Bezie et al. 1998) leading to an increase in arterial stiffness.

The present study sought to examine the development of aortic stiffness in a rat model which rapidly develops hypertension (the SHR) and determine the influence of SNA in this development (Cosson et al. 2009, Hambley et al. 1987a, Judy & Farrell 1979). In comparing the SHR with the WKY at a common age range it was possible to determine the effects of chronic exposure to hypertension on arterial mechanics in the presence and absence of SNA. The baseline data (data acquired before the administration of vasoactive drugs) showed that there were significant differences in the haemodynamics of these two strains of rat. Accompanying the increased MAP, SBP, DBP and PP observed in the SHR was an increase in PWV. These findings are consistent with all other PWV studies which show a strong positive correlation between increased blood pressure and increased PWV. Despite the increased MAP observed in the SHR, there was no correlated increase in arterial diameter compared to the WKY. Such observations have been made previously (Humphrey 2008), and are consistent with a vascular remodelling process whereupon the increased MAP causes an initial increase in arterial diameter. This increases the arterial wall stress and decreases the wall shear stress of the artery. Together these processes trigger a reduction in nitric oxide and endothelin-1, in an attempt to restore wall shear stress (Humphrey 2008). The result is smooth muscle hyperplasia, which causes constriction of the artery and restores the vessel to similar diameters to the normotensive state.

Some strain related differences in haemodynamic values still remained after MAP's were matched by pressure alteration with vasoactive agents. These differences were that the WKY displayed higher  $dP/dt(max)$  at 75 and 100 mmHg. This finding is different to that in other studies where increased  $dP/dt(max)$  is accompanied by increase in PP and HR (Chan et al. 1984b), both of which remained unchanged between strains at this pressure. Furthermore, the SHR received an injection of SNP prior to these measurements being made to reach the baseline MAP of the WKY. This would be expected to increase SNA due to the resultant baroreceptor driven sympathoexcitation in response to reduced blood pressure and thereby increase heart rate and heart rate contractility.

Consistent with the baseline data regarding the diameter differences between the WKY and SHR, the WKY display higher aortic diameters at high blood pressures (125-150 mmHg) compared to the SHR in both the control and denervated state. These data further demonstrate that vascular remodelling induced by chronic hypertension results in reduced aortic diameter. The WKY underwent an acute increase in blood pressure to achieve an equivalent MAP to the SHR; this distending force was able to expand the arterial diameter. However, the SHR having been already exposed to these pressures required no blood pressure modification and instead, the reduced arterial diameter displayed represents the aforementioned arterial remodelling. The fact that the effect is maintained even after denervation also helps to validate this finding, since in the control condition it could be argued that the increase in diameter in the WKY may be a result of the sympathoinhibition produced upon injection of the normotensive animal with PE. However, even when both strains were denervated, the WKY maintained a higher diameter than the SHR despite the fact that both strains were equally sympathoinhibited.



The PWV results shown in this study seemingly differ from previous studies, which have shown a pressure independent increase in aortic PWV in the SHR compared to the WKY. The study by Cosson et al (2007) determines this indirectly via post hoc adjustments for differences in MAP. Another by Ng et al (2012), using a similar protocol of injecting vasoactive drugs to modify blood pressure found that the SHR had a 25% higher total aortic PWV at 100 mmHg compared to that of the WKY. One possible explanation for this difference is that PWV measurements made in the present study were made across the length of only the abdominal aorta; the area of the aorta with the highest concentration of smooth muscle and sympathetic innervation (Kienecker & Knoche 1978b). This was to ensure that the full extent of sympathoinhibition would be captured, with no influence from the rest of the aorta. Ng et al (2012) also found that there was no difference between SHR and WKY in abdominal aortic PWV, and the difference in aortic PWV was largely driven by differences in the thoracic aorta. The authors concluded that these differences were related to the differential expression of elastin and collagen fibres between these two sections of the aorta and the similarities in wall structure of the abdominal aorta between the WKY and SHR aorta (Ng et al 2012).

There were strain specific changes following injection of hexamethonium at each of the measured blood pressures. At low blood pressure (75 mmHg), both strains showed a significant reduction in HR with hexamethonium, however only the SHR had accompanying increases in systolic pressure and PP. Similar findings were observed at the baseline blood pressure of the WKY (100 mmHg), where hexamethonium resulted in reductions in HR in both strains and again the PP of the SHR was changed. These increases in PP in the SHR were responsible for the decreases in compliance seen at 75 mmHg and 100 mmHg, rather than a change in wall stiffness. This was made evident by the lack of change in both

distensibility and PWV. However, the changes in compliance seen in the WKY at these blood pressures were due to changes in arterial stiffness, as made evident from both the changes in PWV and distensibility.

These findings were corroborated with the pressure-distension data recorded at the same MAP's. In the WKY, the greatest change in pressure-distension following hexamethonium occurred at both 75 and 100 mmHg. For the SHR, these were the pressures for which the least change is seen in pressure-distension following hexamethonium was seen. Conversely, at higher blood pressure (150 mmHg) there was a small but greater increase in pressure-distension following hexamethonium in the SHR compared to the WKY. These changes were likely due to the decrease in HR and increase in PP. Such changes in HR and PP could still occur in the SHR due to the baroreceptor set point being higher, thus less sympathoinhibition was present at higher MAP and the effects of hexamethonium were more pronounced.

A previous study showed that the ability of smooth muscle to buffer the effects of increased collagen recruitment lessen as blood pressure increases (Dobrin & Rovick 1969). This is likely due to the strain from the distending pressure inhibiting the binding of actin and myosin fibres within the smooth muscle (Kuhn 1978). This may account for why no changes were seen in arterial stiffness in either the SHR or WKY at high blood pressures.

Consistent with the changes seen in pressure-distension, there was a small but significant reduction in PWV following injection of hexamethonium at pressures ranging from 90-140 mmHg in the WKY and a small but significant reduction in PWV in the SHR at 100 mmHg. Again, the lack of difference observed between strains is likely due to the similarities in the structure of the abdominal aorta in the WKY and SHR. Also of note is the large degree of variation in the PWV measurements between animals. This variation may be due to slight

differences in the placement of the intravascular pressure sensors between each animal, thereby detecting different sections of aorta and their associated stiffness.

Distensibility and compliance did not change with the same consistency as the changes seen in pressure-distension after injection of hexamethonium. There is typically a close relationship between aortic distensibility and pressure-distension (Lénárd et al. 2000). However in this case, the changes in haemodynamic parameters such as HR and PP were sufficient to dissociate these two measurements.

No changes were seen in wall viscoelasticity (as determined by AIC) either between strains or following treatment with hexamethonium. AIC measurements are primarily affected by a combination of  $dP/dt(max)$  and PP. A high  $dP/dt(max)$  with a high PP will cause the vessel to distend quickly and begin loading collagen fibres, causing the initial phase of systole to be highly viscoelastic. During diastole, the extent of arterial recoil is determined by HR wherein a low HR will cause the recoil to be slower thereby allowing the arterial distension to remain more prolonged leading to an increase in the size of the arterial loop.

This study shows that SNA is able to significantly alter aortic stiffness in the normotensive rat. However, the extent to which SNA can elicit control of arterial stiffness is limited to blood pressures of 25 mmHg around the barosensitive set-point of the animal. These results were not apparent in the SHR, which did not show any reduction in arterial stiffness at high blood pressures. Instead, the SHR appeared to exhibit changes in aortic diameters, consistent with that of vascular remodelling.

# **Effect of sympathetic blockade on the arterial stiffness of Lewis and Polycystic Kidney Disease rats**

## **Summary**

The study presented in this chapter investigates the effect of sympathetic nerve activity on abdominal aortic stiffness parameters in hypertension associated with chronic kidney disease. Lewis Polycystic Kidney (LPK) disease rats were compared to their control strain (Lewis) before and following sympathetic blockade by intravenous infusion of hexamethonium. The LPK showed no change in parameter of aortic stiffness following sympathetic blockade and the Lewis showed only small change in pulse wave velocity at 100 mmHg. However, viscoelasticity as measured by area in the curve (AIC) of the pressure distension loop, consistently decreased following withdrawal of sympathetic nerve activity in both the Lewis and LPK. These results suggest a significant role of haemodynamic parameters such as heart rate, pulse pressure and cardiac contractility, affecting the dynamic loading of the vessel wall, in determining viscoelasticity in the Lewis and LPK rat.

### 1.30 Introduction

The previous chapters have demonstrated that sympathetic nerve activity (SNA) imparts approximately a 4% change in arterial stiffness in normotensive rats and 1% in spontaneously hypertensive rats (SHR) at a MAP of 100mmHg. However, the SHR has multiple drivers of hypertension, including metabolic (Pravenec et al. 2004), renal (Anderson et al. 2000) and neurohormonal effects (Imaki et al. 1998). It is thus not due exclusively to an increase in SNA and so these other factors may provide possible confounding variables when SHR are used as controls. Furthermore, it was apparent that these rats had undergone extensive vascular remodelling, as the rats had lived up to 20 weeks in a hypertensive state.

Another hypertensive model is the Lewis Polycystic Kidney (LPK) disease rat. These animals are a model for nephronophthisis 9 (NPHP9), developed due to a single nucleotide polymorphism in the NIMA (never in mitosis gene a)-related kinase 8 (Nek8) gene on chromosome 10 (McCooke et al. 2012). This manifests in hypertension and sympathetic overactivity (Harrison et al. 2010a), reduced compliance (Ng et al. 2011a) and cardiac hypertrophy. Unlike the SHR however, these pathologies begin developing at 3 weeks old and are fully manifest at 12 weeks. Such a rapid development time means that there is less time for arterial remodelling which potentially adds both increased deposition of collagen into the arterial wall as well as smooth muscle hypertrophy which may confound the comparison of the contribution of SNA towards arterial stiffness in SHRs compared with their normotensive controls. Instead, the LPK may represent a more sympathetically driven model of arterial stiffness.

To assess this, LPK rats were compared to their normotensive control, the Lewis rat, before and after sympathetic blockade using hexamethonium. Multiple parameters of arterial

stiffness derived from both aortic diameter measurements and blood pressure measurements were assessed across a range of mean arterial pressures (MAP) as described in previous chapters.

## **1.31 Methods**

### **1.31.1 Animal preparation**

Mixed gender male and female Lewis (n=10) and LPK (n=7) rats aged 12 weeks were studied. Animals were anaesthetized, instrumented and monitored as stated in 0, Section 3.1.

### **1.31.2 Procedures**

#### **Pressure measurement and manipulation**

All animals were instrumented and blood pressure was measured as stated in Chapter 3, Sections 3.3 and 3.4. Hexamethonium (20mg/kg) was used to induce depression of SNA following recording of control measurements.

Diameter measurements and sympathetic nerve measurements were made as described in Chapter 3, Section 3.2 and section 3.3 respectively.

### **1.31.3 Data and statistical analysis**

Primary statistical analysis was done as described in Chapter 3, Section 3.4. Statistical analysis was performed both between strains of rat, with comparisons being made not only against the control conditions but also within each rat following sympathectomy.

In addition, stepwise linear regression was performed to determine the factors that most significantly influenced AIC, distensibility, compliance and PWV with the input variables being: strain of rat (1= Lewis, 2=LPK), type of treatment (0= control, 1= denervated) MAP, heart rate (HR) dP/dt(max), SNA, and pulse pressure (PP). These variables were input into the model in this order for all models. However, the variables of strain was obviously excluded when conducting the within strain comparisons. For this analysis, the models were simply constructed separately for each strain.. This analysis was performed once between both strains and again within each strain of rat. An additional model was constructed post-hoc which sought to determine the factors contributing to dP/dt(max) (Table 7.8). This was done since dP/dt(max) was found to be highly predictive of both AIC and PWV. This model was constructed in the same fashion as above except strain was excluded since it was only the contribution of haemodynamic factors that was of interest.

Further, the ratio of area difference under the ascending distension curve before and after sympathetic denervation was compared both between pressure ranges and between strains. These comparisons were made using unpaired Students t-tests.

## **1.32 Results**

### **1.32.1 Haemodynamic differences between Lewis and LPK**

#### **MAP of 75mmHg (Table 7.1)**

At a MAP of 75 mmHg, LPK rats had a significantly higher PWV than the Lewis rats ( $p<0.05$ ) (Figure 0.1). This was accompanied by lower distensibility ( $p<0.05$ ), compliance ( $p<0.05$ ) and a higher viscoelasticity as measured by AIC ( $p<0.001$ ). There was no difference

in HR, PP, Ds, Dd,  $\Delta D$  or  $dP/dt(max)$ . There was also a significant difference in the pressure-distension intercept at this MAP ( $p<0.001$ , Table 7.5, Table 7.2).

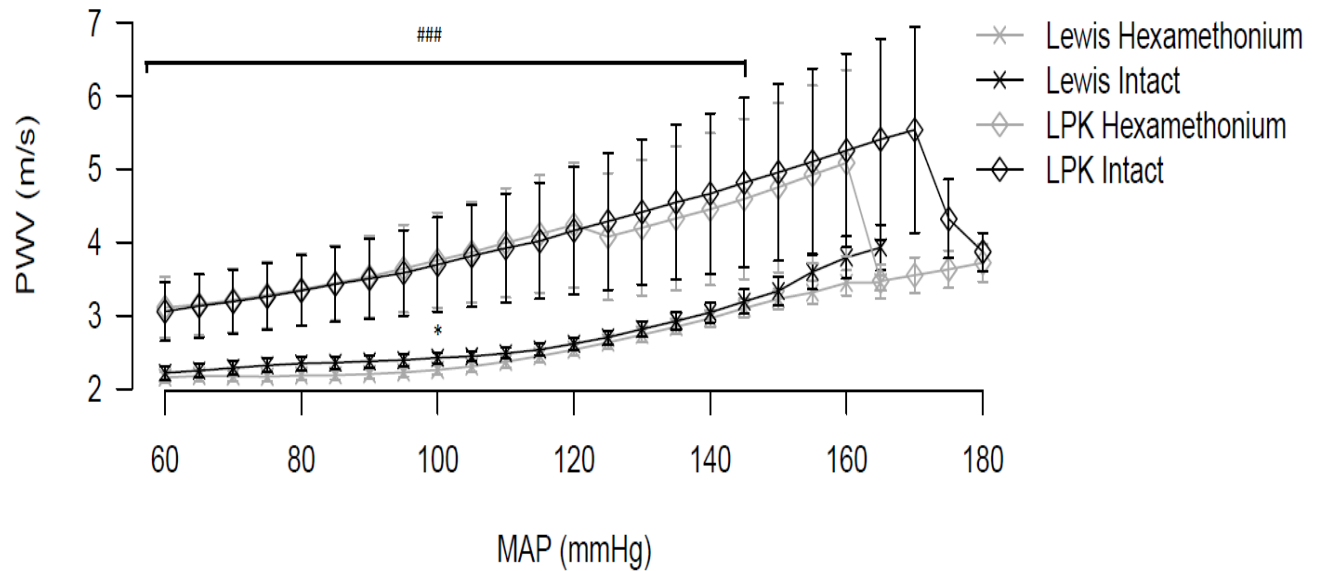


**Figure 0.1:** Comparisons of PWV between Lewis and LPK rats before and after hexamethonium across a range of MAPs. Comparisons were made using an unpaired t test with Bonferroni correction for repeated measures at each blood pressure value shown for comparisons between strain and a paired t-test with the same corrections within strain. \* denotes comparison following hexamethonium and # denotes comparison between strains. \* $p<0.05$ . ### $p<0.001$ . Data are presented as Mean $\pm$ SD



**Table 0.1:** Values at 75mmHg. Comparisons between sympathetic blockade (denervated) and before sympathetic blockade (control).\* p<0.05, \*\* p<0.01, \*\*\*p<0.001. Comparisons between Lewis and LPK in the control state #p<0.05, ##p<0.01, ###p<0.001.

MAP 75mmHg	Lewis		LPK	
	Control	Denervated	Control	Denervated
PWV (m/s)	2.30±0.10	2.24±0.07	3.31±0.45#	3.14±0.43
Distensibility (x10 <sup>-3</sup> ,mmHg <sup>-1</sup> )	3.89±0.28	4.00±0.20	2.64±0.25#	2.83±0.18
Compliance (mm/mmHg)	4.66±0.53	4.58±0.37	2.81±0.49#	2.92±0.42
PP (mmHg)	47.40±2.58	45.30±2.66	59.05±7.14	64.25±10.00
HR (BPM)	437±9	358±11***	440±6	363±11**
AIC (%.mmHg)	178±14	95±17**	537±76###	667±84
DP/dt(max) (mmHg/s)	7740±484	4250±363***	7965±500	5882±627
Systolic Diameter (µm)	1318 ±78	1305±62	1221±99	1215±94
Diastolic Diameter (µm)	1167±66	1136±54	1043±71	1017±72
Diameter Difference (µm)	150±13	169±11	178±30	198±24
Peak Distension (%)	10.77±0.91##	14.30±0.72	9.51±1.18	13.16±2.28

**Table 0.2:** Values at 100mmHg. Comparisons between sympathetic blockade (denervated) and before sympathetic blockade (control).\* p<0.05, \*\* p<0.01, \*\*\*p<0.001. Comparisons between Lewis and LPK in the control state #p<0.05, ##p<0.01, ###p<0.001.

MAP 100mmHg	Lewis		LPK	
	Control	Denervated	Control	Denervated
PWV (m/s)	2.45±0.07	2.30±0.07***	3.68±0.59#	3.52±0.53*
Distensibility (x10 <sup>-3</sup> ,mmHg <sup>-1</sup> )	3.10±0.22	2.78±0.09	1.99±0.14##	2.17±0.23
Compliance (mm/mmHg)	3.93±0.33	3.72±0.20	2.08±0.18###	2.32±0.30
PP (mmHg)	41.90±2.05	33.70±2.00**	68.99±8.78##	64.99±7.17
HR (BPM)	451±7	368±9***	437±9	333±10***
AIC (%.mmHg)	210±30	99±19**	626±42###	426±57**
DP/dt(max)	7620±332	3535±227***	9353±712#	5290±375***
Systolic Diameter (µm)	1437 ±80	1497±83	1220±97	1231±88
Diastolic Diameter (µm)	1272±75	1349±79	1057±88	1064±75
Diameter Difference (µm)	166±12	148±8	163±12	167±22
Peak Distension (%)	11.64±0.75	10.79±0.67	8.90±1.60	12.64±2.13

**Table 0.3:** Values at 125mmHg. Comparisons between sympathetic blockade (denervated) and before sympathetic blockade (control). \* p<0.05, \*\* p<0.01, \*\*\*p<0.001. Comparisons between Lewis and LPK in the control state #p<0.05, ##p<0.01, ###p<0.001.

MAP 125mmHg	Lewis		LPK	
	control	denervated	control	denervated
PWV (m/s)	2.77±0.09	2.68±0.10	3.43±0.33#	3.32±0.29
Distensibility (x10 <sup>-3</sup> ,mmHg <sup>-1</sup> )	1.49x±0.11	1.51±0.18	1.67±0.20	1.53±0.21
Compliance (mm/mmHg)	2.21±0.16	2.23±0.23	1.72±0.22	1.61±0.24
PP (mmHg)	38.80±1.18	36.30±1.30	76.44±9.53###	69.70±8.91
HR (BPM)	434±9	370±8***	440±7	336±9***
AIC (%.mmHg)	125±11	67±13**	768±137###	410±78
dP/dt(max) (mmHg/s)	6150±338	2925±138***	10227±594###	5487±332***
Systolic Diameter (µm)	1600 ±69	1605±51	1206±57##	1188±51
Diastolic Diameter (µm)	1491±67	1509±52	1042±48###	1055±44
Diameter Difference (µm)	109±7	95±9	164±24#	133±25
Peak Distension (%)	6.65±0.65	6.04±0.72	10.02±2.22	10.57±2.59

**Table 0.4:** Values at 150mmHg. Comparisons between sympathetic blockade (denervated) and before sympathetic blockade (control). \* p<0.05, \*\* p<0.01, \*\*\*p<0.001. Comparisons between Lewis and LPK in the control state #p<0.05, ##p<0.01, ###p<0.001.

MAP 150mmHg	Lewis		LPK	
	control	denervated	control	denervated
PWV (m/s)	3.36±0.12	3.33±0.20	4.85±1.10	4.81±1.12
Distensibility (x10 <sup>-3</sup> ,mmHg <sup>-1</sup> )	1.02±0.12	7.90±0.07	1.17±0.20	1.13±0.16
Compliance (mm/mmHg)	1.54±0.17	1.30±0.11	1.39±0.19	1.38±0.21
PP (mmHg)	53.56±1.65	56.33±2.19	81.7±8.12##	73.73±8.70*
HR (BPM)	428±5	379±5***	431±12	348±10**
AIC (%.mmHg)	164±48	101±33*	559±122##	319±29
dP/dt(max) (mmHg/s)	5633±186	2961±81***	8942±798##	5161±421**
Systolic Diameter (µm)	1632 ±69	1741±65	1368±99#	1342±105
Diastolic Diameter (µm)	1543±66	1665±62	1227±97#	1223±95
Diameter Difference (µm)	90±10	76±6	141±22#	119±17
Peak Distension (%)	5.39±0.60	4.40±0.31	8.55±1.64	9.22±1.07

**Table 0.5:** Differences in the systolic phase of the pressure- distension curves before and after sympathetic denervation in the Lewis and LPK rats. For differences between sympathetic blockade: \*p<0.05, \*\*p<0.01, \*\*\*p<0.001; for differences between strains #p<0.05, ##p<0.01, ###p<0.001.

MAP (mmHg)	Lewis				LPK			
	Control		Denervated		Control		Denervated	
	Slope (x10 <sup>-2</sup> %.mmHg)	Intercept (x10 <sup>-2</sup> %.mmHg)	Slope (x10 <sup>-2</sup> %.mmHg)	Intercept (x10 <sup>-2</sup> %.mmHg)	Slope (x10 <sup>-2</sup> %.mmHg)	Intercept (x10 <sup>-2</sup> %.mmHg)	Slope (x10 <sup>-2</sup> %.mmHg)	Intercept (x10 <sup>-2</sup> %.mmHg)
75	8.0±0.5	-1.6±9.8	9.2±0.5	32.3±10.3 ***	4.0±0.2###	29.7±8.2	4.3±0.3	17.3±11.6
100	7.2±0.3	-3.8±8.0	7.7±0.2	-29.8±4.5***	3.1±0.2###	19.0±7.0	4.4±0.2***	21.4±8.7
125	4.9±0.2	6.9±5.7	4.8±0.3	32.2±7.3***	2.7±0.2###	-4.2±9.9	3.9±0.2**	0.4±8.3
150	3.3±0.2	30.3±6.2	2.9±0.1	40.4±4.7	2.5±0.1###	5.7±6.1	3.1±0.1 *	3.4±7.8

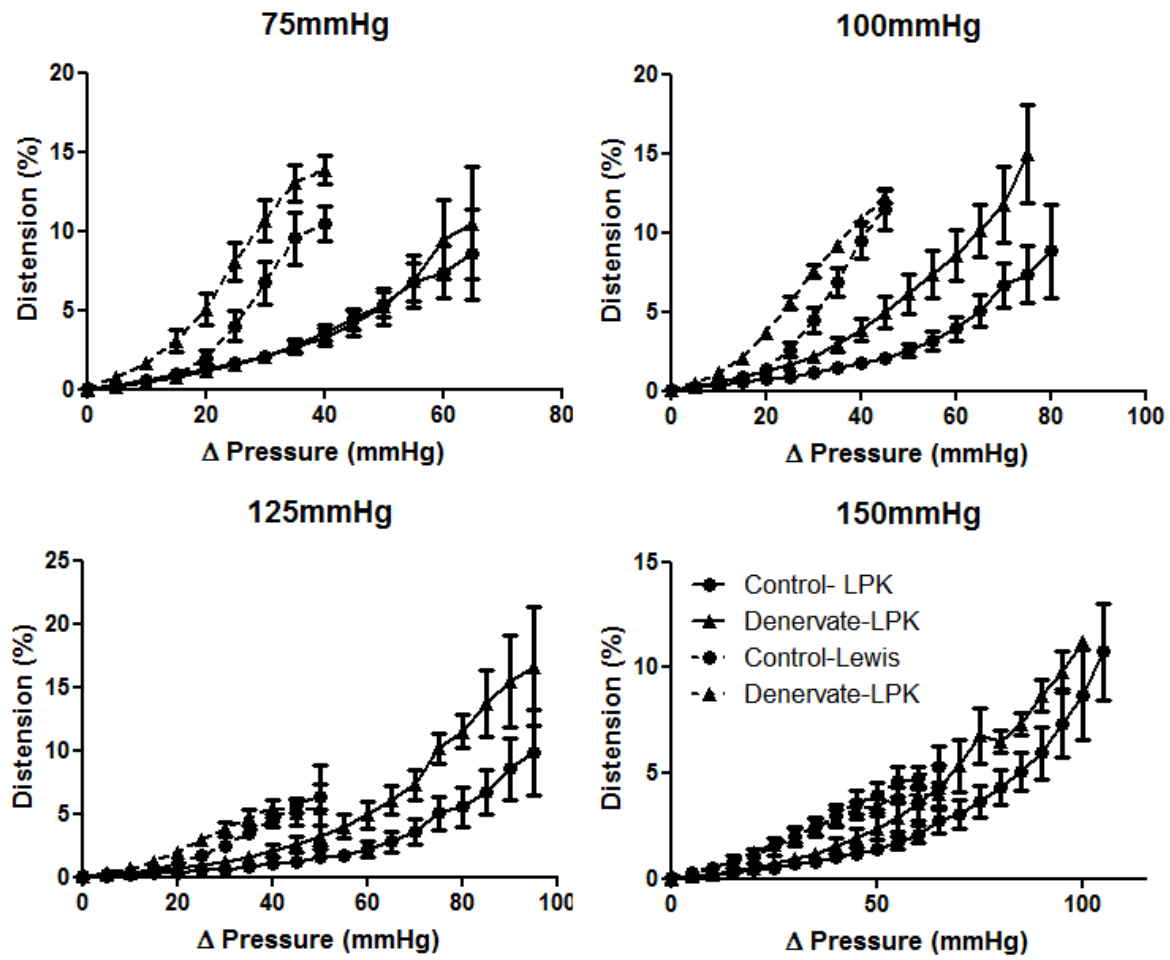


**Figure 0.2:** Pressure-distension curves for Lewis and LPK rats before and after sympathetic denervation across a range of MAP's. See Table 0.5 for statistical differences.

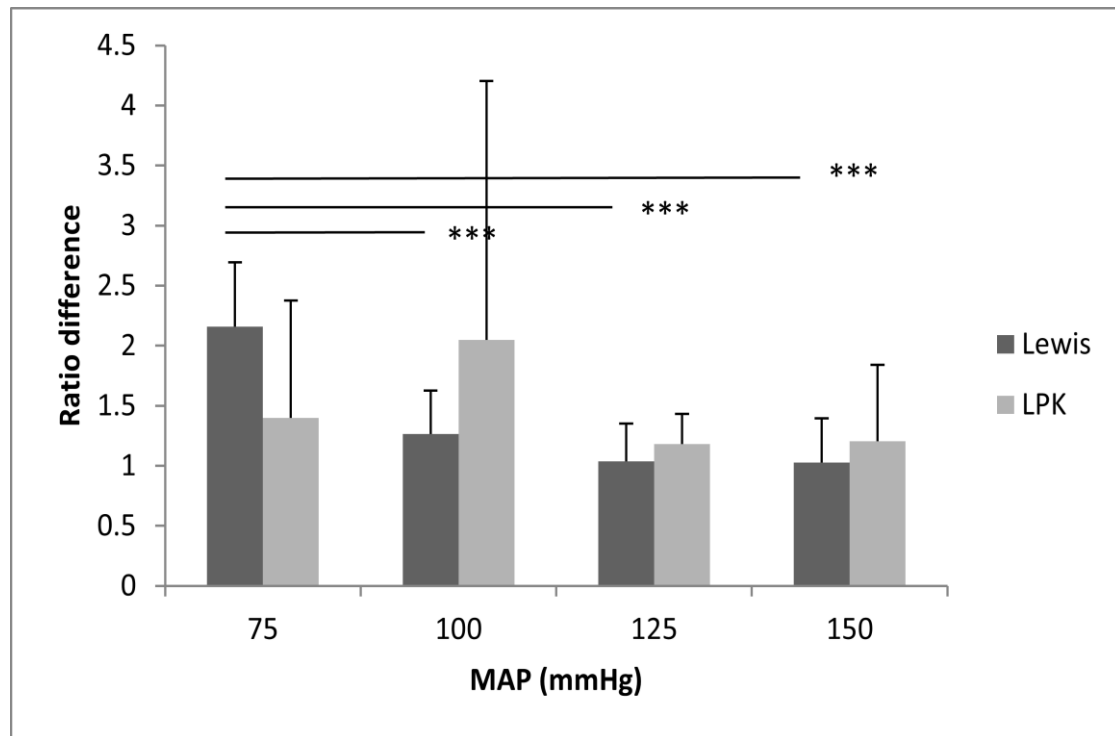


**Figure 0.3:** Comparisons of ratio of difference in area under the distension curve before and after sympathetic denervation between strains and across a range of MAP's. \*\*\* $p < 0.001$ .

#### MAP of 100mmHg (Table 7.2)

At a MAP of 100 mmHg, PWV remained higher in the LPK ( $p < 0.05$ ) (Figure 0.1) and was accompanied with a lower distensibility ( $p < 0.01$ ), compliance ( $p < 0.001$ ) and greater AIC, PP ( $p < 0.01$ ) and peak  $dP/dt(max)$  ( $p < 0.05$ ). There was no difference in HR, Ds, Dd or  $\Delta D$ .

There was also a significant difference in the pressure-distension intercept at this MAP ( $p < 0.001$ ) (Table 7.5, Figure 0.2).

#### MAP of 125mmHg (Table 7.3)

At a MAP of 125 mmHg, despite the higher PWV in the LPK ( $p < 0.05$ ) (Figure 0.1) there was no measured difference in distensibility or compliance. AIC ( $p < 0.001$ ),  $dP/dt(max)$  ( $p < 0.001$ ) and PP ( $p < 0.001$ ) were all greater in the LPK. Both Ds ( $p < 0.01$ ) and Dd ( $p < 0.001$ ) were

higher in the Lewis than the LPK, yet  $\Delta D$  remained higher in the LPK ( $p < 0.05$ ). There was no difference in HR.

There was also a significant difference in the pressure-distension intercept at this MAP ( $p < 0.001$ ) (Table 7.5, Figure 0.2).

#### **MAP of 150mmHg (Table 7.4)**

At a MAP of 150 mmHg there was no difference between PWV (Figure 0.1) or distensibility or compliance. However, AIC, PP and  $dP/dt(\max)$  were all higher in the LPK compared to the Lewis ( $p < 0.01$  for all cases). Both  $D_s$  ( $p < 0.05$ ) and  $D_d$  ( $p < 0.05$ ) were higher in the Lewis than the LPK, yet  $\Delta D$  remained higher in the LPK ( $p < 0.05$ ). There was no difference in HR.

There was also a significant difference in the pressure-distension intercept at this MAP ( $p < 0.001$ ) (Table 7.5, Figure 0.2).

#### **1.32.2 Baroreceptor sensitivity**

There was no significant difference in baroreceptor sensitivity between the Lewis and LPK as determined by the sympathetic baroreflex gain (Lewis:  $1.94 \pm 0.82\%/mmHg$ ; LPK:  $1.69 \pm 0.39\%/mmHg$ ) (Figure 0.4).



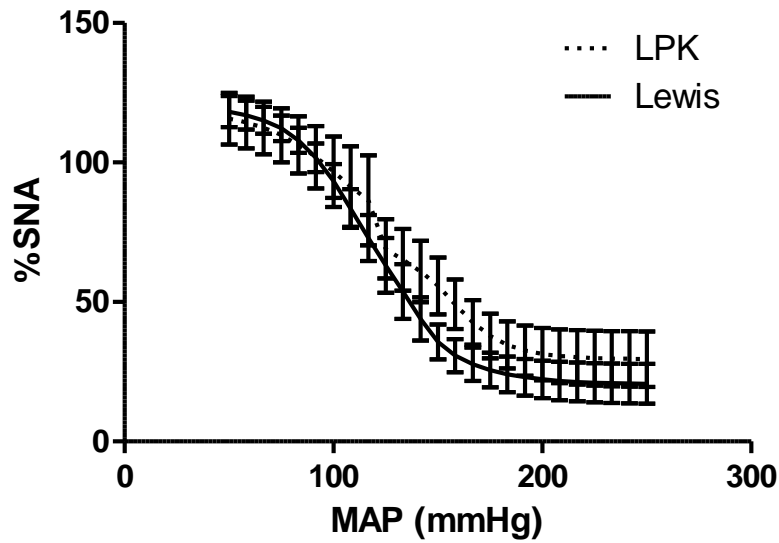


**Figure 0.4:** Baroreceptor sensitivity between the Lewis and LPK. No significant difference was seen between these two strains.

### 1.32.3 Step-wise linear regression between strains

Step-wise linear regression was used to determine the influence of MAP, HR,  $dP/dt(max)$ , PP, PWV, SNA, strain of rat and sympathetic blockade (1=blockade, 0=control) on AIC. The resultant model retained both strain and  $dP/dt(max)$  (Table 0.6).

Step-wise linear regression with PWV as the outcome variable replacing AIC revealed that strain, MAP,  $dP/dt(max)$ , sympathetic blockade and HR were all retained within the model (Table 0.7).

To further determine the relationship between the factors that contribute to alter AIC, step-wise linear regression was conducted upon  $dP/dt(max)$ . The results revealed that the sympathetic blockade, PP, MAP and HR were the biggest determinants of  $dP/dt(max)$  (Table 0.8).

**Table 0.6:** Step-wise linear regression analysis of determinants of AIC between both rat models. Adjusted  $R^2=0.715$ .

Variable	coefficient	$\beta$ coefficient	Part $\text{corr}^2$	p
Rat strain	332.9 $\pm$ 28.28	0.632	0.320	<0.001
dP/dt(max)(mmHg/s)	0.036 $\pm$ 0.005	0.352	0.100	<0.001

**Table 0.7:** Step-wise linear regression analysis of determinants of PWV between both rat models. Adjusted  $R^2=0.436$

Variable	coefficient	$\beta$ coefficient	Part $\text{corr}^2$	p
Rat Strain	2.180 $\pm$ 0.256	0.820	0.332	<0.001
MAP(mmHg)	0.241 $\pm$ 0.084	0.203	0.038	<0.001
dP/dt(max)(mmHg/s)	0.000 $\pm$ 0.000	-0.806	0.172	<0.001
Sympathetic blockade (Blockade=1)	-0.920 $\pm$ .340	-0.355	0.033	<0.001
HR (BPM)	0.008 $\pm$ 0.004	0.0285	0.020	<0.001

**Table 0.8:** Step-wise linear regression analysis of determinants of dP/dt(max) in both rat models. Adjusted  $R^2=0.694$ .

Variable	coefficient	$\beta$ coefficient	Part $\text{corr}^2$	p
Sympathetic blockade (Blockade=1)	-1848 $\pm$ 454	-0.367	0.041	<0.001
PP(mmHg)	58 $\pm$ 6	0.472	0.205	<0.001
MAP (mmHg)	-512 $\pm$ 117	-0.222	0.047	<0.001
HR (BPM)	18.2 $\pm$ 4.8	0.342	0.036	<0.001

### **1.32.4 Effect of sympathectomy on aortic haemodynamics within strains**

#### **MAP 75 mmHg (Table 7.1)**

At a MAP of 75 mmHg, there were significant decreases in HR, AIC and dP/dt(max) following sympathetic blockade in the Lewis rat ( $p<0.001$ ,  $p<0.01$  and  $p<0.001$  respectively). The LPK however, only showed a decrease in HR at this MAP ( $p<0.01$ ).

There was also a significant difference in the pressure-distension intercept following sympathetic blockade at this MAP for the Lewis ( $p<0.001$ , Table 7.5, Figure 0.2).

There was a significant difference in the ratio of difference between the area under the distension curve before and after sympathetic blockade at this MAP in the Lewis rat. These differences were between the ratio of difference at 75 and 100 mmHg, 75 and 125 mmHg and 75 and 150 mmHg (Figure 0.3).

#### **MAP 100 mmHg (Table 7.2)**

At a MAP of 100 mmHg, the Lewis showed significant decreases in PWV ( $p<0.001$ ), PP ( $p<0.01$ ), HR ( $p<0.001$ ), AIC ( $p<0.01$ ) and dP/dt(max) ( $p<0.001$ ) following sympathetic blockade. The LPK showed significant decreases in HR ( $p<0.001$ ), AIC ( $p<0.01$ ) and dP/dt(max) ( $p<0.001$ ).

There was also a significant difference in the pressure-distension intercept following sympathetic blockade at this MAP for both the Lewis and LPK ( $p<0.001$ , Table 7.5, Figure 0.2).

### **MAP 125 mmHg (Table 0.3)**

At a MAP of 125 mmHg, the Lewis showed significant decreases in HR ( $p<0.001$ ), AIC ( $p<0.01$ ) and  $dP/dt(max)$  ( $p<0.001$ ) following sympathetic blockade. Similarly, the LPK showed a decreased in HR ( $p<0.001$ ) and  $dP/dt(max)$  ( $p<0.001$ ) following sympathetic blockade.

There was also a significant difference in the pressure-distension intercept following sympathetic blockade at this MAP for both the Lewis ( $p<0.001$ ) and LPK ( $p<0.01$ , Table 7.5, Figure 0.2).

### **MAP 150 mmHg (Table 0.4)**

At a MAP 150 mmHg, there was a significant reduction in HR ( $p<0.001$ ), AIC ( $p<0.05$ ) and  $dP/dt(max)$  ( $p<0.001$ ) following sympathetic blockade in the Lewis. In the LPK there were significant reductions in PP ( $p<0.05$ ), HR ( $p<0.01$ ) and  $dP/dt(max)$  ( $p<0.01$ ) following sympathetic blockade.

There was also a significant difference in the pressure-distension intercept following sympathetic blockade at this MAP for the LPK ( $p<0.05$ , Table 7.5, Figure 0.2).

### **1.32.5 Step-wise linear regression within strains**

Step-wise multiple linear regression showed that for both the Lewis and the LPK, the most significant factor influencing AIC was  $dP/dt(max)$  (Table 0.9 and Table 0.10 respectively). However, PWV was affected differently between strains, with the Lewis being influenced by MAP, HR and SNA (Table 0.11) whilst the LPK was influenced by  $dP/dt(max)$ , sympathetic blockade and MAP (Table 0.12).

**Table 0.9:** Step-wise linear regression analysis of determinants of AIC in Lewis rat showed that dP/dt(max) (mmHg/s) determined AIC. Adjusted  $R^2=0.453$

Variable	coefficient	$\beta$ coefficient	Part $\text{corr}^2$	p
dP/dt(max) (mmHg/s)	0.024 $\pm$ 0.003	0.679	0.461	<0.001

**Table 0.10:** Step-wise linear regression analysis of determinants of AIC in LPK rat showed that dP/dt(max) (mmHg/s) determined AIC. Adjusted  $R^2=0.252$

Variable	coefficient	$\beta$ coefficient	Part $\text{corr}^2$	p
dP/dt(max) (mmHg/s)	0.048 $\pm$ 0.012	0.518	0.268	<0.001

**Table 0.11:** Step-wise linear regression analysis of determinants of PWV in Lewis rat showed that PWV was most influenced by MAP (mmHg), HR (BPM) and SNA ( $\mu$ V) in descending order. Adjusted  $R^2=0.616$

Variable	coefficient	$\beta$ coefficient	Part $\text{corr}^2$	p
MAP(mmHg)	0.332 $\pm$ 0.037	0.685	0.352	<0.001
HR(BPM)	0.004 $\pm$ 0.001	0.348	0.051	<0.05
SNA( $\mu$ V)	-0.005 $\pm$ 0.002	-0.239	0.036	<0.05

**Table 0.12:** Step-wise linear regression analysis of determinants of PWV in the LPK rat showed that PWV was most influenced by dP/dt(max) (mmHg/s), sympathetic blockade and MAP (mmHg) in descending order. Adjusted  $R^2=0.369$

Variable	coefficient	$\beta$ coefficient	Part $\text{corr}^2$	p
dP/dt(max) (mmHg/s)	-0.001 $\pm$ 0.000	-0.813	0.342	<0.001
Neurogenic blockade (blockade=1)	-2.112 $\pm$ 0.568	-0.600	0.186	<0.05
MAP (mmHg)	-2.112 $\pm$ 0.568	-0.600	0.072	<0.05

## **1.33 Discussion**

### **1.33.1 Difference between strains**

This study shows that there was a significant difference between the arterial haemodynamics of the Lewis and LPK rat. Differences were confirmed using data both derived from blood pressure measurements and aortic diameter measurements across a range of mean blood pressures. Such differences reflect entirely different vascular wall properties between strains.

Previous studies have recognised the effect of polycystitis on the development of hypertension in both the LPK rat model (Phillips et al. 2007) as well as in humans (Klein et al. 2001a). These investigations show the influence of impaired renal function on the development of hypertension but also hypothesize an additional contribution of increased SNA and its interaction with arterial vasculature. Indeed, further research from the Phillips group has shown that SNA is increased in the LPK as represented by increased basal HR (Harrison et al. 2010a). However, yet undetermined is the level of control such increases in SNA have on large arteries.

The LPK displayed increased arterial stiffness at MAP of 75 mmHg and 100 mmHg compared with the Lewis for all metrics of arterial stiffness including distensibility, PWV and distension. However, this effect became more attenuated as the MAP was increased to 125 mmHg and 150 mmHg. This highlights the importance of the pressure dependent nature of arterial stiffness, namely that the effects of vascular wall remodelling may be present at low pressures but are absent at high blood pressures. These results differ somewhat from previous research by Ng et al (2011), who showed that the LPK maintained a higher PWV throughout the same range of blood pressures (Ng et al. 2011a). One possible reason for these differences could be the segment of aorta covered in each study. Ng et al (2011) measured aortic PWV

along the entire aorta whereas this study measured PWV along the abdominal aorta. Measurement of PWV across different sections of aorta have previously shown completely different stiffness profiles (Ng et al. 2012) and aortic stiffening with age is known to vary within aortic regions (Hickson et al. 2010, Rogers et al. 2001).

In this study there was a marked increase in PP between strains (at MAPs ranging from 100-150 mmHg) in the absence of any change in HR. The consequence of this was a significantly increased maximal rate of change in pressure, as measured by  $dp/dt(max)$ . Such changes would suggest that the resultant pressure and distension waveforms would be different and therefore potentially contribute to the changes in arterial stiffness. However, there was only a difference in peak distension at 150 mmHg between the LPK and Lewis. At mean pressures of 75 mmHg and 100 mmHg there was no significant difference in the maximum distension of the LPK and the Lewis despite a significant increase in systolic pressure. These results alongside the PWV data suggest the arteries of the LPK become relatively stiffer at lower blood pressures.

When distension was displayed as a function of pressure, there was a significant difference between the resultant curves of the LPK and Lewis rats. At all MAP's, the LPK showed a significantly lower slope than the Lewis. This result emphasises the increased arterial stiffness of the LPK, since the same amount of arterial pressure change did not produce an equal change in distension. These results are still consistent with those found for the other metrics of stiffness across all blood pressures, for whilst there were still differences in distension at higher blood pressures, they were far less pronounced.

In the present study, the combination of increased PP, reduced HR and reduced  $dp/dt(max)$  were the primary cause of increased AIC in the LPK compared with the Lewis. PP influences

the AIC by having one measurement cover a greater pressure range throughout the cardiac cycle thus allowing the pressure-distension curve to cover a greater area. HR and  $dP/dt(\max)$  reflect the time intervals associated with the cardiac cycle. If both values are increased with no change in PP, the vessel is forced through a highly viscoelastic systolic phase and a normal diastolic phase whereas the lower HR and  $dP/dt(\max)$  allows the systolic phase to increase the distension more gradually during the systolic phase and recoil slower during diastole.

Of note in these data are the differences between the pressure distension curves observed here in rats and those observed in previous studies on humans. In human brachial and radial arteries (Tardy & Meister 1991), the diameter expansion that occurs following systole initially increases at an exponential angle and then plateaus at higher pressures (Figure 0.5a). The hysteresis loop during diastole then decreases its diameter and follows the same curve down. This loop is consistent with the present understanding of arterial mechanics, whereby at low pressures the load is taken up by the elastin fibres thus displaying higher compliance at this point on the curve. At higher pressures, the stiff collagen fibres begin to bear the load of pressure resulting in a stiffer profile. Incidentally, the reduction in diameter throughout diastole observed in this example is likely due to myogenically induced arterial contraction. The same pressure-distension curves were also observed in the human carotid artery (Lénárd et al. 2000)



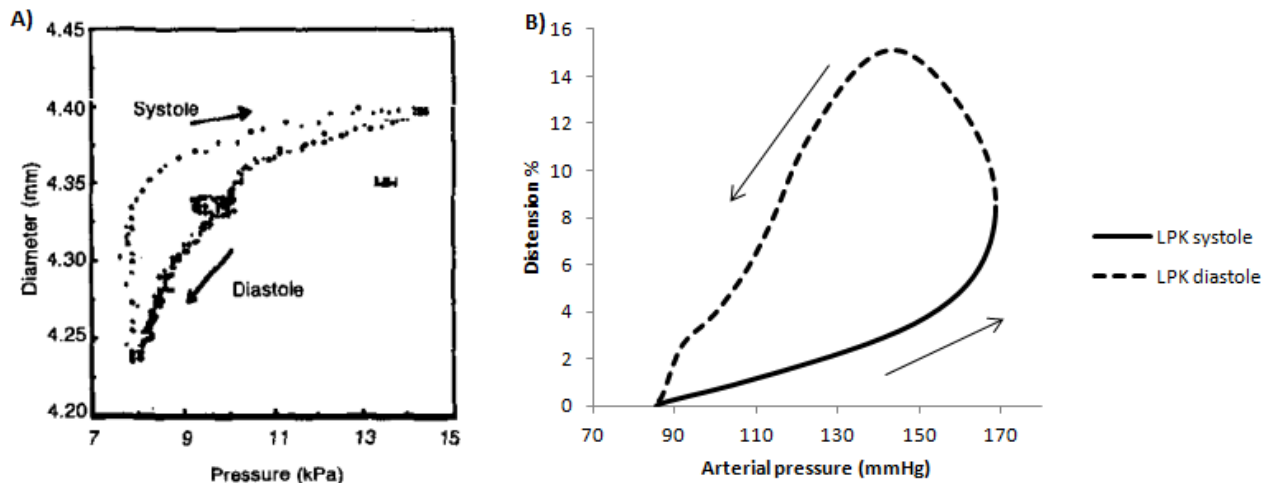


**Figure 0.5:** (a) Pressure-diameter curve from the brachial artery of a human. Systole is characterized by an exponential increase in diameter at low blood pressures followed by a plateau at higher blood pressures. Image from Tardy & Meister, 1991. (b) Pressure-diameter curve from the abdominal aorta of the LPK rat. Systole is characterized by a small increase in diameter at low blood pressures and an exponential increase in diameter during late systole and early diastole.

In rats, the pressure-distension loops are entirely opposite. During systole, the arterial diameter initially does not change much with respect to pressure, then as pressure increases the artery expands. This expansion continues through early diastole despite the lack of distending force. A possible reason for this phase delay is the HR in the rat is much faster than in humans but the pulse pressure is similar, resulting in a very short time for the distending pressure to affect wall distension, for example it takes only approximately 40ms to reach maximum distension in the rat compared to 150ms for humans (Rhodes and Phlanzer, 2003). Such a rapid increase in pressure forces the diameter expansion to lag behind, resulting in the small amount of distension during the initial phase of systole. However, as systole finishes, the inertia is still being applied to the arterial wall, resulting in a large increase in diameter with relatively little change in pressure.

These observations have also been made by other groups assessing arterial stiffness using arterial wall tracking in rats (Vayssettes-Courchay et al. 2011b). However, this work did not

elucidate the difference of the pressure-distension curves between rat and human arteries. To the authors knowledge, this is the first study to recognise that the rat and human arteries are exposed to different time-dependent distending stressors. The rat arterial vasculature is subject to similar distending pressure as in that of the human. However, the HR is significantly higher in the rat and this results in a significantly higher  $dP/dt(max)$ . The higher  $dP/dt(max)$  is not coupled with any change in the wall thickness to radius ratio ( $h/r$ ) compared with the normal human  $h/r$  (Wolinsky & Glagov 1969), therefore the increases in viscoelasticity observed here are being borne entirely by the arterial wall. The potential effects of such wall stress will require further research.

There was no difference in baroreceptor activity between both Lewis and LPK as determined by the lack of change in gain. Although some studies have shown there to be a positive correlation between polycystic kidney disease and SNA (Klein et al. 2001b), these results do not differ significantly from previous studies which also showed a lack of difference in SNA gain between Lewis and LPK (Harrison et al. 2010b).

There was also no difference shown in the any haemodynamic parameters between sexes (data not shown). These results have also been observed by the founder of the LPK strain Professor Jacqueline Phillips (unpublished data).

### **1.33.2 Sympathetic effects on arterial haemodynamics**

The effects of sympathetic blockade on large artery mechanics in the Lewis and LPK reflects systemic changes in SNA, not limited to the aorta. In addition to altering vascular smooth muscle tone, sympathetic blockade also reduced HR and  $dP/dt(max)$ . Similar to the differences seen between LPK and Lewis, these parameters also altered aortic viscoelasticity within strains. One of the most salient findings in this study was the dissociation of the

effects of sympathetic blockade on the traditional metrics for arterial stiffness (PWV, compliance and distensibility) which were moderately changed within rat strains and the metrics of viscoelasticity (distension and AIC) which were changed markedly. These findings suggest that the main effect of sympathetic denervation was on cardiac function, affecting contractility, and so the dynamic loading of the vascular wall as quantified by  $dP/dt(max)$ , as opposed to a predominantly direct effect on aortic smooth muscle.

SNA has a marked pressure-dependent effect on arterial stiffness within the two strains of rats studied. In the Lewis strain, sympathetic denervation produced a significant increase in shift in the pressure-distension curve at 75 mmHg and 100 mmHg. With increasing pressure, this effect became more attenuated and was absent at a MAP of 150 mmHg. Conversely, the LPK showed no effect of sympathetic blockade on distension at 75 mmHg, with large increases present at 100 and 125 mmHg as well as some preserved increase in distension at 150 mmHg.

The pressure ranges for which the largest change in distension occurred reflected the resting anaesthetised blood pressure of each of these strains of animal. That is, the Lewis had an anaesthetised resting MAP of  $82 \pm 8$  mmHg whilst the LPK had a resting MAP of  $124 \pm 5$  mmHg. Arterial remodelling occurs around the pressures to which an animal is exposed and occurs more rapidly at higher blood pressures (Liu & Fung 1996). Typically, this remodelling is characterized by an increase in smooth muscle density, thus giving the artery greater potential to actively change its tone despite an increase in blood pressure (Aars 1971, Fridez et al. 2002). This may account for why the LPK rats were able to continue to show differentiation in its pressure-distension curves at 150 mmHg with sympathectomy whilst the Lewis rats could not. Similar results are also found in the previous chapter with respect to the differences between WKY's and SHR's.

As the present study showed a reduction in both HR and  $dP/dt(\max)$  following sympathectomy, it was necessary to conduct step-wise multiple linear regression to determine which factors, including SNA, were the drivers of the changes in arterial stiffness and viscoelasticity. This revealed that indeed the majority of the variance seen in AIC was attributable to  $dP/dt(\max)$  (Table 7.6). This result is consistent with the previously established concept that the shape of pressure-distension loops in rats is highly influenced by HR and consequently the  $dP/dt(\max)$ . Indeed, this was to such an extent that it completely inverts the shape of the ascending pressure distension relationship compared to humans (Figure 0.5a vs Figure 0.5b). One must then account for the result thusly: when  $dP/dt(\max)$  is reduced as a result of the reduction in HR and cardiac contractility, the aorta has more time to increase its diameter resulting in a steadier ascending pressure-distension curve, therefore making it more similar to the descending pressure-distension curve, and as a result AIC is decreased.

A particular finding was that despite there being no difference between the systolic pressure-distension phase of the Lewis control and the Lewis denervated at a MAP of 150 mmHg, there was still a difference between their measured AIC. Indeed there are still differences in both  $dP/dt(\max)$  and HR at this pressure range, and this occurred despite the expectation that the sympathoinhibition following phenylephrine infusion would be close to that of hexamethonium. In fact, the HR changes during a phenylephrine challenge are small compared to those achieved after hexamethonium has had time to completely affect HR and contractility (Figure 0.6). Furthermore, intravenous phenylephrine produced a transient increase in  $dP/dt(\max)$  due to increased venous return (Cannesson et al. 2012) compared to the sustained decrease following hexamethonium (Figure 0.6). Therefore, it is likely that the decreased HR in the denervated state increased the time for elastic recoil during diastole thus decreasing the AIC.

Conversely, it was shown that at 75 mmHg, sympathetic denervation was unable to produce any change in distension in the LPK despite a reduction in both HR and  $dP/dt(\max)$ . At this pressure range, it may be that the distending pressure was not sufficient for the effects of  $dP/dt(\max)$  to have any effect on viscoelasticity. This is supported by the observation that the LPK had a significantly higher PWV at MAP's of 75-125 mmHg. Thus, the aorta is still relatively stiff at these pressures due to the increased deposition of collagen and smooth muscle cells (Ng et al. 2011b), therefore the reduced  $dP/dt(\max)$  cannot alleviate the influence of the passive properties of the aorta.

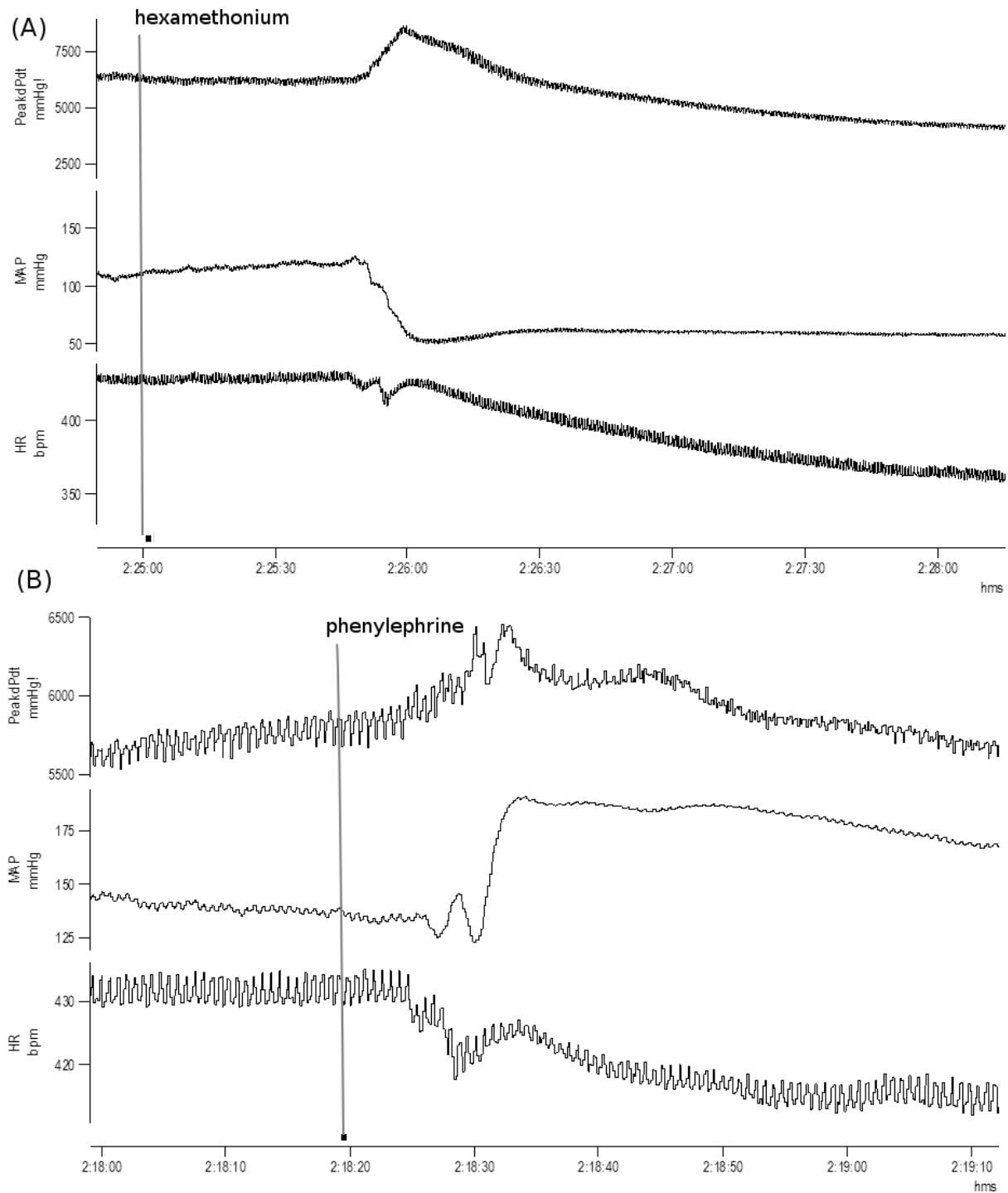


**Figure 0.6:** Comparison of HR and  $dP/dt(\max)$  changes following injection of hexamethonium (A) and injection of phenylephrine (B). Following hexamethonium there is a significant and persistent decrease in both HR and  $dP/dt(\max)$  as the drug causes complete sympathetic blockade. However, the phenylephrine induced changes in HR are small and transient and do not affect  $dP/dt(\max)$ .

This study did not find any significant changes in stiffness as measured by distensibility or following sympathetic blockade and only a change in PWV at a MAP of 100 mmHg in the

Lewis rat. This may either be explained by unseen changes in wall thickness which counter the directional change in PWV (see Moens-Korteweg equation, Chapter 3) or by the lack of sensitivity of PWV to measure acute changes in arterial stiffness in rodents. At the time of writing, there have been only two studies in rats that have shown a change in PWV independent of blood pressure after administration agents affecting acute manipulations (Fitch et al. 2001, Tan et al. 2012b).

Unlike the findings in the aforementioned study by Tan et al, 2012, step-wise linear regression revealed that HR did not contribute the most to the changes seen in PWV. Indeed, the contributors to changes in PWV differed between strains of rat. In the Lewis, PWV was most significantly affected by MAP then HR and SNA, while the LPK was most affected by  $dP/dt(max)$ , sympathetic blockade then MAP. These results further demonstrate the factors most influencing the arterial stiffness of the LPK are those which alter the rate at which the arterial wall is loaded and unloaded.

### **1.34 Conclusions**

These results demonstrate that whilst the direct effects of sympathetic tone on aortic smooth muscle may not strongly affect aortic stiffness in these strains of rats, changes in sympathetically mediated cardiovascular outputs such as HR and cardiac contractility are sufficient to cause marked changes in the stiffness profile of arteries. However, given the newly discovered differences in murine systolic pressure-distension curve compared to human P-D curves, it is apparent that rat aortic stiffness may have a stronger dependence on factors that alter the rate of cardiac contraction, and so the dynamic loading of artery walls. Further studies are needed to assess whether this is consistent in humans.

## Conclusions

Presently, CVD poses a great human and financial health toll. Contributing to the development of CVD is arterial stiffness as is made evident from both its known pathophysiology (O'Rourke & Hashimoto 2007) and the plethora of epidemiological studies which indicate its predictive value of cardiovascular diseases and all-cause mortality in both the hypertensive and normal population (Blacher et al. 1999, Laurent et al. 2001, Mattace-Raso et al. 2006). As such, arterial stiffness is now recognised by the European Society of Hypertension as a metric to be measured in the treatment of hypertension (Mancia et al. 2007).

It was in the spirit of further understanding the physiology of arterial stiffness that this thesis was written. For it is known that alteration of arterial smooth muscle tone is sufficient to cause changes in arterial stiffness in a variety of different sized arteries (Bank et al. 1995a, Bia et al. 2003b, Dobrin & Rovick 1969, Weber et al. 1996). It was therefore hypothesized that manipulation of SNA which innervates the smooth muscle of large arteries may also be sufficient to change arterial stiffness, thereby potentially providing a site of action for the treatment of arterial stiffness and consequently CVD.

In order to test this hypothesis, arterial stiffness data were captured using both pressure sensor catheters to derive PWV as well as ultrasound to obtain arterial diameters throughout the cardiac cycle (Chapter 3). These diameter data combined with pressure data allowed for



the calculation of compliance based arterial stiffness measurements. This provided a robust means of calculation of arterial stiffness which effectively measured both the changes in material stiffness of the arterial wall (mostly via PWV) but also the change in the capacitance function of the arterial wall (mostly via compliance, distensibility, AIC). Sympathetic denervation and blockade was performed to determine the contribution of sympathetic tone to arterial stiffness as well as other haemodynamic parameters simultaneously being recorded.

The first study which attempted to determine the contribution of SNA to arterial stiffness involved a unilateral physical denervation of the left lesser splanchnic nerve, which innervates the abdominal aorta (Chapter 4). The results showed no significant differences in arterial stiffness. A previous study by Gerova et al (Gerová et al. 1973) had shown that both the left and right sympathetic projections to the abdominal aorta contributed to 50% of the vascular tone, it was therefore considered that a change in arterial stiffness might be observed equal to half of SNA's potential. However, it was observed that following the aortic denervation, there was a reduction in blood pressure (consistent with the loss of some peripheral tone provided by the nerve) followed by a compensatory return to baseline blood pressure due to sympathoexcitation mediated by the baroreflex. It was surmised that this compensatory change in blood pressure was achieved by the remaining right splanchnic nerve, thus providing the abdominal aorta with SNA equivalent to the control condition and obfuscating any potential changes in arterial stiffness.

Since it would not be possible to apply the same physical denervation to both sides of the animal and still maintain static positioning of the ultrasound probe on the abdominal aorta, global sympathectomy was achieved via the nicotinic antagonist hexamethonium (Hunter 1950, Mathias 1991). In addition to this, the diameter data was further examined throughout the cardiac cycle allowing for the creation of pressure-distension loops which provided

insight into the changes in arterial stiffness as the aorta transitioned through systole and diastole. These new methodologies were first used on normotensive WKY's and showed that at mean arterial pressures (MAP) of 25 mmHg around the resting anaesthetized blood pressure (100mmHg), a significant decrease in arterial stiffness was observed as determined by both PWV and pressure-distension measurements (Chapter 5). These results suggested that at resting and lower blood pressures, aortic smooth muscle is capable of modifying arterial stiffness. However, as the distending pressure is increased, the passive collagen fibres in the arterial wall are increasingly loaded leaving no capacity for changes in smooth muscle tone to alter arterial stiffness.

SHR's were used as a model known for both increased SNA and their predisposition toward arterial stiffness (Chapter 6). It was hypothesized that as they exhibited a higher baseline SNA, removal of SNA would result in a greater change in arterial stiffness compared to their normotensive counterparts (WKY). It was also expected that the SHR would show reductions in aortic stiffness at high blood pressures due to the absence of a sympathoinhibited control condition, as was present in the WKY. The findings for the SHR were similar to that of the WKY; arterial stiffness was reduced following sympathectomy at 100mmHg, although to a much lesser extent. There were no significant changes in stiffness at high blood pressures. It was concluded that in spite of, or perhaps due to the apparent arterial remodelling seen in the SHR, the reduction in SNA was unable to produce enough change in smooth muscle tone to reduce aortic stiffness at high blood pressures.

In order to determine whether the effects seen in the SHR were due to arterial remodelling or the effects of distending pressure on arterial stiffness, sympathectomy was conducted on a more rapidly developing rodent model of hypertension, the Lewis Polycystic Kidney (LPK) diseases rat and their normotensive control, the Lewis rat (Chapter 7). The hypertension seen

in the LPK is fully manifest at 12 weeks of age, therefore they were afforded less time to undergo markedly significant arterial remodelling. Both the Lewis and LPK showed decreased arterial stiffness following sympathectomy around the resting anesthetized blood pressures of each strain. However, both of these strains showed additional cardiac contribution towards the pressure-distension derived arterial stiffness. Specifically, it was found that the combination of reduced heart rate and cardiac contractility (as determined by the rate of change in blood pressure:  $dP/dt(max)$ ) resulting from the sympathectomy changed the viscoelasticity of the artery. This study provided evidence that the effect of SNA on arterial stiffness may not be limited to the tonic effects on arterial smooth muscle but also other sympathetic efferents, including innervation of cardiac muscle affecting contractility and so changing the dynamic loading of the artery wall. These cardiac effects were only apparent in both the Lewis and LPK rats, the WKY and SHR did not show consistent differences in  $dP/dt(max)$  either between strains or following sympathetic denervation. This likely accounts for the absence of the lack of change in viscoelasticity in Chapters 4-6.

The work in this thesis provides a robust quantification on the contribution of SNA towards large artery stiffness *in-vivo*. The findings of this work provide an additional avenue for consideration in the diagnosis and treatment of arterial stiffness in the management of CVD.

### **1.35 Limitations**

Experiments showed significant variability in PWV between animal strains. A possible reason for this may have been slight variations in the area of aorta examined between rats. Great care was always taken to place the pressure transducers across the length of the aorta by observing the shape of the pressure waveform and where applicable, observing the catheters with ultrasound. However, this was not always possible. Therefore, in certain rats

there may have been recordings of a segment of the thoracic aorta in addition to abdominal aorta, which has previously been shown to significantly alter the observed PWV (Ng et al. 2012).

Also, it should again be reiterated that the changes seen in these studies following sympathetic denervation of the anaesthetized rat aorta do not necessarily translate to the human aorta. Rather, this work is meant to model the effects of sympathetic input into smooth muscle of large arteries in humans some of which contain significantly more arterial smooth muscle than the aorta such as the brachial artery or indeed any peripheral large artery.

### **1.36 Future Work**

This thesis has shown that there is a relatively small but significant effect of acute changes in SNA on arterial stiffness and viscoelasticity. Such changes may need to be considered when designing therapies in the treatment of hypertension. One such therapy is baroreceptor field stimulation, designed for the treatment of resistant hypertensive patients. By maintaining stimulation of the baroreceptors, sustained sympathoinhibition is induced to reduce blood pressure. This in turn may produce changes in arterial stiffness akin to those seen following sympathetic blockade. A pilot study was conducted to determine the effects of baroreceptor stimulation on PWV and pulse pressure amplification, the results of which are describe in Appendix B.

In addition to the acute changes in aortic stiffness, chronic changes in SNA may lead to significant changes in arterial stiffness. Evidence comes from the recognition of the trophic role SNA has on the maintenance of arterial wall structure (Kacem & Sercombe 2008, Kacem et al. 1997, 2006). Constant sympathetic input is required to smooth muscle to prevent the

dedifferentiation of smooth muscle cells into a phenotype that leads to atherosclerosis. Further investigation may be required to determine whether this pathology contributes to arterial stiffness.

### **1.37 List of Findings**

The following lists the major findings and conclusions of this thesis:

- (i) Unilateral physical denervation is insufficient to produce a change in arterial stiffness. This is likely due to compensation of sympathetic tone by the remaining contralateral sympathetic projection.
- (ii) Sympathetic denervation produces a decrease in arterial stiffness at MAP's around the resting anaesthetized blood pressure of WKY's.
- (iii) Chronic exposure to high blood pressures induces vascular remodelling which alters aortic diameters.
- (iv) Significantly altering cardiac function via removal of sympathetic activity can significantly affect arterial viscoelasticity by altering the dynamic loading characteristics of the wall of conduit arteries.
- (v) Rats display a very different pressure-distension profile compared to humans owing to their significantly higher heart rates and  $dP/dt(max)$ .

Collectively, the findings of this thesis lead to a greater understanding of the function of SNA in determining large artery stiffness. This work therefore exists as part of the greater effort to understand the multitude of factors responsible for the development arterial stiffness.

# **Appendix A**

## **Vascular properties in response to sympathetic blockade in hypertension: the effect of age**

### **Summary**

The effects of age related increases in SNA on the development of arterial stiffness in the SHR were studied. SHR's display a marked increase in basal SNA compared to their normotensive controls (WKY). This increase in SNA begins developing early in the life of these animals. It was hypothesized that as these rats aged there would be a concordant increase in arterial stiffness with SNA due to an increase in aortic smooth muscle tone. It was further hypothesized that these increases in stiffness may be reduced by application of sympathetic blockade resulting in greater reductions in aortic stiffness following sympathetic blockade as the rats aged. No age-related changes in arterial stiffness, and only small changes in haemodynamic some parameters measured were found before or during sympathetic blockade in both the normotensive and hypertensive rats. Further studies may need to employ both a greater cohort of animals and a longer aging period to observe the age related effects of SNA on arterial stiffness.

## **A.1 Introduction**

It has been shown that aging is associated with an increase in sympathetic nerve activity (SNA). It is thought that this contributes to the development of hypertension in the elderly. It is hypothesized that the additional SNA also contributes to increased arterial stiffness in hypertension by means of aortic smooth muscle tone.

A rat model known for its rapid development of both hypertension and increased basal SNA is the spontaneously hypertensive rat (SHR). It has been shown by Judy & Farrell (Judy & Farrell 1979) that both mean arterial pressure (MAP) and SNA increase rapidly in the SHR from the ages of 5-15 weeks followed by a plateau in both of these parameters. It was therefore hypothesized that throughout this period one may be able to observe an associated increase in aortic stiffness with age, consistent with increased recruitment of aortic smooth muscle resulting from increasing SNA. Furthermore, it was hypothesized that the chemical removal of SNA by means of hexamethonium would reduce the tone of the aorta, resulting in greater reductions in aortic stiffness following sympathetic blockade as the rats aged.

This appendix offers an age-based breakdown of the averaged results presented in Chapter 6.

## **A.2 Methods**

### **A.2.1 Animals**

Male Wistar Kyoto (WKY) rats and spontaneously hypertensive rats (SHR) were separated into three groups each studied at a different age: 10 weeks (n= WKY, 10 SHR), 15 weeks (n=4 WKY, 9 SHR) and 20 weeks (n=5 WKY, 8 SHR). Animals weighed  $300\pm 50$  g and were



sourced from the Animal Resource Centre in Perth Australia. All animals were anaesthetized and monitored as per Section 3.1.

### **A.2.2 Procedures**

All animals were instrumented and blood pressure was measured as described in Chapter 3, Sections 3.3 and 3.4. Diameter measurements were made as described in Chapter 3, Section 3.2. Sympathetic nerve recordings were made as described in Chapter 3, Section 3.3

### **A.2.3 Data and statistical analysis**

Arterial stiffness data were analysed as per chapter 3.4.

Both strains were compared at their resting anaesthetized blood pressure at each age group. Comparisons were made using unpaired Students t-tests. In addition, all haemodynamic parameters were compared within discrete MAP groups (75mmHg, 100mmHg, 125mmHg, 150mmHg) with respect to animal strain, age and state of SNA.

## **A3. Results**

### **A.3.1 Haemodynamic comparisons between strains and ages at resting anesthetized blood pressures**

Resting anaesthetized MAP was increased at all ages in the SHR compared to the WKY (10 weeks:  $92 \pm 13$  mmHg vs  $140 \pm 16$  mmHg,  $p < 0.001$ ; 15 weeks:  $100 \pm 21$  mmHg vs  $140 \pm 18$  mmHg,  $p < 0.01$ ; 20 weeks:  $101 \pm 8$  mmHg vs  $126 \pm 12$  mmHg,  $p < 0.01$ , Table 1). Systolic pressure was also higher in SHR (10 weeks:  $112 \pm 12$  mmHg vs  $170 \pm 18$  mmHg,  $p < 0.001$ ; 15 weeks:  $122 \pm 29$  mmHg vs  $169 \pm 21$  mmHg,  $p < 0.001$ ; 20 weeks:  $120 \pm 10$  mmHg vs  $156 \pm 14$

mmHg,  $p<0.001$ , Table 1), as was pulse pressure (10 weeks:  $37\pm6$  mmHg vs  $53\pm5$  mmHg,  $p<0.001$ ; 15 weeks:  $40\pm11$  mmHg vs  $52\pm7$  mmHg,  $p<0.01$ ; 20 weeks:  $38\pm8$  mmHg vs  $53\pm10$  mmHg,  $p<0.05$ , table 1). These increases in blood pressure were accompanied by an increase in PWV at 15 and 20 weeks (15 weeks:  $4.09\pm0.29$  m/s vs  $7.92\pm2.24$ m/s,  $p<0.01$ ; 20 weeks:  $4.25\pm1.24$ m/s vs.  $7.70\pm1.85$ m/s,  $p<0.01$ , Table 1). There was no difference in heart rate between strains at any age. Nor were there any differences in any measured parameter between ages.

**Table A.1:** Baseline haemodynamic values for both SHR and WKY at the ages studied. Significant differences between WKY and SHR are indicated with \* $p<0.05$ , \*\* $p<0.01$ , \*\*\* $p<0.001$ .

	10 weeks		15 weeks		20 weeks	
	WKY	SHR	WKY	SHR	WKY	SHR
MAP (mmHg)	$92\pm 13$	$140\pm16^{***}$	$100\pm21$	$140\pm18^{**}$	$101\pm8$	$126\pm12^{**}$
HR (BPM)	$412\pm20$	$400\pm33$	$408\pm27$	$407\pm16$	$394\pm32$	$396\pm19$
Systolic Pressure (mmHg)	$112\pm12$	$170\pm18^{***}$	$122\pm29$	$169\pm21^{**}$	$120\pm10$	$156\pm14^{***}$
Diastolic Pressure (mmHg)	$74\pm14$	$116\pm16$	$82\pm18$	$116\pm17$	$83\pm9$	$103\pm11$
Pulse Pressure (mmHg)	$37\pm6$	$53\pm5^{***}$	$40\pm11$	$52\pm7^{**}$	$38\pm8$	$53\pm10^*$
dP/dt(max) (mmHg/s)	$4164\pm179$ 7	$4033\pm919$	$4300\pm179$ 4	$4317\pm891$	$4840\pm186$ 4	$4131\pm1803$
PWV (mmHg)	$4.89\pm1.13$	$5.46\pm0.65$	$4.09\pm0.29$	$7.92\pm2.24^*$ *	$4.25\pm1.24$	$7.70\pm1.85^*$ *

### A.3.2 Pressure matched differences in haemodynamic parameters between WKY and SHR

Only two differences were observed between haemodynamic parameters within a given age range and across all MAPs. These included a significant decrease in distensibility of the 15 week old denervated SHR compared to the 15 week old denervated WKY at 75mmHg (WKY denervate:  $3.66\times10^{-3}\pm0.38\times10^{-3}$  mmHg<sup>-1</sup>; SHR denervate:  $2.22\times10^{-3}\pm0.38\times10^{-3}$  mmHg<sup>-1</sup>: Table A.1). Also a significant increase in pulse pressure (PP) in the 20 week old denervated

SHR compared to the 20 week old denervated WKY (WKY denervate:  $56 \pm 3$  mmHg; SHR denervate:  $64 \pm 3$  mmHg; Table A.4). All differences between strain and SNA averaged across all ages are examined in Chapter 6.

**Table A.2:** Comparison of haemodynamic parameters at a MAP of 75 mmHg between WKY's and SHR's across three age ranges and before and after sympathetic denervation. A significant difference is observed between the aortic distensibility of the 15 week old denervated WKY and 15 week old denervated SHR. \*\*\*p<0.001.

75mmHg	10 weeks		15 weeks		20 weeks	
	WKY	SHR	WKY	SHR	WKY	SHR
<b>Control</b>						
Systolic (mmHg)	93±3	94±2	95±4	91±2	91±3	91±2
Diastolic (mmHg)	56±2	58±2	56±4	60±2	57±2	56±2
PP (mmHg)	38±4	38±3	36±6	33±3	35±4	36±3
Heart rate (bpm)	396±15	382±10	408±21	392±10	402±15	387±11
dP/dt(max) (mmHg/s)	4950±741	4106±494	5500±1048	3425±524	5337±741	3471±560
Compliance (mm/mmHg)	4.32±0.66	7.20±0.44	5.45±0.94	3.49±0.47	4.41±0.66	4.15±0.50
Distensibility (x10 <sup>-3</sup> /mmHg)	3.73±0.53	5.09±0.35	4.55±0.74	3.13±0.37	3.50±0.53	3.29±0.37
PWV (m/s)	4.32±0.47	3.26±0.32	4.07±0.67	3.73±0.33	4.31±0.67	3.73±0.36
<b>Denervated</b>						
Systolic (mmHg)	97±3	98±2	94±4	98±2	95±3	98±2
Diastolic (mmHg)	55±2	55±2	54±4	58±2	55±2	54±2
PP (mmHg)	41±4	43±3	42±6	47±3	36±4	44±3
Heart rate (bpm)	348±15	347±10	318±21	333±10	336±15	332±11
dP/dt(max) (mmHg/s)	4975±741	4172±494	4450±1048	3038±524	4067±741	2941±560
Compliance (mm/mmHg)	6.74±0.66	6.00±0.44	7.46±0.94	3.16±0.47	4.40±0.66	3.62±0.50
Distensibility (x10 <sup>-3</sup> /mmHg)	5.39±0.52	5.09±0.35	5.99±0.73***	3.13±0.37***	3.13±0.52	3.10±0.37
PWV (m/s)	3.93±0.47	3.30±0.32	3.72±0.67	3.72±0.33	4.24±0.67	3.72±0.36

**Table A.3:** Comparison of haemodynamic parameters at a MAP of 100 mmHg between WKY's and SHR's across three age ranges and before and after sympathetic denervation. No significant difference was observed between any parameters as a function of age.

100mmHg	10 weeks		15 weeks		20 weeks	
	WKY	SHR	WKY	SHR	WKY	SHR
<b>Control</b>						
Systolic (mmHg)	127±2	123±3	119±3	120±2	123±2	128±2
Diastolic (mmHg)	79±2	80±3	83±3	81±2	81±2	84±2
PP (mmHg)	38±3	40±5	49±4	39±3	39±4	46±4
Heart rate (bpm)	398±11	333±15	388±13	381±9	395±12	384±12
dP/dt(max) (mmHg/s)	4094±467	2683±660	4750±660	3516±381	4790±510	3229±512
Compliance (mm/mmHg)	3.91±0.62	3.92±0.87	5.09±0.76	3.10±0.50	4.12±0.68	3.34±0.68
Distensibility (x10 <sup>-3</sup> /mmHg)	3.21±0.34	3.38±0.48	3.94±0.49	2.54±0.28	2.75±0.38	2.33±0.38
PWV (m/s)	4.69±0.36	5.58±0.51	5.54±0.63	4.16±0.30	4.73±0.63	4.36±0.40
<b>Denervated</b>						
Systolic (mmHg)	126±2	131±3	126±3	126±2	126±2	134±2
Diastolic (mmHg)	76±2	73±3	79±2	76±2	79±2	81±2
PP (mmHg)	46±3	58±5	49±4	53±3	46±4	55±4
Heart rate (bpm)	331±11	297±15	344±13	324±9	352±12	336±12
dP/dt(max) (mmHg/s)	4030±467	4133±660	4401±572	3872±381	4438±512	3974±511
Compliance (mm/mmHg)	5.52±0.62	3.14±0.87	6.08±0.76	2.66±0.50	4.38±0.68	2.74±0.68
Distensibility (x10 <sup>-3</sup> /mmHg)	3.77±0.34	2.52±0.48	4.04±0.42	2.33±0.28	3.16±0.38	1.83±0.38
PWV (m/s)	4.57±0.36	5.40±0.51	3.19±0.63	4.10±0.30	4.54±0.63	4.64±0.40

**Table A.4:** Comparison of haemodynamic parameters at a MAP of 125 mmHg between WKY's and SHR's across three age ranges and before and after sympathetic denervation.

125mmHg	10 weeks		15 weeks		20 weeks	
	WKY	SHR	WKY	SHR	WKY	SHR
<b>Control</b>						
Systolic (mmHg)	148±4		160±5	154±6	156±4	159±5
Diastolic (mmHg)	106±3		112±3	105±4	105±3	104±3
PP (mmHg)	46±3		50±4	54±4	50±3	55±4
Heart rate (bpm)	379±11		358±14	393±16	359±11	380±14
dP/dt(max) (mmHg/s)	3719±560		4038±686	4617±792	4244±560	4480±686
Compliance (mm/mmHg)	2.75±1.06		4.36±0.91	2.05±0.15	3.16±2.49	2.31±0.61
Distensibility (x10 <sup>-3</sup> /mmHg)	1.63±0.37		1.89±0.37	1.69±0.53	1.94±0.41	1.88±0.46
PWV (m/s)	5.73±0.51		4.41±0.73	5.73±0.73	5.37±0.89	5.77±0.73
<b>Denervated</b>						
Systolic (mmHg)	147±4		163±5	158±6	152±4	161±5
Diastolic (mmHg)	100±3		112±3	96±4	104±3	99±3
PP (mmHg)	49±3		50±4	66±4	49±3	64±4
Heart rate (bpm)	347±11		339±14	334±16	344±11	330±14
dP/dt(max) (mmHg/s)	3755±560		3212±686	5167±792	3892±560	4892±686
Compliance (mm/mmHg)	3.22±1.22		4.14±0.88	1.95±0.30	4.19±2.71	2.47±0.81
Distensibility (x10 <sup>-3</sup> /mmHg)	1.89±0.37		2.78±0.46	1.57±0.53	2.64±0.41	2.01±0.46
PWV (m/s)	5.64±0.51		5.00±0.89	5.52±0.73	5.18±0.89	5.72±0.73

**Table A.5:** Comparison of haemodynamic parameters at a MAP of 150mmHg between WKY's and SHR's across three age ranges and before and after sympathetic denervation. A significant difference was observed between the pulse pressure (PP) of the denervated 20 week old WKY compared to the denervated 20 week old SHR. \*\*p<0.01.

150mmHg	10 weeks		15 weeks		20 weeks	
	WKY	SHR	WKY	SHR	WKY	SHR
<b>Control</b>						
Systolic (mmHg)	182±4	176±3	186±6	183±3	180±4	184±3
Diastolic (mmHg)	120±3	122±2	122±5	128±2	125±3	127±3
PP (mmHg)	65±3	56±2	70±5	56±2	57±3	59±3
Heart rate (bpm)	372±15	377±11	358±24	396±11	327±15	372±14
dP/dt(max) (mmHg/s)	4034±372	3670±263	4100±589	4514±277	3730±372	3406±340
Compliance (mm/mmHg)	2.48±1.91	2.89±1.07	1.94±0.33	1.89±0.40	2.03±1.21	2.23±1.04
Distensibility (x10 <sup>-3</sup> /mmHg)	1.47±0.23	1.65±0.16	1.01±0.37	1.43±0.17	1.14±0.23	1.36±0.21
PWV (m/s)	7.61±0.67	5.40±0.47	6.09±1.05	5.96±0.50	5.95±1.05	6.59±0.61
<b>Denervated</b>						
Systolic (mmHg)	181±4	176±3	186±6	180±3	180±4	187±3
Diastolic (mmHg)	119±3	119±2	122±5	125±2	120±3	123±3
PP (mmHg)	65±3	58±2	62±5	57±2	56±3**	64±3**
Heart rate (bpm)	347±15	340±11	338±24	329±11	350±15	344±14
dP/dt(max) (mmHg/s)	3582±372	3244±263	3250±589	3828±277	3665±372	3754±340
Compliance (mm/mmHg)	1.72±0.56	3.33±1.12	2.33±0.41	1.95±0.39	2.36±1.78	2.06±0.61
Distensibility (x10 <sup>-3</sup> /mmHg)	0.96±0.23	1.61±0.16	1.15±0.36	1.45±0.17	1.14±0.23	1.31±0.21
PWV (m/s)	7.32±0.67	5.41±0.47	5.98±1.05	6.00±0.50	5.95±1.05	6.60±0.61

## A.4 Discussion

This sub-analysis of the study presented in Chapter 6 sought to examine the development of aortic stiffness over an age range that has previously been shown to be the period of hypertension development in the SHR (Cosson et al. 2007, Hambley et al. 1987b, Judy & Farrell 1979). The results showed that there is no significant effect of SNA on the development of arterial stiffness between the ages of 10 weeks and 20 weeks. Indeed, it was also shown that there were no significant changes in any haemodynamic parameter across the age ranges studied in both the WKY and SHR.

In relation to the resting anesthetized blood pressures of all the rats that at the age of 10 weeks, there was already a significant difference in the MAP of the WKY and SHR. As both strains aged, there were no further changes in any of the haemodynamic parameters measured. These results differ from those of (Cosson et al. 2007) who showed both an increased progression of SBP, DBP, MAP, HR and PWV as both the WKY and SHR aged. However, these changes occurred largely between the ages of 6 weeks and 12 weeks, a period not covered in the present study. This may indicate that there are greater cardiovascular changes in the 6 to 12 week period than in the 10 to 20 week period.

Alternative explanations for the lack of significance seen between age in this study is the relatively low sample sizes acquired for each age range. The sample size was sufficient for the study design as presented in Chapter 6, but lacked statistical power in the sub-analysis breakdown as presented here.

Future research into determining the effect of SNA on the development of hypertension might do well to extend the scope of the aging study to greater than 6 months. For whilst the



magnitude of SNA and MAP does begin to plateau at 20 weeks (Cosson et al. 2007, Hambley et al. 1987b, Judy & Farrell 1979), more time allows for increases in sympathetic nerve density at the site of efferent organs (Burgi et al. 2011, Thrasivoulou & Cowen 1995). Such increases in nerve density to the aortic smooth muscle may cause increased aortic tone resulting in increased arterial stiffness.

# **Appendix B**

## **Aortic stiffness and pressure waveform parameters during baroreceptor field stimulation driven changes in sympathetic nerve activity**

### **Summary**

Long term baroreceptor field stimulation is proposed as a treatment for human resistant hypertension and has been made feasible through the advent of baroreceptor activation through field stimulation. The mechanism of blood pressure lowering through baroreceptor stimulation is a reduction in sympathetic output. This appendix summarises a pilot study that investigated the effect of field stimulation of the baroreceptors in rodents on aortic parameters of stiffness and waveform shape. It was found that acute field stimulation to invoke a baroreceptor response lowered blood pressure in a manner that has the same end effect on aortic stiffness and parameters of aortic waveform shape as when blood pressure was lowered with a peripheral vasodilator. Further investigations are required to quantify the effect of long term blood pressure lowering through field stimulation of the baroreceptors on aortic parameters.

This work was the subject of an oral presentation at the European Society of Hypertension Conference, 2013 (Butlin et al. 2013) and contributes to work under the Australia Research Council Linkage Grant LP120100463 with industry partner CVRx, manufacturers of field baroreceptor stimulation devices.

## **B.1 Introduction**

The baroreceptor mechanism regulates blood pressure through a negative feedback loop, with stretch receptors embedded in the arteries (aortic arch, carotid sinus) detecting increased vessel extension driven by rises in blood pressure, converted to afferent signals and inverted to drive a decrease in SNA and thus a decrease in blood pressure through the subsequent cardiovascular effect. If baroreceptor activity were driven independent of a blood pressure increase, it provides a possible model to investigate physiological changes in SNA and the effect upon aortic wall mechanics.

Baroreceptor stimulation has long been known as a possible blood pressure lowering mechanism and therapy (Braunwald & Epstein 1967). However, direct stimulation of baroreceptor related nerves did not prove to be a successful long term treatment due to deterioration of the stimulation contact. More recently, field stimulation of the baroreceptor complex has proved a successful acute (Heusser et al. 2010) and long term method of blood pressure lowering therapy (Bakris et al. 2012). However, the effect of baroreceptor field stimulation, and indeed baroreceptor stimulation in general, upon the aorta has not been studied. This pilot study begins an investigation along these lines by evaluating parameters of stiffness and pressure waveform shape in the descending aorta of rodents during acute lowering of blood pressure driven by field stimulation of the baroreceptor complex.

## **B.2 Methods**

Spontaneously hypertensive rats (13 weeks old,  $n=3$ ) were anaesthetised (urethane). The right carotid artery was exposed and instrumented with a field stimulator just before the carotid bifurcation, and therefore near the carotid baroreceptor sinus (Figure B.1). Two high fidelity

pressure sensors were introduced into the aorta as outlined previously (Chapter 3) but placed in the thoracic and abdominal aorta for measurement of thoracic aortic blood pressure and PWV in the descending trunk of the aorta. Pulse pressure amplification ( $PP_{amp}$ , Equation B.1) and form factor (FF, a parameter of waveform shape, Equation B.2) were calculated.

Blood pressure was lowered sequentially (in a randomised order) by continuous baroreceptor field stimulation, pulsed baroreceptor field stimulation (1 second on, 1 second off), and intravenous infusion of sodium nitroprusside (SNP, blood pressure control arm, as outlined previously in Chapter 3). Unipolar stimulation was at 1 kHz with a 0.53 ms pulse width. The stimulating voltage was determined by first attaining the voltage at which mean blood pressure dropped by 5 mmHg, then multiplying this threshold voltage by 3. In trials of various voltages, a voltage of 3 times the threshold voltage appeared to give the maximal decrease in blood pressure (results not shown).

$$PP_{amp} = \frac{PP_{distal}}{PP_{proximal}} \quad \text{Equation B.1}$$

$$FF = \frac{MAP - DP}{PP} \quad \text{Equation B.2}$$

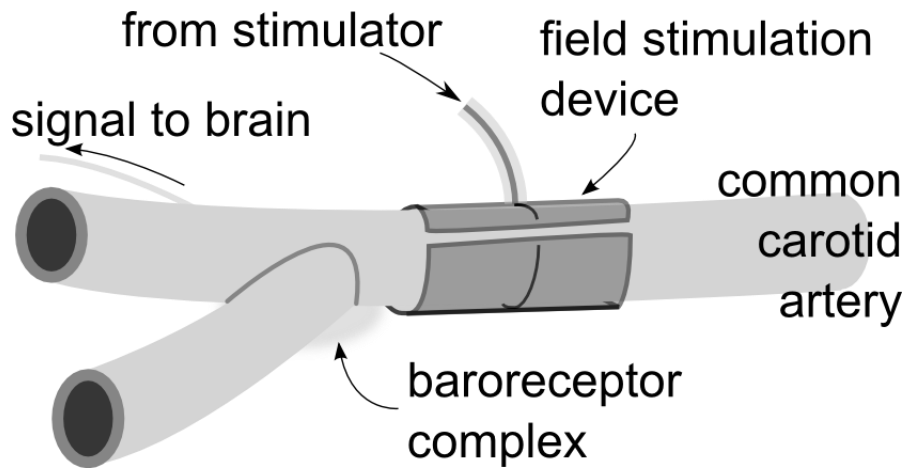


**Figure B.1:** Carotid baroreceptor field stimulation device for the rat. A unipolar electrode was placed around the common carotid artery, immediately below the bifurcation, held within a silastic tube.

Haemodynamic measurements were extracted for a 30% decrease in mean arterial pressure for the three modes of blood pressure lowering. Results were compared by paired t-test to ascertain if there were any differences in the arterial parameters in response to the different modes of blood pressure reduction.

### B.3 Results

Both continuous and pulsed field stimulation of the baroreceptors rapidly decreased blood pressure, heart rate, aortic PWV (Figure B.2),  $PP_{amp}$ , and FF (Table B.1). The direction of the response was similar in all repeated measurements in all rats. There were no significant differences in any of the parameters measured whether blood pressure was lowered through continuous or pulsed baroreceptor field stimulation or infusion of SNP (Table B.1).

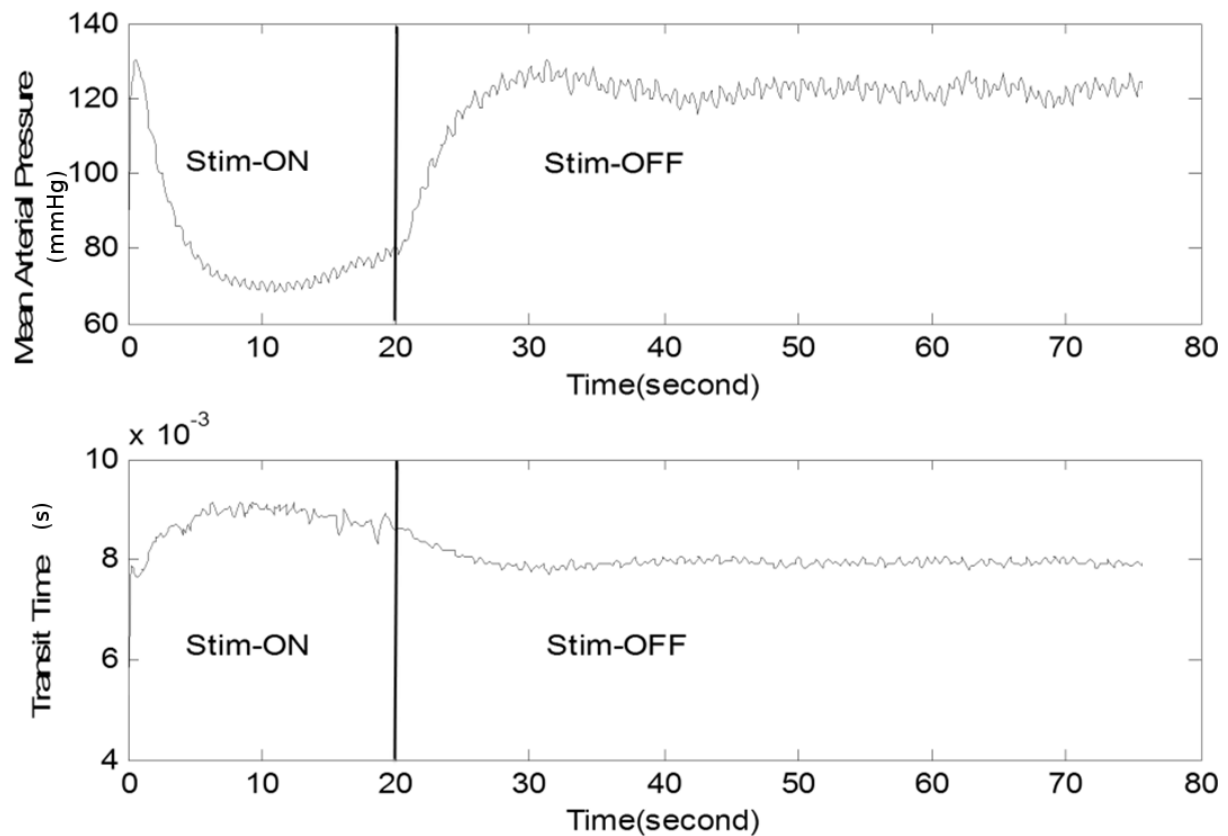


**Figure B.2:** An example recording within one rat during (Stim-ON) and following (Stim-OFF) acute baroreceptor field stimulation. A rapid blood pressure drop is associated with a rise in aortic transit time (increase in PWV). Upon switching field stimulation off, blood pressure and transit time rapidly return to baseline.

**Table B.1:** The change in pulse wave velocity (PWV), pulse pressure amplification (PPamp), and form factor (FF) following a 30% decrease in MAP driven by either continuous field stimulation of the carotid baroreceptor complex, pulse field stimulation of the baroreceptor complex, or lowering of blood pressure through vasodilation driven by sodium nitroprusside (SNP) infusion. There were no significant differences between any of the blood pressure lowering mechanisms for any of the parameters measured.

	value at 30% decrease in MAP		
	$\Delta$ PWV (%)	$\Delta$ PP <sub>amp</sub> (%)	$\Delta$ FF (%)
continuous field stimulation	$-10.0 \pm 2.9$	$-58 \pm 44$	$-3.3 \pm 8.3$
pulse field stimulation	$-6.6 \pm 1.8$	$-79 \pm 58$	$-5.5 \pm 11.7$
SNP infusion	$-13.4 \pm 4.7$	$-183 \pm 159$	$-4.2 \pm 7.0$

## B.4 Discussion

This pilot study indicates that in terms of the aortic pressure waveform, and the peripheral vascular influence on aortic pressure through wave reflection, there was no substantial difference between the use of baroreceptor field stimulation and the use of a peripheral vasodilator.

Although SNA was not measured in this pilot study, the mechanism of baroreceptor lowering of blood pressure is assumed to be driven through a reduction in SNA, whereas the vasoactive (SNP) mechanism of lowering of blood pressure would, if anything, cause an increase in SNA. This pilot study therefore provides an investigation of physiological changes in SNA and the effect that has on descending aortic PWV, the amplification of the pulse pressure along the aortic trunk, and a cursive investigation of wave reflection parameters through calculation of the form factor. Within the range of SNA changes in this study, there were no observed differences in aortic stiffness or wave reflection parameters.

There are two probable reasons behind this observation and the deviation from observations in the chapters of this thesis. Firstly, the change in SNA activity may not have been large enough to effect any changes in the aorta. Throughout this thesis, SNA reduction was produced by complete sympathetic blockade. It is probable that baroreceptor stimulation does not completely block all SNA, and further studies investigating baroreceptor stimulation during SNA recording will need to be conducted to confirm this. The probable relatively smaller reduction in SNA with baroreceptor stimulation may not have been enough to impart changes in the descending aorta, as observed in complete sympathetic blockade experiments in this thesis.

The second reason for the absence of any changes in aortic properties with baroreceptor driven changes in SNA is the site of measurement. All studies in this thesis investigated the abdominal aorta, where as this pilot study investigate the entire (thoracic and abdominal) descending aorta. The thoracic aorta contains relatively less smooth muscle than the abdominal aorta and therefore would have comparatively less change in response to SNA reduction.

This pilot study shows that field stimulation of the baroreceptor complex does not cause any changes in the average descending aorta of the rat. However, further studies are needed to investigate the effect on the abdominal aorta, including compliance and viscoelasticity measures utilising diameter measurements (Chapter 3) coupled with simultaneous recording of SNA.



# **Appendix C**

## **Animal Ethics Approval forms**

## ANIMAL RESEARCH AUTHORITY (ARA)

AEC Reference No.: 2010/003 – 2

Date of Expiry: 5 March 2012

**Full Approval Duration: 6 March 2010 to 5 March 2012 (24 months)**  
(initial 12 months plus 12 month extension granted Feb 2011)

This ARA remains in force until the Date of Expiry (unless suspended, cancelled or surrendered) and is contingent upon receipt of a Final Report at the end of this period (see Approval email for submission details).

**Principal Investigator:**

Prof Albert Avolio  
Australian School of Advanced Medicine  
Macquarie University NSW 2109  
0408 657 616  
[Alberto.avolio@mq.edu.au](mailto:Alberto.avolio@mq.edu.au)

**Associate Investigators:**

George Lindesay 0434 984 207  
Mark Butlin 0422 908 895

**Other people participating:**

Keith Ng 0433 538 697  
Wendy Liu 0404 413 580  
Isabella Tan 0416 192 968  
Prof Paul Pilowsky 0431 500 553  
A/Prof Ann Goodchild 0410 601 302  
Dr Simon McMullan 0402 073 146  
Dr Qi-Jian Sun 0413 733 250  
Dr Natasha Kumar 0413 339 954  
Melissa Farnham 0415 821 096  
Cara Hildreth 0402 836 705

**In case of emergency, please contact:**

**Animal Welfare Officer** 9850 7758 / 0439 497 383  
**Central Animal House Manager Christine Sutter:** 9850 7780 / 0428 861 163  
**or the Principal Investigator / Associate Investigator named above**

The above-named are authorised by MACQUARIE UNIVERSITY ANIMAL ETHICS COMMITTEE to conduct the following research:

**Title of the project:** The effect of sympathetic nerve input on large artery stiffness in conditions of normotension and hypertension

**Type of animal research and aims of project:**

Research (Cardiovascular) – This project aims to quantify the contribution of aortic sympathetic nerve input on the stiffness of large arteries and thus the impact on increasing blood pressure in normotension and hypertension.

**Surgical Procedures category:** 2 (Animal unconscious without recovery)

All procedures must be performed in accordance with the AEC approved protocol, unless Conditions of Approval state otherwise.

**Maximum numbers approved:**

Species	Strain	Age/Sex/Weight	Total	Supplier/Source
Rat	Spontaneously Hypertensive Rat (SHR)	24-26wks/male	15	ARC Perth
		10-12wks/male	15	
Rat	Wistar Kyoto (WKY)	24-26wks/male	15	ARC Perth
		10-12wks/male	15	

**Location of research:**

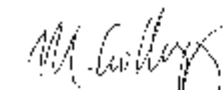
Location	Full street address
Australian School of Advanced Medicine	Level 1, Clinic Building, 2 Technology Place, Macquarie University NSW 2109
Central Animal House Facility	Building F9A, Research Park Drive, Macquarie University NSW 2109

**Amendments approved by the AEC since initial approval:**

1. 12-month extension to the ARA (Approved Feb 2011)

**Conditions of Approval: N/A**

Being animal research carried out in accordance with the Code of Practice for a recognised research purpose and in connection with animals (other than exempt animals) that have been obtained from the holder of an animal suppliers licence.



Prof Michael Gillings (Chair, Animal Ethics Committee)

Approval Date of Progress Report: 17 February 2011

## ANIMAL RESEARCH AUTHORITY (ARA)

AEC Reference No.: 2010/044 - 8

Date of Expiry: 31 August 2014

Full Approval Duration: 1 September 2010 to 31 August 2014 (48 months)

This ARA remains in force until the Date of Expiry (unless suspended, cancelled or surrendered) and will only be renewed upon receipt of a satisfactory Progress Report before expiry of this period (see Approval email for submission details).

**Principal Investigator:**

Dr Mark Butlin  
Australian School of Advanced Medicine  
Macquarie University NSW 2109  
[Mark.butlin@mq.edu.au](mailto:Mark.butlin@mq.edu.au) 0422 908 895

**Associate Investigators:**

Prof Alberto Avolio 0408 657 616  
Zahra Parisa Kouchaki 0403 491 774

**Other people participating:**

George Lindesay 0434 984 207  
Kayla Viegas 0424 024 776  
Omar Al-Adhami 0426 299 791  
Cara Hildreth 0402 836 705

**In case of emergency, please contact:**

Animal Welfare Officer - 9850 7758 / 0439 497 383

Manager, CAF - 9850 7780 / 0428 861 163

or the Principal Investigator / Associate Investigator named

The above-named are authorised by MACQUARIE UNIVERSITY ANIMAL ETHICS COMMITTEE to conduct the following research:

**Title of the project:** Large artery dimension, structure and stiffness in development of hypertension

**Purpose:** 4 - Research: human or animal biology

**Aims:** This project aims to observe if there are any differences in large artery dimensions, the amount and distribution of components in the artery wall, and the stiffness of the artery, in the presence or absence of high blood pressure (hypertension).

**Surgical Procedures category:** 2: Animal unconscious without recovery

**All procedures must be performed in accordance with the AEC approved protocol, unless Conditions of Approval state otherwise.**

**Maximum numbers approved:**

Species	Strain	Age/Sex/Weight	Year 1	Year 2	Year 3	Total	Supplier/Source
Rat	Spontaneously Hypertensive Rat (SHR)	12 weeks	16	16	17	49	ARC Perth
Rat	Wistar Kyoto (WKY)	12 weeks	16	16	17	49	ARC Perth
Rat	Sprague-Dawley (SD)	12 weeks	16	16	17	49	ARC Perth
TOTAL			48	80	68	147	

**Location of research:**

Location	Full street address
Australian School of Advanced Medicine	Level 1, Clinic Building, 2 Technology Place, Macquarie University NSW 2109
Central Animal Facility	Building F9A, Research Park Drive, Macquarie University NSW 2109

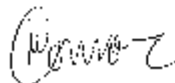
**Amendments approved by the AEC since initial approval:**

- 1) Approved AEC meeting 14 Oct 2010: addition of new Personnel: Kayla Viegas
- 2) Approved AEC meeting 2 Dec 2010: addition of new strain Fischer-344 rat, n=49
- 3) Approved AEC meeting 19 May 2011: addition of new personnel: Cara Hildreth and Omar Al-Adhami
- 4) Approved AEC meeting 11 August 2011: addition of ventilation under anaesthesia and neuromuscular blockade
- 5) Approved AEC meeting 14 June 2012: addition of Tegan Hunter as Associate Investigator
- 6) Approved AEC meeting 13 March 2013: addition of Parisa Kouchaki as Associate Investigator & removal of Tegan Hunter
- 7) Approved AEC meeting 13 August 2013: extension of approval duration by 1 year and removal of 49 Fischer-344 rats from the study

**Conditions of Approval:**

1. The PI must consult the Manager, CAF (Christine Sutter) to make arrangements for use of space and/or resources in the facility. An email is required from the Manager to the AEC (via [animal.ethics@mq.edu.au](mailto:animal.ethics@mq.edu.au)) confirming whether the facility can accommodate requirements for this protocol. – documented 24/02/2011

Being animal research carried out in accordance with the Code of Practice for a recognised research purpose and in connection with animals (other than exempt animals) that have been obtained from the holder of an animal suppliers licence.



Professor Mark Connor (Chair, Animal Ethics Committee)

Approval Date: 19 September 2013

# ANIMAL RESEARCH AUTHORITY (ARA)

AEC Reference No.: 2011/044 – 14

Date of Expiry: 11 September 2014

Full Approval Duration: 12 September 2011 to 11 September 2014 (36 months)

This ARA remains in force until the Date of Expiry (unless suspended, cancelled or surrendered) and will only be renewed upon receipt of a satisfactory Progress Report before expiry (see Approval email for submission details).

**Principal Investigator:**  
Prof. Jacqueline Phillips  
Australian School of Advanced Medicine  
Macquarie University NSW 2109  
0409 225 707  
[Jacqueline.phillips@mq.edu.au](mailto:Jacqueline.phillips@mq.edu.au)

**Associate Investigators:**  
Alberto Avolio 0408 657 616  
Cara Hildreth 0412 266 420  
Mark Butlin 0422 908 893  
Melissa Farnham 0415 821 096  
QJ-Jian Sun 0413 733 250  
**Other people participating:**  
Ms Alice Ding 0433 663 967  
Ms Divya Sarma Kandukuri 0432 435 396  
Mr Omar Al-Adhami 0426 292 791  
Mr Ibrahim Salman 0426 286 182  
Barbara Zangerl 0426 849 669  
George Lindsey (02) 9850 9812  
Yimin Yao 0422 672 307  
Rochelle Boyd 0409 322 382  
Ko Jin Quek 0404 124 209  
Manash Saha 0469 344 124

**In case of emergency, please contact:**  
the Principal Investigator / Associate Investigator named above,  
Animal Welfare Officer - 9850 7758 / 0439 497 383,  
or Manager, CAF - 9850 7780 / 0428 861 163

The above-named are authorised by MACQUARIE UNIVERSITY  
ANIMAL ETHICS COMMITTEE to conduct the following research:

**Title of the project:** Do stiff blood vessels or overactive nerves cause long-term high blood pressure in kidney disease?

**Purpose:** 4 – Research: human or animal biology

**Aim:** This project aims to use an animal model to determine if drugs which block the hormone angiotensin II therapy for hypertension reduces the stiffness of blood vessels or elevated nerve activity.

**Surgical Procedures category:** 3 (Minor conscious intervention)

**All procedures must be performed as per the AEC-approved protocol, unless stated otherwise by the AEC and/or AWO.**

Maximum numbers approved:

Species	Strain	Sex	Age	TOTAL	Supplier/Source
Rat	Lewis	M/F	3-18 wks	156	ARC Perth
Rat	LPK	M/F	3-18 wks	156	ARC Perth/Westmead Hospital
Rat	SHR	M/F	4-24 wks	156	ARC Perth
Rat	WKY	M/F	4-24 wks	156	ARC Perth
TOTAL				624	

Location of research:

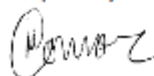
Location	Full street address
Australian School of Advanced Medicine	Level 1, Clinic Building, 2 Technology Place, Macquarie University NSW 2109
Central Animal Facility	Building F9A, Research Park Drive, Macquarie University NSW 2109

Conditions of Approval: N/A

Amendments approved by the AEC since initial approval:

1. Addition of new personnel to protocol: Barbara Zangerl (approved May 2012).
2. Addition of new personnel to protocol: George Lindsey (approved June 2012).
3. Addition of new personnel to protocol: Yimin Yao subject to adequate supervision (approved July 2012).
4. Addition of Melissa Farnham as Associate Investigator (approved July 2012).
5. Modification of experimental procedure (approved 16 August 2012).
6. Change of age of animals used (approved 16 August 2012).
7. Addition of new personnel to protocol: Marie-Ange Kouassi (approved September 2012).
8. Addition of new personnel to protocol: Rochelle Boyd (approved & ratified December 2012).
9. Addition of new personnel to protocol: Ko Jin Quek (approved February 2013).
10. Addition of new personnel to protocol: Manash Saha as Student (Executive approved 17 April 2013, ratified by AEC 18 April 2013).
11. Increase dose range of Valsartan to 60mg/kg/day for LPK rats (Executive approved 23 May 2013, ratified by AEC 13 June 2013).
12. Add procedures performed under anaesthesia to include manipulation of blood pressure & venous return (Approved 13 June 2013).
13. Addition of QJ-Jian Sun as Associate investigator (Executive approved 6 August 2013, ratified by AEC 15 August 2013).
14. Alternative method to provide drug treatment (Executive approved 3 August 2013, ratified by AEC 15 August 2013).
15. Increase maximum dose of Amlodipine to 20mg/kg/day and begin BP treatment for SHR at the earlier age of 8 weeks (Executive approved 30 August 2013, ratified by AEC 19 September 2013).

Being animal research carried out in accordance with the Code of Practice for a recognised research purpose and in connection with animals (other than exempt animals) that have been obtained from the holder of an animal supplier's license.



Prof Mark Connor (Chair, Animal Ethics Committee)

Approval Date: 19 September 2013

Adapted from Form C (issued under part IV of the Animal Research Act, 1985)

## ANIMAL RESEARCH AUTHORITY (ARA)

AEC Reference No.: 2012/002-2

Date of Expiry: 22 February 2014

**Full Approval Duration:** 23 February 2012 to 22 February 2015 (12 Months + 24 month extension)

*This ARA remains in force until the Date of Expiry (unless suspended, cancelled or surrendered) and will only be renewed upon receipt of a satisfactory Progress Report before expiry / is contingent upon receipt of a Final Report at the end of this period (see Approval email for submission details).*

**Principal Investigator:**  
Dr Mark Butlin  
Lecturer, Australian School of Advanced Medicine  
Mark.butlin@mq.edu.au  
0422 908 895

**Associate Investigators:**  
George Lindesay 0434 984 207  
Albert Avolio 0408 657 616  
Zahra Kouchaki 9812 3575

**In case of emergency, please contact:**  
*the Principal Investigator / Associate Investigator named above*  
**OR Manager, CAF: 9850 7780 / 0428 861 163 and Animal Welfare Officer: 9850 7758 / 0439 497 383**

The above-named are authorised by MACQUARIE UNIVERSITY ANIMAL ETHICS COMMITTEE to conduct the following research:

**Title of the project:** Effect of acute baroreceptor stimulation on aortic haemodynamics.

**Purpose:** 4 - Research: Animal or human biology

**Aims:** This project aims to investigate the effect of a device which stimulates the baroreceptors, on the sympathetic outflow of the brain and the stiffness of the aorta in rats.

**Surgical Procedures category:** 2 – Animal Unconscious without Recovery

**All procedures must be performed as per the AEC-approved protocol, unless stated otherwise by the AEC and/or AWO.**

Maximum numbers approved (for the Full Approval Duration):

Species	Strain	Age/Sex/Weight	Total	Supplier/Source
02 - Rat	WKY	10-20 weeks/~250g-450g /male	48	ARC Perth
02 - Rat	SHR	10-20 weeks/~250g-450g /male	48	ARC Perth
TOTAL			96	

**Location of research:**

Location	Full street address
Central Animal Facility	Building F9A, Research Park Drive, Macquarie University NSW 2109
ASAM	Building F10A, 2 Technology Place, Macquarie University NSW 2109

**Amendments approved by the AEC since initial approval:**

1. Addition of Zahra Kouchaki as Associate Investigator (Approved February 2013)
2. Extend approval duration by 2 years (Approved February 2013)

**Conditions of Approval:** N/A

Being animal research carried out in accordance with the Code of Practice for a recognised research purpose and in connection with animals (other than exempt animals) that have been obtained from the holder of an animal suppliers licence.



Dr. Kandy White (Deputy Chair, Animal Ethics Committee)

**Approval Date:** 14 February 2013

# References

- Aars H. 1971. Effects of Altered Smooth Muscle Tone on Aortic Diameter and Aortic Baroreceptor Activity in Anesthetized Rabbits. *Circ. Res.* 28(2):254–62
- Access E. 2005. The shifting burden of cardiovascular disease in Australia. *Publ. Rep.*
- Anderson WP, Kett MM, Stevenson KM, Edgley a. J, Denton KM, Fitzgerald SM. 2000. Renovascular Hypertension: Structural Changes in the Renal Vasculature. *Hypertension.* 36(4):648–52
- Armentano RL, Barra JG, Santana DB, Pessana FM, Graf S, et al. 2006. Smart damping modulation of carotid wall energetics in human hypertension: effects of angiotensin-converting enzyme inhibition. *Hypertension.* 47(3):384–90
- Avolio A, Butlin M, Tan I. 2013. Importance of pressure pulse amplification in the association of resting heart rate and arterial stiffness. *Hypertension.* 62(6):e46
- Avolio AP, Chen SG, Wang RP, Zhang CL, Li MF, O'Rourke MF. 1983. Effects of aging on changing arterial compliance and left ventricular load in a northern Chinese urban community. *Circulation.* 68(1):50–58
- Bakris GL, Nadim MK, Haller H, Lovett EG, Schafer JE, Bisognano JD. 2012. Baroreflex activation therapy provides durable benefit in patients with resistant hypertension: results of long-term follow-up in the Rheos Pivotal Trial. *J. Am. Soc. Hypertens.* 6(2):152–58
- Bank a J, Wilson RF, Kubo SH, Holte JE, Dresing TJ, Wang H. 1995a. Direct effects of smooth muscle relaxation and contraction on in vivo human brachial artery elastic properties. *Circ. Res.* 77(5):1008–16
- Bank AJ, Wang H, Holte JE, Mullen K, Shammass R, Kubo SH. 1996. Contribution of collagen, elastin, and smooth muscle to in vivo human brachial artery wall stress and elastic modulus. *Circulation.* 94(12):3263–70
- Bank AJ, Wilson RF, Kubo SH, Holte JE, Dresing TJ, Wang H. 1995b. Direct effects of smooth muscle relaxation and contraction on in vivo human brachial artery elastic properties. *Circ. Res.* 77(5):1008–16
- Barra JG, Armentano RL, Levenson J, Fischer EI, Pichel RH, Simon A. 1993. Assessment of smooth muscle contribution to descending thoracic aortic elastic mechanics in conscious dogs. *Circ. Res.* 73(6):1040–50
- Bevan RD, Tsuru H. 1981. Functional and structural changes in the rabbit ear artery after sympathetic denervation. *Circ. Res.* 49(2):478–85

- Bezie Y, Lamaziere J-MD, Laurent S, Challande P, Cunha RS, et al. 1998. Fibronectin Expression and Aortic Wall Elastic Modulus in Spontaneously Hypertensive Rats. *Arterioscler. Thromb. Vasc. Biol.* 18(7):1027–34
- Bia D, Armentano RL, Grignola JC, Craiem D, Zócalo Y a, et al. 2003a. The vascular smooth muscle of great arteries: Local control site of arterial buffering function? *Rev. española Cardiol.* 56(12):1202–9
- Bia D, Armentano RL, Grignola JC, Craiem D, Zócalo Y a, et al. 2003b. [The vascular smooth muscle of great arteries: local control site of arterial buffering function?]. *Rev. española Cardiol.* 56(12):1202–9
- Blacher J, Asmar R, Djane S, London GM, Safar ME. 1999. Aortic pulse wave velocity as a marker of cardiovascular risk in hypertensive patients. *Hypertension.* 33(5):1111–17
- Boehm S, Huck S. 1997. Receptors controlling transmitter release from sympathetic neurons in vitro. *Prog. Neurobiol.* 51(3):225–42
- Braunwald E, Epstein S. 1967. Relief of angina pectoris by electrical stimulation of the carotid-sinus nerves. ... *Engl. J.* .... 277(24):1278–83
- Burgi K, Cavalleri MT, Alves AS, Britto LRG, Antunes VR, Michelini LC. 2011. Tyrosine hydroxylase immunoreactivity as indicator of sympathetic activity: simultaneous evaluation in different tissues of hypertensive rats. *Am. J. Physiol. Regul. Integr. Comp. Physiol.* 300(2):R264–71
- Butlin M, Hammond A, Lindesay G, Viegas K, Avolio A. 2012. In-vitro and in-vivo use of vasoactive agents in characterising aortic stiffness in rats: testing the assumptions. *Hypertension.* 30:e42
- Butlin M, Lindesay G, Georgakopoulos D, Pilowsky P, Goldys E, Town G. 2013. Effect of baroreceptor field stimulation on rat aortic stiffness and waveform parameters. *23rd Eur. Meet. Hypertens. Cardiovasc. Prot.*
- Cannesson M, Jian Z, Chen G, Vu TQ, Hatib F. 2012. Effects of phenylephrine on cardiac output and venous return depend on the position of the heart on the Frank-Starling relationship. *J. Appl. Physiol.* 113(2):281–89
- Casey DP, Curry TB, Joyner MJ, Charkoudian N, Hart EC. 2011. Relationship between muscle sympathetic nerve activity and aortic wave reflection characteristics in young men and women. *Hypertension.* 57(3):421–27
- Chan S, Ong B, Wong P. 1984a. Suppression of arterial pressure, heart rate and cardiac contractility following microinjection of kainic acid into the nucleus ambiguus of the rat. *Neurosci. Lett.* 47:57–62
- Chan S, Ong B, Wong P. 1984b. Suppression of arterial pressure, heart rate and cardiac contractility following microinjection of kainic acid into the nucleus ambiguus of the rat. *Neurosci. Lett.* 47:57–62

- Climie RED, Nikolic SB, Otahal P, Keith LJ, Sharman JE. 2013. Augmentation index and arterial stiffness in patients with type 2 diabetes mellitus. *Artery Res.* 7(3-4):194–200
- Cosson E, Herisse M, Laude D, Thomas F, Valensi P, et al. 2007. Aortic stiffness and pulse pressure amplification in Wistar-Kyoto and spontaneously hypertensive rats. *Am. J. Physiol. Heart Circ. Physiol.* 292(5):H2506–12
- Cosson E, Valensi P, Laude D, Mesangeau D, Dabire H. 2009. Arterial stiffness and the autonomic nervous system during the development of Zucker diabetic fatty rats. *Diabetes Metab.* 35(5):364–70
- Danpinid A, Luo J, Vappou J, Terdtoon P, Konofagou EE. 2010. In vivo characterization of the aortic wall stress-strain relationship. *Ultrasonics.* 50(7):654–65
- Davies JE, Baksi J, Francis DP, Hadjiloizou N, Whinnett ZI, et al. 2010. The arterial reservoir pressure increases with aging and is the major determinant of the aortic augmentation index. , pp. 580–86
- Delacrétaz E, Hayoz D, Hutter D, Allemann Y. 2001. Radial artery compliance in response to mental stress in normotensive offspring of hypertensive parents. *Clin. Exp. Hypertens.* 23(7):545–53
- Dobrin P, Canfield T. 1977. Identification of smooth muscle series elastic component in intact carotid artery. *Am. J. Physiol.* 232(2):H122–30
- Dobrin PB, Rovick AA. 1969. Influence of vascular smooth muscle on contractile mechanics and elasticity of arteries. *Am. J. Physiol.* 217(6):1644–51
- Doonan RJ, Scheffler P, Lalli M, Kimoff RJ, Petridou ET, et al. 2011. Increased arterial stiffness in obstructive sleep apnea: a systematic review. *Hypertens. Res.* 34(1):23–32
- Dotevall G. 1994. Involvement of cardiac, respiratory and gastrointestinal functions in neural responses to stressful events. *Integr. Physiol. Behav. Sci.* 29(4):374–82
- Drager LF, Bortolotto L a, Figueiredo AC, Krieger EM, Lorenzi GF. 2007. Effects of continuous positive airway pressure on early signs of atherosclerosis in obstructive sleep apnea. *Am. J. Respir. Crit. Care Med.* 176(7):706–12
- Dumont RJ, Okonkwo DO, Verma S, Hurlbert RJ, Boulos PT, et al. 2001. Acute spinal cord injury, part I: pathophysiologic mechanisms. *Clin. Neuropharmacol.* 24(5):254–64
- Eastwood PR, Malhotra A, Palmer LJ, Kezirian EJ, Horner RL, et al. 2010. Obstructive Sleep Apnoea: From pathogenesis to treatment: Current controversies and future directions. *Respirology.* 15(4):587–95
- Esler M. 2000. The sympathetic system and hypertension. *Am. J. Hypertens.* 13(6 Pt 2):99S–105S
- Feng J, Zhang D, Chen B. 2012. Endothelial mechanisms of endothelial dysfunction in patients with obstructive sleep apnea. *Sleep Breath.* 16(2):283–94



- Fitch RM, Vergona R, Sullivan ME, Wang Y-XX. 2001. Nitric oxide synthase inhibition increases aortic stiffness measured by pulse wave velocity in rats. *Cardiovasc. Res.* 51(2):351–58
- Fridez P, Makino a., Kakoi D, Miyazaki H, Meister J-J, et al. 2002. Adaptation of conduit artery vascular smooth muscle tone to induced hypertension. *Ann. Biomed. Eng.* 30(7):905–16
- Fronek K. 1983. Trophic effect of the sympathetic nervous system on vascular smooth muscle. *Ann. Biomed. Eng.* 11(6):607–15
- Gerova M, Gero J, Dolezel S, Blazkova Huzulakova I, Gerová M, Blazková-Huzuláková I. 1973. Sympathetic control of canine abdominal aorta. *Circ. Res.* 33(2):149–59
- Gerová M, Gero J, Dolezel S, Blazková-Huzuláková I. 1973. Sympathetic control of canine abdominal aorta. *Circ. Res.* 33(2):149–59
- Glasser S, Arnett D. 1998. The importance of arterial compliance in cardiovascular drug therapy. *J. Clin. Pharmacol.* 38(3):202–12
- Greene L a, Rein G. 1978. Release of norepinephrine from neurons in dissociated cell cultures of chick sympathetic ganglia via stimulation of nicotinic and muscarinic acetylcholine receptors. *J. Neurochem.* 30(3):579–86
- Greenwood JP, Scott EM, Stoker JB, Mary D a. 2001. Hypertensive left ventricular hypertrophy: relation to peripheral sympathetic drive. *J. Am. Coll. Cardiol.* 38(6):1711–17
- Guyenet PG. 2006. The sympathetic control of blood pressure. *Nat. Rev. Neurosci.* 7(5):335–46
- Hambley JW, Johnston G a, Rogers LJ. 1987a. Blood pressure development in SHR and WKY rats: effects of neonatal monosodium glutamate treatment and evidence for transient hypertension in WKY rats. *Neurosci. Lett.* 83(1-2):190–94
- Hambley JW, Johnston G a, Rogers LJ. 1987b. Blood pressure development in SHR and WKY rats: effects of neonatal monosodium glutamate treatment and evidence for transient hypertension in WKY rats. *Neurosci. Lett.* 83(1-2):190–94
- Hamlin RL, del Rio C. 2012. dP/dt(max)--a measure of “baroinometry”. *J. Pharmacol. Toxicol. Methods.* 66(2):63–65
- Hansen L, Parker I, Sutliff RL, Platt MO, Gleason RL. 2013. Endothelial dysfunction, arterial stiffening, and intima-media thickening in large arteries from HIV-1 transgenic mice. *Ann. Biomed. Eng.* 41(4):682–93
- Harkness ML, Harkness RD, McDonald D a. 1957a. The collagen and elastin content of the arterial wall in the dog. *Proc. R. Soc. Lond. B. Biol. Sci.* 146(925):541–51

- Harkness ML, Harkness RD, McDonald D a. 1957b. The collagen and elastin content of the arterial wall in the dog. *Proc. R. Soc. Lond. B. Biol. Sci.* 146(925):541–51
- Harrison JL, Hildreth CM, Callahan SM, Goodchild AK, Phillips JK. 2010a. Cardiovascular autonomic dysfunction in a novel rodent model of polycystic kidney disease. *Auton. Neurosci.* 152(1-2):60–66
- Harrison JL, Hildreth CM, Callahan SM, Goodchild AK, Phillips JK. 2010b. Cardiovascular autonomic dysfunction in a novel rodent model of polycystic kidney disease. *Auton. Neurosci.* 152(1-2):60–66
- Hayoz D. 1995. Flow-diameter phase shift: A potential indicator of conduit artery function. *Hypertension.* 26(1):20–25
- Hayoz D, Tardy Y, Rutschmann B, Mignot JP, Achakri H, et al. 1993. Spontaneous diameter oscillations of the radial artery in humans. *Am. J. Physiol.* 264(6 Pt 2):H2080–4
- Hering D, Kucharska W, Kara T, Somers VK, Narkiewicz K. 2010. Smoking is associated with chronic sympathetic activation in hypertension. *Blood Press.* 19(3):152–55
- Heusser K, Tank J, Engeli S, Diedrich A, Menne J, et al. 2010. Carotid baroreceptor stimulation, sympathetic activity, baroreflex function, and blood pressure in hypertensive patients. *Hypertension.* 55(3):619–26
- Hickson SS, Butlin M, Graves M, Taviani V, Avolio AP, et al. 2010. The relationship of age with regional aortic stiffness and diameter. *JACC. Cardiovasc. Imaging.* 3(12):1247–55
- Hughes A, Wang J-J, Bouwmeester C, Davies J, Shrive N, et al. 2012. The reservoir-wave paradigm. *J. Hypertens.* 30(9):1880–1; author reply 1881–3
- Humphrey JD. 2008. Mechanisms of arterial remodeling in hypertension: coupled roles of wall shear and intramural stress. *Hypertension.* 52(2):195–200
- Humphrey JD, Na S. 2002. Elastodynamics and Arterial Wall Stress. *Ann. Biomed. Eng.* 30(4):509–23
- Hunter A. 1950. Hexamethonium Bromide. *Lancet.* 255:251–52
- Imaki T, Naruse M, Harada S, Chikada N, Nakajima K. 1998. Stress-Induced Changes of Gene Expression in the Paraventricular Nucleus are Enhanced in Spontaneously Hypertensive Rats. . 10(9):635–43
- Jelic S, Bartels MN, Mateika JH, Ngai P, DeMeersman RE, Basner RC. 2002. Arterial stiffness increases during obstructive sleep apneas. *Sleep.* 25(8):850–55
- Judy WV, Farrell SK. 1979. Arterial baroreceptor reflex control of sympathetic nerve activity in the spontaneously hypertensive rat. *Hypertension.* 1(6):605–14

- Kacem K, Bonvento G, Seylaz J. 1997. Effect of sympathectomy on the phenotype of smooth muscle cells of middle cerebral and ear arteries of hyperlipidaemic rabbits. *Histochem. J.* 29(4):279–86
- Kacem K, Sercombe R. 2008. Similar pathological effects of sympathectomy and hypercholesterolemia on arterial smooth muscle cells and fibroblasts. *Acta Histochem.* 110(4):302–13
- Kacem K, Sercombe C, Hammami M, Vicaut E, Sercombe R. 2006. Sympathectomy causes aggravated lesions and dedifferentiation in large rabbit atherosclerotic arteries without involving nitric oxide. *J. Vasc. Res.* 43(3):289–305
- Kandlikar SS, Fink GD. 2011. Splanchnic sympathetic nerves in the development of mild DOCA-salt hypertension. *Am. J. Physiol. Heart Circ. Physiol.* 301(5):H1965–73
- Karrer HE. 1961. An electron microscope study of the aorta in young and in aging mice. *J. Ultrastructure Res.* 5(1):1–27
- Kienecker E, Knoche H. 1978a. Sympathetic innervation of the pulmonary artery, ascending aorta, and coronar glomera of the rabbit. *Cell Tissue Res.* 333:329–33
- Kienecker EW, Knoche H. 1978b. Sympathetic Innervation of the Pulmonary Artery , Ascending Aorta , and Coronar Glomera of the Rabbit. *Cell Tissue Res.* 188(2):329–33
- Kim JW, Park CG, Hong SJ, Park SM, Rha SW, et al. 2005a. Acute and chronic effects of cigarette smoking on arterial stiffness. *Blood Press.* 14(2):80–85
- Kim JW, Park CG, Hong SJ, Park SM, Rha SW, et al. 2005b. Acute and chronic effects of cigarette smoking on arterial stiffness. *Blood Press.* 14(2):80–85
- Klein IHHT, Ligtenberg G, Oey PL, Koomans HA, Blankestijn PJ. 2001a. Sympathetic Activity Is Increased in Polycystic Kidney Disease and Is Associated with Hypertension. *J. Am. Soc. Nephrol.* 12:2427–33
- Klein IHHT, Ligtenberg G, Oey PL, Koomans HA, Blankestijn PJ. 2001b. Sympathetic Activity Is Increased in Polycystic Kidney Disease and Is Associated with Hypertension. *J. Am. Soc. Nephrol.* 12:2427–33
- Kool MJ, Lustermaans FA, Breed JG, Struyker-Boudier HA, Hoeks AP, Van Bortel LM. 1993. Effect of perindopril and amiloride/hydrochlorothiazide on haemodynamics and vessel wall properties of large arteries. *J. Hypertens. Suppl.* 11(5):S362–3
- Kool MJ, Spek JJ, Struyker Boudier HA, Hoeks AP, Reneman RS, et al. 1995. Acute and subacute effects of nicorandil and isosorbide dinitrate on vessel wall properties of large arteries and hemodynamics in healthy volunteers. *Cardiovasc. Drugs Ther.* 9(2):331–37
- Krug R, Boese JM, Schad LR. 2003. Determination of aortic compliance from magnetic resonance images using an automatic active contour model. *Phys. Med. Biol.* 48(15):2391–2404

- Krum H, Schlaich M, Whitbourn R, Sobotka PA, Sadowski J, et al. 2009. Catheter-based renal sympathetic denervation for resistant hypertension: a multicentre safety and proof-of-principle cohort study. *Lancet*. 373(9671):1275–81
- Kubo T, Hagiwara Y, Endo S, Fukumori R. 2002. Activation of hypothalamic angiotensin receptors produces pressor responses via cholinergic inputs to the rostral ventrolateral medulla in normotensive and hypertensive rats. *Brain Res*. 953(1-2):232–45
- Kuhn HJ. 1978. Cross bridge slippage induced by the ATP analogue AMP-PNP and stretch in glycerol-extracted fibrillar muscle fibres. *Biophys. Struct. Mech*. 4(2):159–68
- Lambert G. 2001. Paring down on Descartes: a review of brain noradrenaline and sympathetic nervous function. *Clin. Exp. Pharmacol.* .... 2(June):979–83
- Laurent S, Boutouyrie P, Asmar R, Gautier I, Laloux B, et al. 2001. Aortic stiffness is an independent predictor of all-cause and cardiovascular mortality in hypertensive patients. *Hypertension*. 37(5):1236–41
- Lénárd Z, Fülöp D, Visontai Z. 2000. Static versus dynamic distensibility of the carotid artery in humans. *J. Vasc.* .... 1082:103–11
- Leone N, Ducimetière P, Gariépy J, Courbon D, Tzourio C, et al. 2008. Distension of the carotid artery and risk of coronary events: the three-city study. *Arterioscler. Thromb. Vasc. Biol*. 28(7):1392–97
- Liao D, Arnett DK, Tyroler H a., Riley W a., Chambless LE, et al. 1999. Arterial Stiffness and the Development of Hypertension : The ARIC Study. *Hypertension*. 34(2):201–6
- Liu S, Fung Y. 1996. Indicial functions of arterial remodeling in response to locally altered blood pressure. *Am. J. Physiol.* .... 270(4):H1323–H1333
- London GM, Guerin AP. 1999. Influence of arterial pulse and reflected waves on blood pressure and cardiac function. *Am. Heart J*. 138(3 II):220–24
- Lydakis C, Momen A, Blaha C, Herr M, Leuenberger UA, Sinoway LI. 2008. Changes of elastic properties of central arteries during acute static exercise and lower body negative pressure. *Eur. J. Appl. Physiol*. 102(6):633–41
- Malpas S. 2010. Sympathetic nervous system overactivity and its role in the development of cardiovascular disease. *Physiol. Rev*. 90:513–57
- Mancia G, De Backer G, Dominiczak A, Cifkova R, Fagard R, et al. 2007. 2007 ESH-ESC Guidelines for the management of arterial hypertension: the task force for the management of arterial hypertension of the European Society of Hypertension (ESH) and of the European Society of Cardiology (ESC). *Blood Press*. 16(3):135–232
- Mangell P, Länne T, Sonesson B, Hansen F, Bergqvist D. 1996. Regional differences in mechanical properties between major arteries--an experimental study in sheep. *Eur. J. Vasc. Endovasc. Surg*. 12(2):189–95

- Mangoni AA, Mircoli L, Giannattasio C, Mancia G, Ferrari AU. 1997. Effect of sympathectomy on mechanical properties of common carotid and femoral arteries. *Hypertension*. 30(5):1085–88
- Mano T, Iwase S. 2003. Sympathetic nerve activity in hypotension and orthostatic intolerance. *Acta Physiol. Scand*. 177(3):359–65
- Mathias CJ. 1991. Management of hypertension by reduction in sympathetic activity. *Hypertension*. 17(4):69–74
- Matsukawa K, Ninomiya I. 1989. Anesthetic effects on tonic and reflex renal sympathetic nerve activity in awake cats. *Am. J. Physiol*. 256(2 Pt 2):R371–8
- Matsukawa T, Mano T, Gotoh E, Ishii M. 1993. Elevated sympathetic nerve activity in patients with accelerated essential hypertension. *J. Clin. Invest*. 92(1):25–28
- Mattace-Raso FUS, van der Cammen TJM, Hofman A, van Popele NM, Bos ML, et al. 2006. Arterial stiffness and risk of coronary heart disease and stroke: the Rotterdam Study. *Circulation*. 113(5):657–63
- McCooke J, Appels R, Barrero R. 2012. A novel mutation causing nephronophthisis in the Lewis polycystic kidney rat localises to a conserved RCC1 domain in Nek8. *BMC ...*. 13:393
- McEniery CM, Yasmin, Hall IR, Qasem A, Wilkinson IB, Cockcroft JR. 2005. Normal vascular aging: differential effects on wave reflection and aortic pulse wave velocity: the Anglo-Cardiff Collaborative Trial (ACCT). *J. Am. Coll. Cardiol*. 46(9):1753–60
- Mello J de, Orsi A, Padovani C. 2004. Structure of the aortic wall in the guinea pig and rat. *Braz. J. Morphol. ....* 21:35–38
- Milch R. 1965. Matrix properties of the arterial wall. *Monogr. Surg. Sci*. 2(4):261–342
- Mitchell GF, Hwang S-J, Vasan RS, Larson MG, Pencina MJ, et al. 2010a. Arterial stiffness and cardiovascular events: the Framingham Heart Study. *Circulation*. 121(4):505–11
- Mitchell GF, Hwang S-J, Vasan RS, Larson MG, Pencina MJ, et al. 2010b. Arterial stiffness and cardiovascular events: the Framingham Heart Study. *Circulation*. 121(4):505–11
- Mitchell GF, Lacourcière Y, Ouellet J-P, Izzo JL, Neutel J, et al. 2003. Determinants of elevated pulse pressure in middle-aged and older subjects with uncomplicated systolic hypertension: the role of proximal aortic diameter and the aortic pressure-flow relationship. *Circulation*. 108(13):1592–98
- Mynard JP. 2013. Assessment of conceptual inconsistencies in the hybrid reservoir-wave model. *Conf. Proc. ... Annu. Int. Conf. IEEE Eng. Med. Biol. Soc. IEEE Eng. Med. Biol. Soc. Annu. Conf*. 2013:213–16

- Mynard JP, Penny DJ, Davidson MR, Smolich JJ. 2012. The reservoir-wave paradigm introduces error into arterial wave analysis: a computer modelling and in-vivo study. *J. Hypertens.* 30(4):734–43
- Najjar SS, Scuteri A, Lakatta EG. 2005. Arterial aging: is it an immutable cardiovascular risk factor? *Hypertension.* 46(3):454–62
- Narkiewicz K, van de Borne PJH, Hausberg M, Cooley RL, Winniford MD, et al. 1998. Cigarette Smoking Increases Sympathetic Outflow in Humans. *Circulation.* 98(6):528–34
- Neuhuber W, Schrödl F. 2011. Autonomic control of the eye and the iris. *Auton. Neurosci.* 165(1):67–79
- Ng K, Butlin M, Avolio AP. 2012. Persistent effect of early, brief angiotensin-converting enzyme inhibition on segmental pressure dependency of aortic stiffness in spontaneously hypertensive rats. *J. Hypertens.* 30(9):1782–90
- Ng K, Hildreth CM, Phillips JK, Avolio AP. 2011a. Aortic stiffness is associated with vascular calcification and remodeling in a chronic kidney disease rat model. *Am. J. Physiol. Renal Physiol.* 300(6):F1431–6
- Ng K, Hildreth CM, Phillips JK, Avolio AP. 2011b. Aortic stiffness is associated with vascular calcification and remodeling in a chronic kidney disease rat model. *Am. J. Physiol. Renal Physiol.* 300(6):F1431–6
- Ng a. V., Callister R, Johnson DG, Seals DR. 1993. Age and gender influence muscle sympathetic nerve activity at rest in healthy humans. *Hypertension.* 21(4):498–503
- Nichols WW, O'Rourke MF, Vlachopoulos C. 2011. *Blood Flow in Arteries*. Boca Raton: CRC Press. 6th ed.
- O'Rourke M, Hashimoto J. 2007. Mechanical Factors in Arterial AgingA Clinical Perspective. *J. ....* 50(1):1–13
- O'Rourke MF, Nichols WW. 2005. Aortic diameter, aortic stiffness, and wave reflection increase with age and isolated systolic hypertension. *Hypertension.* 45(4):652–58
- O'Rourke MF, Staessen J a, Vlachopoulos C, Duprez D, Plante GE. 2002. Clinical applications of arterial stiffness; definitions and reference values. *Am. J. Hypertens.* 15(5):426–44
- Okada Y, Galbreath MM, Shibata S, Jarvis SS, Vangundy TB, et al. 2011. Relationship Between Sympathetic Baroreflex Sensitivity and Arterial Stiffness in Elderly Men and Women. *Hypertension*, pp. 98–104
- Osborn JL, Plato CF, Gordin E, He XR. 1997. Long-term increases in renal sympathetic nerve activity and hypertension. *Clin. Exp. Pharmacol. Physiol.* 24(1):72–76

- Palmieri E a, Fazio S, Palmieri V, Lombardi G, Biondi B. 2004. Myocardial contractility and total arterial stiffness in patients with overt hyperthyroidism: acute effects of beta1-adrenergic blockade. *Eur. J. Endocrinol.* 150(6):757–62
- Phillips BG, Somers VK. 2000. Neural and humoral mechanisms mediating cardiovascular responses to obstructive sleep apnea. *Respir. Physiol.* 119(2-3):181–87
- Phillips JK, Hopwood D, Loxley R a, Ghatora K, Coombes JD, et al. 2007. Temporal relationship between renal cyst development, hypertension and cardiac hypertrophy in a new rat model of autosomal recessive polycystic kidney disease. *Kidney Blood Press. Res.* 30(3):129–44
- Prado CM, Rossi M a. 2006. Circumferential wall tension due to hypertension plays a pivotal role in aorta remodelling. *Int. J. Exp. Pathol.* 87(6):425–36
- Pravenec M, Zídek V, Landa V, Simáková M, Mlejnek P, et al. 2004. Genetic analysis of “metabolic syndrome” in the spontaneously hypertensive rat. *Physiol. Res.* 53 Suppl 1:S15–22
- Rogers WJ, Hu YL, Coast D, Vido D a, Kramer CM, et al. 2001. Age-associated changes in regional aortic pulse wave velocity. *J. Am. Coll. Cardiol.* 38(4):1123–29
- Rourke MFO, Hashimoto J. 2007. Mechanical Factors in Arterial Aging. *J. Am. Coll. Cardiol.* 50(1):1–13
- Rovick A, Dobrin PB. 1969. Influence of vascular smooth muscle on contractile mechanics and elasticity of arteries. *Am. J. Physiol.* 217(6):1644–51
- Schiffrin EL, Hayoz D. 1997. How to assess vascular remodelling in small and medium-sized muscular arteries in humans. *J. Hypertens.* 15(6):571–84
- Schultz MG, Davies JE, Roberts-Thomson P, Black JA, Hughes AD, Sharman JE. 2013a. Exercise central (aortic) blood pressure is predominantly driven by forward traveling waves, not wave reflection. *Hypertension.* 62(1):175–82
- Schultz MG, Otahal P, Cleland VJ, Blizzard L, Marwick TH, Sharman JE. 2013b. Exercise-induced hypertension, cardiovascular events, and mortality in patients undergoing exercise stress testing: a systematic review and meta-analysis. *Am. J. Hypertens.* 26(3):357–66
- Segal SS. 2005. Regulation of blood flow in the microcirculation. *Microcirculation.* 12(1):33–45
- Shields R. 1993. Functional anatomy of the autonomic nervous system. *J. Clin. Neurophysiol.* 10(1):2–13
- Shiina K, Tomiyama H, Takata Y, Yoshida M, Kato K, et al. 2010. Effects of CPAP therapy on the sympathovagal balance and arterial stiffness in obstructive sleep apnea. *Respir. Med.* 104(6):911–16

- Sinoway LI, Li J. 2005. A perspective on the muscle reflex: implications for congestive heart failure. *J. Appl. Physiol.* 99(1):5–22
- Smith ML, Niedermaier ON, Hardy SM, Decker MJ, Strohl KP. 1996. Role of hypoxemia in sleep apnea-induced sympathoexcitation. *J. Auton. Nerv. Syst.* 56(3):184–90
- Sonesson B, Vernerström E, Hansen F, Länne T. 1997. Influence of sympathetic stimulation on the mechanical properties of the aorta in humans. *Acta Physiol. Scand.* 159(2):139–45
- Spieker LE. 2002. Mental Stress Induces Prolonged Endothelial Dysfunction via Endothelin-A Receptors. *Circulation.* 105(24):2817–20
- Sundlöf G, Wallin B. 1978. Human muscle nerve sympathetic activity at rest. Relationship to blood pressure and age. *J. Physiol.* 274(1):621
- Świerblewska E, Hering D, Kara T, Kunicka K, Kruszewski P, et al. 2010. An independent relationship between muscle sympathetic nerve activity and pulse wave velocity in normal humans. *J. Hypertens.* 28(5):979–84
- Tan I, Butlin M, Liu YY, Ng K, Avolio AP. 2012a. Heart rate dependence of aortic pulse wave velocity at different arterial pressures in rats. *Hypertension.* 60(2):528–33
- Tan I, Butlin M, Liu YY, Ng K, Avolio AP. 2012b. Heart rate dependence of aortic pulse wave velocity at different arterial pressures in rats. *Hypertension.* 60(2):528–33
- Tardy Y, Meister J. 1991. Non-invasive estimate of the mechanical properties of peripheral arteries from ultrasonic and photoplethysmographic measurements. ... *Meas.* 39:
- Thrasivoulou C, Cowen T. 1995. Regulation of rat sympathetic nerve density by target tissues and NGF in maturity and old age. *Eur. J. Neurosci.* 7(3):381–87
- Van Bortel LM, Kool MJ, Struijker Boudier HA. 1995. Effects of Antihypertensive Agents on Local Arterial Distensibility and Compliance. *Hypertension.* 26(3):531–34
- Vayssettes-Courchay C, Ragonnet C, Isabelle M, Verbeuren TJ. 2011a. Aortic stiffness in vivo in hypertensive rat via echo-tracking: analysis of the pulsatile distension waveform. *Am. J. Physiol. Heart Circ. Physiol.* 301(2):H382–90
- Vayssettes-Courchay C, Ragonnet C, Isabelle M, Verbeuren TJ. 2011b. Aortic stiffness in vivo in hypertensive rat via echo-tracking: analysis of the pulsatile distension waveform. *Am. J. Physiol. Heart Circ. Physiol.* 301(2):H382–90
- Vlachopoulos C, Kosmopoulou F, Alexopoulos N, Ioakeimidis N, Siasos G, Stefanadis C. 2006. Acute mental stress has a prolonged unfavorable effect on arterial stiffness and wave reflections. *Psychosom. Med.* 68(2):231–37
- Weber R, Stergiopoulos N, Brunner HR, Hayoz D. 1996. Contributions of vascular tone and structure to elastic properties of a medium-sized artery. *Hypertension.* 27(3ii):816–22



- Wilkinson IB, Fuchs S a, Jansen IM, Spratt JC, Murray GD, et al. 1998. Reproducibility of pulse wave velocity and augmentation index measured by pulse wave analysis. *J. Hypertens.* 16(12 Pt 2):2079–84
- Wolinsky H, Glagov S. 1969. Comparison of Abdominal and Thoracic Aortic Medial Structure in Mammals. *Circ. Res.* 25(6):677–86

